THE EINSTEIN ALL-SKY SLEW SURVEY

Grant NAG5-1201

Final Report

For the Period 1 August 1989 through 31 July 1991

Principal Investigator
Dr. Martin S. Elvis

May 1992

Prepared for:

National Aeronautics and Space Administration
Goddard Space Flight Center
Greenbelt, Maryland 20771

Smithsonian Institution
Astrophysical Observatory
Cambridge, Massachusetts 02138

The Smithsonian Astrophysical Observatory
is a member of the
Harvard-Smithsonian Center for Astrophysics

The NASA Technical Officer for this grant is Dr. Donald K. West, National Aeronautics and Space Administration, Code 684, Space and Earth Sciences Directorate, Goddard Space Flight center, Greenbelt, Maryland 20771.

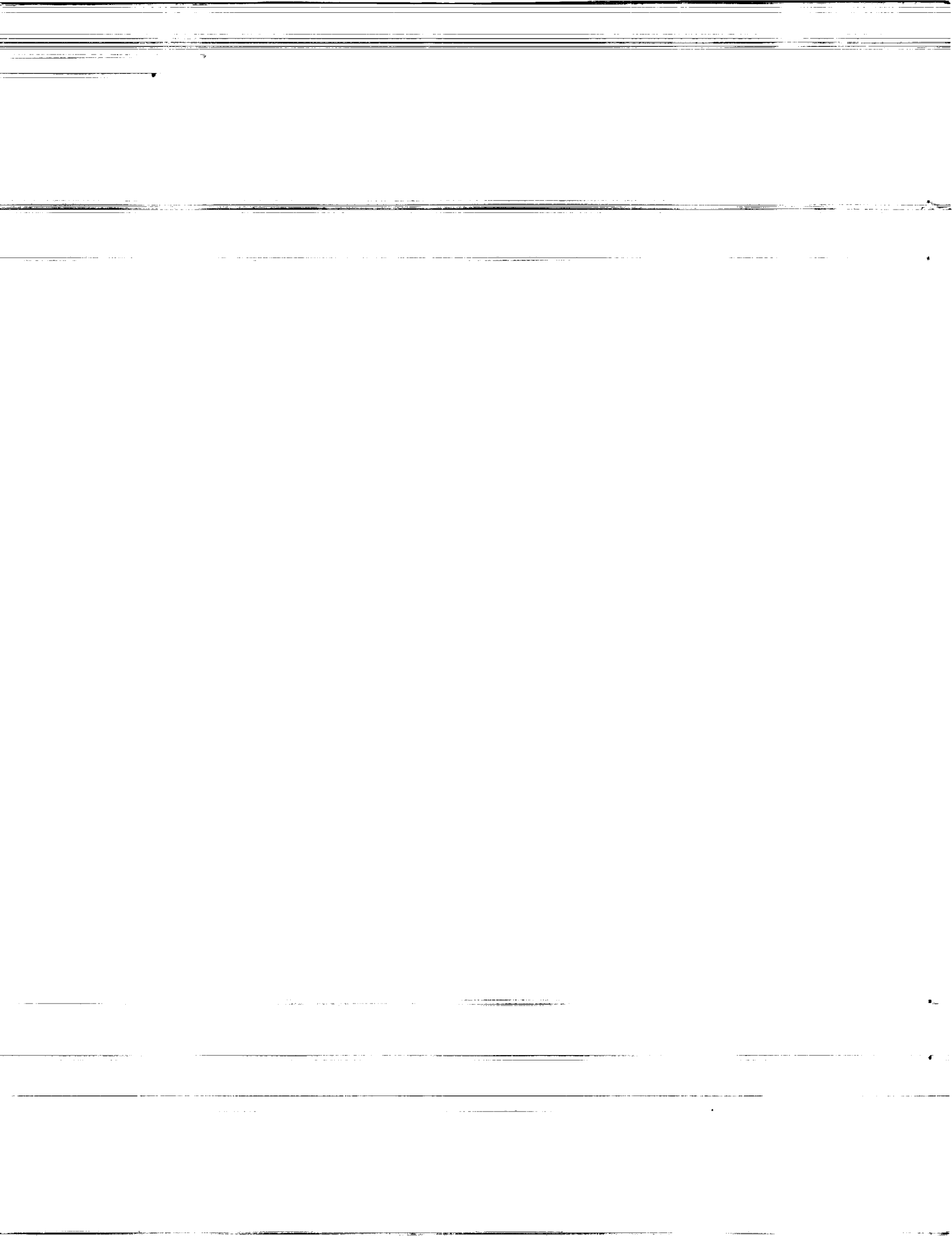

PRIMARY

The First *Einstein* IPC Slew Survey produced a list of 819 X-ray sources, with $f_X \sim 10^{-12} - -10^{-10}$erg cm^{-2} s^{-1} and positional accuracy of $\sim 1.2'$ (90% radius). The aim of this program was to identify these X-ray sources.

A postdoctoral fellow, Jonathan Schachter, was hired on this program for this purpose. The result is that the first identifications from the ADP program are extensive. From the entire survey we have so far identified 637 objects (78%) with known types of sources (e.g., CV, QSO). There are 133 objects newly discovered X-ray sources in this subset.

This part of the search used archival material only - catalogs of X-ray sources, stars, active galaxies, and clusters of galaxies. Appendix B is the Ap.J. Supplement paper which details the production of the Slew Survey and lists (in table 6, column 16) all the catalog identifications. Table 7 highlights the 133 new sources with identifications. A summary of the identifications is given in table 5. Among the identifications are a number of Abell clusters, including a surprising number at relatively high redshift. This may be in contradiction with the result of Edge *et al.*, who claim to see a decrease in the number of luminous clusters with redshift. Careful analysis of the Slew Survey completeness criteria will be needed to test this impression.

There are 313 new X-ray sources in the Slew Survey. 506 objects in the Slew Survey were previously known to be X-ray sources. Of these 191 were detected with HEAO-A3 and many more with pointed IPC observations (with a sizable sample of objects in common). This overlap with HEAO-A3 means we have *soft* x-ray fluxes for a large sample of hard X-ray selected objects. These identifications were also invaluable in 'debugging' the aspect solution and exposure map generation for the Slew Survey.

One of our new sources is a newly discovered ROSAT/WFC EUV detection, and turns out to be an uncataloged white dwarf (Cooke *et al.* 1992). The Slew Survey data show that this object has a soft IPC spectrum, which demonstrates that the use

of IPC pulse height data may be a useful means of selecting sub-classes of sources in the Slew Survey. This information is now being used in cross-comparisons of the Slew Survey and ROSAT All Sky Survey. Preliminary results find some 35 Slew Survey sources were not detected in the ROSAT All Sky Survey. This surprising result implies either large amplitude variability or a heavily cut-off spectrum for these objects. A real possibility is that these are the sought after 'obscured population' needed to reconcile *Ginga* fluctuations analysis with the *Einstein* and ROSAT source counts. This is now under active investigation.

The next phase in the program is to use more archival material in the form of the available multi-wavelength sky surveys - the Palomar/UK Schmidt, Green Bank/Parkes, and IRAS surveys sky maps- together with new VLA observations to identify the great majority of the remaining sources. Our use of this material is more thorough than is normal and details of the methodology were given in a paper at the first 'Astronomical Data Analysis Software and Systems Meeting' (see appendix C.)

The first fruit of this program is the discovery of thirteen new, bright, BL Lac objects using VLA fluxes and positions and POSS magnitudes to make the X-ray identification. A total of 85 BL Lac objects are now confidently predicted in the final Slew Survey list (c.f. a *total* of 87 in the Hewitt and Burbidge 1987 Catalog). Australia Telescope (radio) observing time has been granted to pursue the sources not accessible from the VLA, giving us whole sky coverage.

An optical identification program is well underway, with R. Remillard (MIT), S. Saar (CfA), and M. Donahue (Carnegie, Pasadena) as major collaborators. Several dozen candidate identifications have already been made and are ready for final analysis.

We have successfully brought up the *Einstein* Medium Survey simulation tool and are investigating its use for simulating the Slew Survey. Simulations of the survey are essential to defining statistically complete samples for studies of all populations of astrophysical object in the Slew Survey.

A list of all published papers, talks and abstracts for this program is given in appendix A. Appendix C contains copies of the published conference proceedings and of the paper detailing the BL Lac discovery program and initial results (draft only-final version in preparation).

The ADP program has successfully led to a large fractio of the sources in the Slew Survey being identified.

OMIT

Appendix A

REFERENCES

First Identification of Einstein IPC Slew Survey Sources, 1990, J. Schachter, J.C. McDowell, D. Plummer, and M. Elvis, *BAAS*, 22, 1195.

The Einstein Slew Survey Catalog, 1991, J.F. Schachter, M. Elvis, D. Plummer, G. Fabbiano, and J. Huckra, Proceedings of "Digitized Optical Sky Surveys", eds. H.T. MacGillivray and E.B. Thomson, [Kluwer], p.441.

Identifications of Einstein Slew Survey Sources, 1991, J.F. Schachter, M. Elvis, D. Plummer, and G. Fabbiano, in "Frontiers of X-ray Astronomy" ed. K. Koyama, in press.

The First Einstein Slew Survey Catalog, J. Schachter, D. Plummer and M. Elvis, 1991, *Bull. APS*, Spring 1991, Washington, D.C.

A Study of Time Variability in the Einstein Slew Survey, P. Slane, D. Plummer, and M. Elvis, 1991 *BAAS*, 23, 957.

Counterparts of Sources in the Einstein Slew Survey, J. Schachter, M. Elvis, and D. Plummer, 1991, *BAAS*, 23, 58.

Identifications of Sources in the Einstein Slew Survey: Results and Methods, J. Schachter, M. Elvis, D. Plummer, and R. Remillard, 1991 *BAAS*, 23, No. 4, 1431.

Einstein Slew Survey: Data Analysis Innovations, 1992, M. Elvis, D. Plummer, J. Schachter, and G. Fabbiano, in Proceedings of 1st ADASS, ed. D.M. Worrall, PASP Conference Series, in press.

The Einstein Slew Survey, 1992, M. Elvis, D. Plummer, J. Schachter, and G. Fabbiano), *Ap.J. Suppl.*, in press. (May).

Thirteen New BL Lac Objects Discovered by an Efficient X-ray/Radio/Optical Technique, 1992, J. Schachter, J. Stocke, E. Perlman, M. Elvis, J. Luu, J.P. Huchra, R. Humphreys, R. Remillard, and J. Wellin, *Ap.J. Letters*, in preparation.

Appendix B
The Einstein IPC Slew Survey

THE ASTROPHYSICAL JOURNAL SUPPLEMENT SERIES, 80:257–303, 1992 May

THE *EINSTEIN* SLEW SURVEY

MARTIN ELVIS, DAVID PLUMMER, JONATHAN SCHACHTER, AND G. FABBIANO
Harvard-Smithsonian Center for Astrophysics, 60 Garden Street, Cambridge, MA 02138
Received 1991 May 31; accepted 1991 August 15

ABSTRACT

A catalog of 819 sources detected in the *Einstein* IPC Slew Survey of the X-ray sky is presented; 313 of the sources were not previously known as X-ray sources. Typical count rates are 0.1 IPC count s^{-1}, roughly equivalent to a flux of 3×10^{-12} ergs cm^{-2} s^{-1}. The sources have positional uncertainties of 1'.2 (90% confidence) radius, based on a subset of 452 sources identified with previously known pointlike X-ray sources (i.e. extent less than 3').

Identifications based on a number of existing catalogs of X-ray and optical objects are proposed for 637 of the sources, 78% of the survey, (within a 3' error radius) including 133 identifications of new X-ray sources. A public identification data base for the Slew Survey sources will be maintained at CfA, and contributions to this data base are invited.

Subject headings: BL Lacertae objects: general — catalogs — quasars: general — X-rays: general — X-rays: stars — surveys

1. INTRODUCTION

Sky surveys have always played a major role in astronomy. In the present era in astronomy, we are rapidly accumulating new sky surveys across the whole spectrum. In particular, the advent of imaging telescopes has made X-ray surveys possible that are comparable in sensitivity to those at other wavelengths. The *Einstein Observatory* (*HEAO 2;* Giacconi et al. 1979a) was the first imaging X-ray astronomy satellite, and many papers have reported on surveys of restricted regions of the sky made using pointed observations taken with the Imaging Proportional Counter (IPC, Gorenstein, Harnden, & Fabricant 1981) on board *Einstein.* (The "Medium Survey," e.g. Gioia et al. 1990; the "Deep Survey," e.g. Primini et al. 1991; Table 1). As a result we are in the peculiar position in the soft X-ray band covered by *Einstein* (~0.2–3.5 keV), of knowing more about the faint sources than about the bright sources. The limited sky coverage of the Medium and Deep Surveys results in their having effective *upper* limits to their sensitivity as well as lower limits since bright sources are rare on the sky (Fig. 1; Table 1). This limitation complicates log N–log S and source evolution studies (Fig. 1) since for bright source counts we have to refer to the hard X-ray surveys, usually to the Piccinotti et al. (1982) *HEAO* A-2 survey which covered the 2–10 keV energy band. For example, Schmidt (1990) has emphasized how the Piccinotti et al. and the Medium Survey source counts are in contradiction for AGNs and clusters of galaxies (although evolution may explain these problems; Gioia et al. 1990). What is needed is a log N–log S with the same instrument over the whole X-ray flux range. A survey of the bright sources in the soft X-ray range is thus important, and only a survey covering most of the sky can find the relatively rare bright sources. A survey using the same instrument as used for the *Einstein* Medium and Deep Surveys would greatly simplify interpretation. Samples of bright sources selected uniformly by their X-ray properties are also valuable for follow-up detailed work with other instruments, e.g., *ROSAT, ASTRO-D.*

We have constructed a survey of the sky with the *Einstein* IPC using the "Slew" data taken when the satellite was moving ("slewing") from one target to the next. By co-adding all these slews, we have achieved a useful sensitivity over a large solid angle, some 50% of the sky. The main properties of the *Einstein* IPC Slew Survey are given in Table 2. Because it was not clear that this survey could be constructed successfully, it was not attempted earlier. The resources needed to process the data were large, making the effort too large for the uncertain payoff. Computer processing power and on-line storage capacity have grown by orders of magnitude in the last few years so that it is now possible for projects of this size to be carried out experimentally by a small team relatively quickly, and thus at low risk. This paper describes the *Einstein* Slew Survey and presents the resulting catalog of X-ray sources.

The complete information content of the Slew Survey is more than the source catalog. A CD-ROM issued by SAO (Plummer et al. 1991) contains the full data on the individual photons in the Slew Survey and the aspect solution file for each slew. This enables a user to derive fluxes and upper limits for any position on the sky covered by the Slew Survey. The CD-ROM also contains more information on the source detections (see "lists/unix/srcs.lis," "lists/vms/srcs.lis," etc.). The CD-ROM is available from SAO (send requests by e-mail to the *Einstein* Data Products Office, edpo@cfa.harvard.edu), or via the *Einstein* On-Line Information System, *einline* (Harris et al. 1991).

2. DATA SELECTION

For the survey we selected all the data taken while the *Einstein* satellite was slewing with the IPC at the focus ("SLEW" mode data—hence the survey name). Only the IPC data is valuable for this survey. Table 3 compares a "figure of merit" for this type of work for the four focal plane instruments on *Einstein.* The combination of wide field of view, high quantum efficiency, and large fraction of time in the focal plane make

TABLE 1

Einstein SURVEYS

Name	Area[a]	f_{lim}[b] (upper[c])	f_{lim}[b] (lower)	Number of Sources	References
Deep	2.3	$\sim 7 \times 10^{-14}$	$\sim 4 \times 10^{-14}$	25	Primini et al. 1991
Medium	780	$\sim 5 \times 10^{-12}$	$\sim 2 \times 10^{-13}$	835	Gioia et al. 1990
Slew	35,060[d]	$\sim 1 \times 10^{-9}$	$\sim 3 \times 10^{-12}$	819	This paper

[a] Square degrees (deg^2).
[b] Units: ergs cm^{-2} s^{-1}.
[c] Defined as the flux below which 90% of the sources lie.
[d] Defined by the minimum exposure (1.0 s) at which a source was detected.

the IPC over 100 times more valuable than the next most useful instrument, the HRI. Only slews for which IPC targets lay at each end were used (i.e., no instrument changes during the slew). Also only slews in which data dropouts were small (<1 major frame; 40.96 s) were included. This gave 2799 useful slews with a total instrument on-time of 10^6 s of data, and 2.6×10^6 photons.

All photon events were accepted: unlike the processing of the pointed data, no Sun/Earth angle or pulse height event (PHA) screening was made. Screening proved unnecessary for most of the survey since its purpose is to reduce the background, which is negligible for the short exposures in the Slew Survey. In processing we omitted photons from regions near the IPC "ribs" (features produced by the window support structure of the IPC; Harnden et al. 1984), and near to the edges of the detector. Edge photons are not processed in the standard, pointed, data either.

Figure 2 shows the exposure map for the Slew Survey. The concentration of exposure near the ecliptic poles is clear. This concentration occurs for all Earth-orbiting satellites with fixed solar panels since one axis must point toward the Sun and the satellite lies in the ecliptic plane. The spacecraft is then only free to rotate along arcs of ecliptic longitude. There is lower than average exposure in parts of the Galactic plane, because the IPC was turned off if it was expected to slew across the brightest few sources, and these are concentrated in the Galactic plane. This was a protection against detector gas breakdown that could be induced by too many counts being detected in a small region. The Slew Survey thus has zero exposure on the Crab Nebula. This policy was not always successfully followed and we do have exposure on GX 5-1, which was fortunate for our purposes since it allowed a "proof-of-concept" at an early stage (Fig. 3).

Figure 4 is an exposure histogram showing the fraction of the sky covered to a given exposure depth. From this, and the log N–log S of the Medium Survey (Gioia et al. 1990), one can predict that the Slew Survey will contain of order 1000 sources, which in fact is a quite accurate prediction.

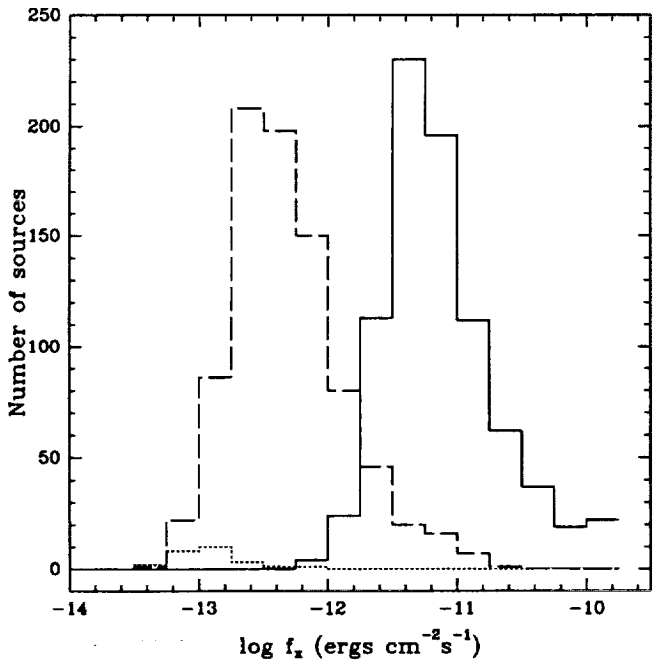

FIG. 1.—Distribution of source fluxes from the Slew Survey (*solid line*) compared with those of the extended Medium Survey (*dashed line;* Gioia et al. 1990) and the Deep Survey (*dotted line;* Primini et al. 1991)

3. ASPECT SOLUTION

The key to producing a Slew Survey is to solve for the pointing position of the satellite with time as it slews across the sky (the "aspect" or "aspect solution"). To determine the *Einstein* aspect during slews it was necessary to use the on-board gyro-

TABLE 2

Einstein IPC SLEW SURVEY PROPERTIES

Property	Value
Observing time	0.99×10^6 s
Effective exposure[a]	0.47×10^6 s
Total number of photons	2.6×10^6
Mean background	~0.7 photons per source box[b]
Minimum number of photons per source (for mean background)	5 ($P_{mand} \sim 1 \times 10^{-6}$)
Mean exposure	12 s
Mean limiting count rate	0.45 counts s^{-1}
Mean limiting flux[c]	14×10^{-12} ergs cm^{-2} s^{-1}
Number of sources	1075
Identifications[d]	Stars: $m_V < 7$ AGN: $m_V < 17$

[a] Including corrections for vignetting and excluding the "ribs" regions.
[b] 6′ × 6′ box.
[c] 0.2–4.0 keV, for a conversion factor of 3.26×10^{-11} ergs per count appropriate for a power-law energy index of 0.5 and a Galactic N_H of 2.0×10^{20} atoms cm^{-2} as used in the *Einstein* Medium Survey (Gioia et al. 1984)
[d] Based on Medium Survey nomogram (Maccacaro et al. 1988).

TABLE 3

RELATIVE VALUE OF *Einstein* INSTRUMENTS FOR SLEW SURVEYING

Instrument	(FOV × % time × QE)[a]	Figure of Merit
IPC	1800 × ~0.5 × 0.7	630
HRI	216 × ~0.2 × 0.1	4.3
SSS	9 × ~0.15 × 0.9	1.2
FPCS	≤90 × ~0.15 × 0.01	0.14

[a] FOV = field of view in square arcminutes; % time = fraction of time in focal plane; QE = quantum efficiency.

scope rate data ("gyro data"). The on-board star trackers, which are the primary means of providing the aspect solution for the pointed observations, could not be used since the satellite moved some 5′–6′ during a single readout interval (1 minor frame = 0.32 s, the standard minimum read-out interval for a NASA mission), while the star trackers could only follow stars at rates of $<2' s^{-1}$ (Koch et al. 1978).

At any time during the mission, three of the six gyros in the gyro assembly were operating. Each gyro yields a spin rate every minor frame, and the gyros are oriented so that any set of three will give sufficient information to determine rotations about the three spacecraft axes. The existing calibration of the gyro rates to rotation rates was designed only to be accurate enough to bring the spacecraft to a direction where the star trackers, with their ~2° field of view, could acquire a field. Accurate pointing depended on the star trackers.

To use the gyros alone for deriving a Slew aspect required that the existing calibration be checked and modified to give solutions accurate at the arcminute level anywhere during a slew. Two things made this possible: (1) the level of accuracy required is of order 1′—similar to the IPC point spread function—which is some 30 times less demanding than for pointed observations; and (2) enough well-positioned X-ray sources are known which are bright enough to be detected in a single slew. These sources give us an internal check on the quality of our aspect solution on several hundred individual slews, thus allowing a reliable Slew aspect solution to be developed.

Figure 5 shows the initial offsets between the slew-derived position and the accurate positions for known X-ray sources in the *HEAO 1* A-3 (Remillard et al. 1991) and pointed IPC catalogs (2E; Harris et al. 1991) detected in individual slews. The coordinates are oriented along and perpendicular to the slew direction. Several features can be seen: There is a concentration of points near the origin, implying that a good fraction of the time the gyro system does give good aspect during slews; this concentration is however offset along the slew direction by ~3′–5′; there is a "tail" of poorly positioned sources along the slew direction; and there is a "halo" of poorly positioned sources extending to large distances from the central cluster near the origin.

The offset of the central cluster is due to an ambiguity in the documentation of the timing information. We determined empirically that the aspect data and photon data sent in a single data packet (minor frame) refer to different times: the photon data to the current minor frame, and the aspect data to the preceding minor frame. This is negligible in pointed mode but in Slew mode leads to the observed offset.

The "tail" of poor aspect slews we found to be due to the

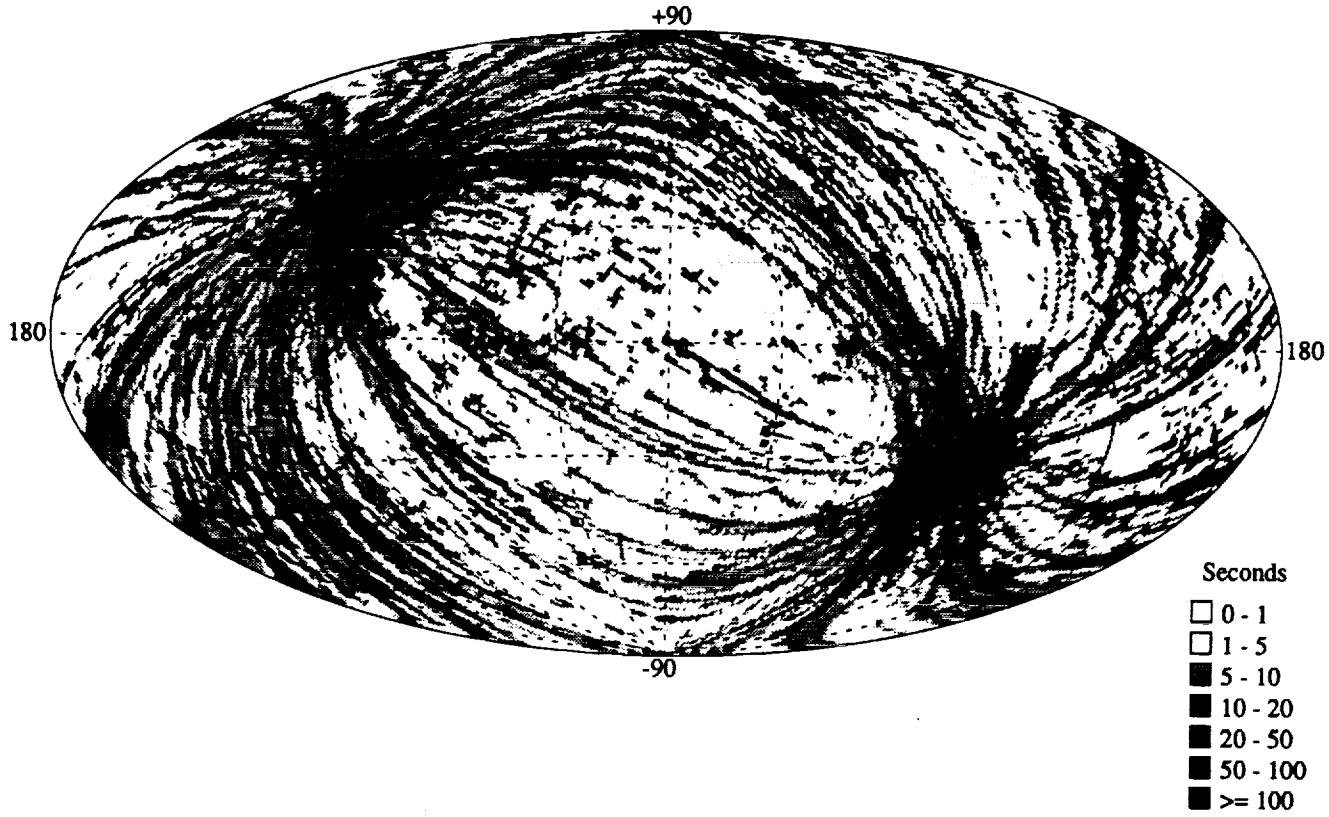

FIG. 2.—Exposure map for the Slew Survey in Galactic coordinates. Slew paths are readily seen going in great circles between the ecliptic poles.

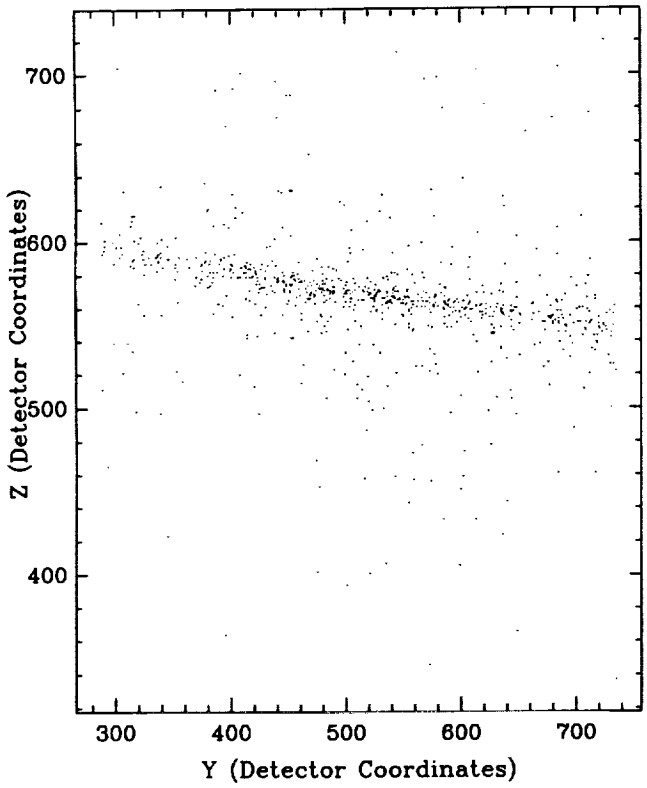

FIG. 3a

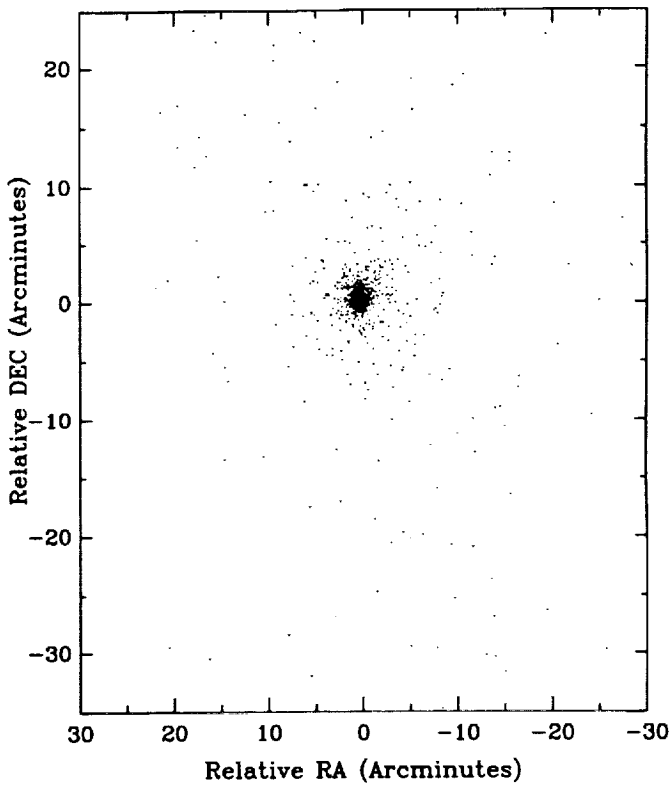

FIG. 3b

FIG. 3.—GX 5-1 (1ES 1758-250) seen before (*a*) and after (*b*) Slew aspect was applied. Applying the Slew aspect correction, which takes into account the motion of the satellite, produces a well-defined image (*b*). The background over the whole 1° × 1° field shown is 65 counts for an exposure of 14 s.

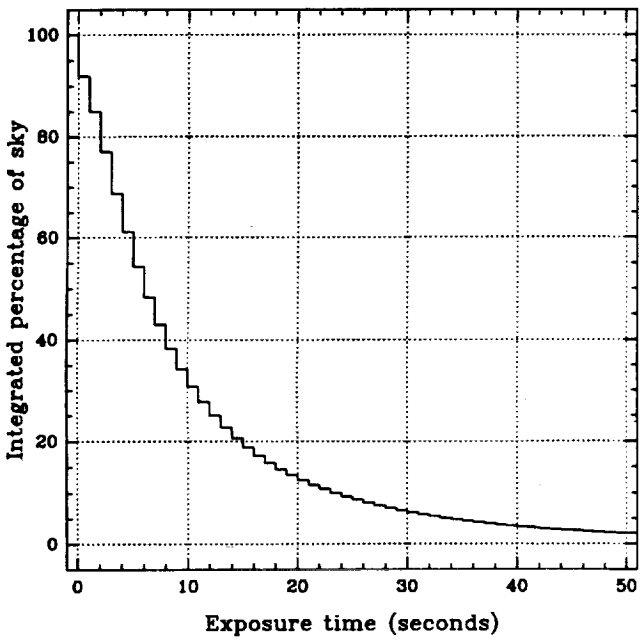

FIG. 4.—Fraction of the sky to a given exposure in the Slew Survey

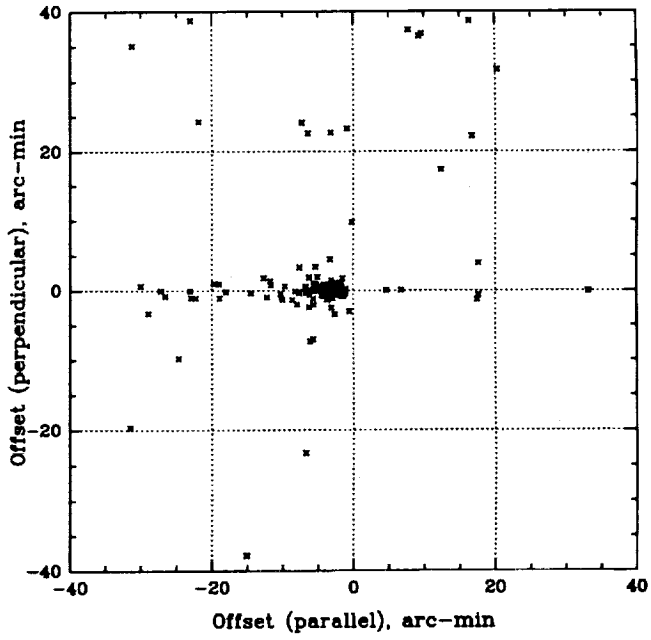

FIG. 5.—Initial offsets in arcminutes between Slew-derived and accurate X-ray source positions for 172 known X-ray sources (Remillard et al. 1991; 2E Catalog) detected in individual slews.

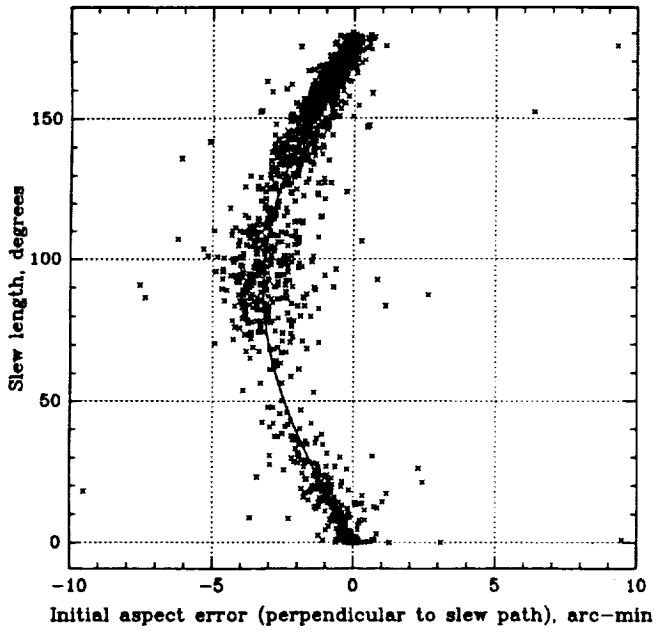

FIG. 6*a*

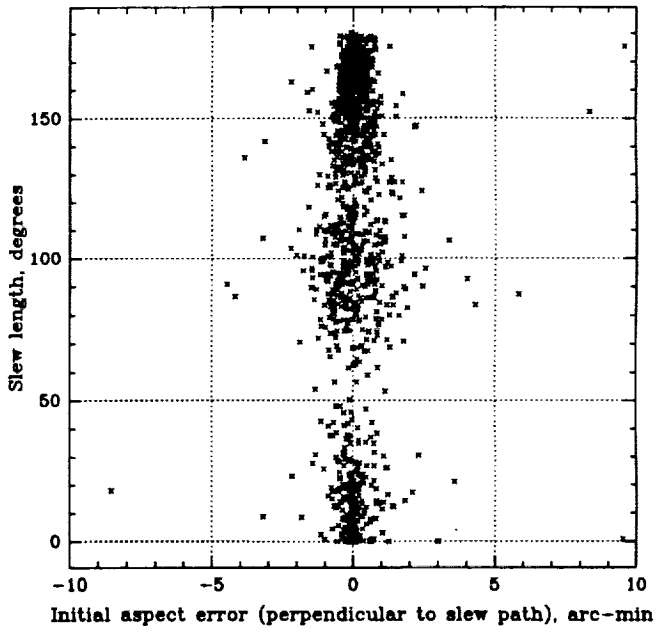

FIG. 6*b*

FIG. 6.—(*a*) Offset in arcminutes (perpendicular to slew direction) between the Slew-calculated position at the end of the slew and the accurate position from the pointed, star tracker, solution vs. slew length in degrees. The plot is for the data before the application of the correction made by rotating the assumed plane of the gyro assembly and is for gyro combination B. The solid curve shows the size of the correction. (*b*) Offsets as in (*a*) after gyro orientation corrections.

quality of the pointed aspect at the start of the slew. The 'MAP-MODE' star tracker aspect (where the trackers send back the positions of all stars in the field) is not sufficiently reliable (e.g., Harris, Stern, & Biretta 1990), and it is essential to go back into the pointed observation until "LOCKED" star tracker aspect is found. (In LOCKED aspect the tracker records only the position of the chosen guide star.) Errors of a few arcseconds in the starting position extrapolate to large errors when the spacecraft slews through tens of degrees.

The cause of much of the spread seen in Figure 5 is seen in Figure 6*a*. This shows the offset perpendicular to the slew direction as a function of position along the slew path. The clear "bow" shape arises naturally from a displacement of the gyro assembly from its assumed orientation with respect to the spacecraft axes. This offset can be illustrated by imagining a vector rotating 180° within a given plane. This represents the actual rotation of the satellite. Now consider a second vector parallel to the first vector at its original position. Rotate the second vector within a second plane tilted slightly from the first plane such that they intersect along the line of the vectors' original direction. The second vector represents the rotation of the satellite as reported by the displaced gyros. The two vectors will be coincident at the start and end of the 180° rotation but will be offset in between, reaching a maximum at 90°. The offset at 90° exactly equals the relative offset of the two planes, and therefore the offset of the gyro assembly. By rotating the gyro assembly axes according to the maximum observed offset, the "bow" distortions in the derived positions can be virtually eliminated (Fig. 6*b*). A separate set of corrections is needed for each set of gyros which indicates that the rotations are not of the gyro assembly as a whole but of the individual gyros mounted in the assembly. Errors in the assumed gyro orientations of a few arcminutes are entirely negligible for pointed observations. The rotations for each set of gyros were fixed and are given in Table 4.

In addition the conversion from gyro spin rate to angular rotation is only calibrated to a level sufficient for pointed operation. In the Slew Survey this conversion is critical and leads to errors when extrapolating the gyro solution over large slew angles. We calculate the initial offset between the known, star tracker–derived, pointing position and the gyro-extrapolated position at the end of the each slew. Each offset is measured as a small difference, δ, in R.A., decl., and Roll angle. Since we measure three δ's and can adjust the scale factors for three gyros, there is sufficient information to force this offset to be zero for each slew. The corrections needed are of order 3′. We used the following procedure: using the initial offsets we guess an appropriate trial scale factor for each gyro in turn. This leads to a change in the three δ's for each of the three gyros. The resulting 3×3 matrix forms a set of simultaneous equations

TABLE 4

OFFSETS FOR EACH SET OF GYROS

Gyro Combination[a]	Gyros in Use	ΔX	ΔY
A	1, 2, 3	0.0	0.0
B	2, 3, 5	3.2	0.0
C	2, 3, 4	4.25	1.25
D	2, 4, 6	6.0	0.0
E	3, 5, 6	6.0	1.75
G	3, 4, 6	4.75	1.75

[a] Gyro combination F did not contribute usable slews to the survey.

which can be solved to give scale factors for each gyro that will exactly set the δ's to zero. This procedure produces a sufficiently accurate aspect solution, as determined, post facto by the identification process (see § 6). The scale factors, however, are mostly not systematic. This suggests that there is a residual aspect error that could, if corrected, improve the Slew Survey aspect. The solution may lie in treating the orientation of each gyro separately instead of "rotating" the whole gyro assembly.

Finally, slews having scale factor corrections larger than 2% were found to introduce greater errors in position. In very short slews, for example, the aspect became so bad that sources were distorted into smears that were not detected at all. We simply excluded any slews for which we derived scale factor corrections larger than 2% (8.6% of the total), leaving the total of 2799 useful slews.

The offsets of the Slew positions from the accurate positions of known X-ray sources in the *HEAO 1* A-3 catalog (Remillard et al. 1991) and the Bright Star Catalog (Hoffleit & Jaschek 1982) for the final set of corrected aspect slews gave the offset diagram seen in Figure 7*a*. The true reliability of the Slew Survey aspect solution is better than is immediately apparent from Figure 7*a* since false identifications produce a significant "background" at radii > 3′. Figure 7*b* shows the distribution of offsets from a false set of Slew Survey sources obtained by shifting all the Slew Survey sources by 1° in R.A. Figure 7*c* shows a plot of the average background due to false identifications plotted against the radial histogram of Figure 7*a*. Subtracting this background rate implies a 90% confidence radius of order an arcminute for the Slew Survey aspect. Figure 7*d* shows an integrated histogram with the background subtracted which allows the derivation of confidence radii of the reader's choice. We derive a 90% confidence radius of 1.′2 and a 95% radius of 2′ from Figure 7*d*.

4. SOURCE DETECTION

The short exposures of the Slew Survey over most of the sky lead to an expectation value of 0.1 photons in a standard 2.′4 square IPC detection cell. Since we expect ~1000 sources over the sky, approximately 99.996% of the 2.58×10^7 detection cells would be empty of sources. The "sliding box" detection algorithm used for the pointed data (Harnden et al. 1984) is thus highly inefficient for the slew survey.

4.1. *Percolation Algorithm*

Instead, we have developed a "percolation" algorithm that tests each photon for the presence of unusual numbers of near neighbors. Since there are only $\sim 3 \times 10^6$ photons in the survey this takes a factor of ~50 fewer operations than the sliding box method. The percolation algorithm is exactly analogous to the method described by Huchra & Geller (1984) for the selection of groups of galaxies from the CfA Redshift Survey (bright galaxies, like Slew Survey photons, are sparsely distributed on the sky) except that the Slew Survey contains only the two dimensions of R.A. and decl., and has no equivalent of the redshift dimension. The Slew Survey percolation algorithm loops through every photon in the field and searches for other photons within the percolation length. If another photon is found, it is added to the group and subsequently searched for neighbors. The process continues until no more photons lie within a percolation length. Figure 8 describes the process in a flowchart. These groups constitute our candidate sources for the Slew Survey. This algorithm has the advantage of not being biased against extended sources as is a sliding box (by subtracting a source-enhanced background). It does, of course, have a surface brightness limit when the mean distance between source photons exceeds the percolation length. A percolation length of 2′ (~ double the FWHM of the IPC point spread function) produced good results except in regions of high exposure where the background began to become important (see below). All groups detected by the percolation algorithm with fewer than three photons were automatically rejected.

4.2. *Exposure Map*

It was then necessary to determine which photon groupings constituted significant sources. This significance is highly dependent on the local background and the distribution of exposure time around a source. Figure 9 illustrates some of the difficulties. The contours are isoexposure levels. Each field covers 30′ × 30′, and the exposure map has a resolution of 1′. Detailed structure on the few arcminute scale is evident. Because of the random nature of the slew paths, there is no predictable structure to the exposure maps. Figure 9 also shows the individual photons in the regions. Each frame is centered on a Slew Survey source which illustrates that the size of the point-spread function is comparable with the exposure map structure. It is clear that the detailed exposure distribution in the surrounding region must be calculated in order to compare the background from this region with the number of counts detected in the "source" region defined by the percolation detect algorithm.

The exposure maps were generated from the aspect solution and the timing gap records (".tgr" files) for each slew ("HUT"). A template of the relative exposure within the 1° IPC field of view was made including corrections for vignetting and ribs at the full 8″ resolution of the detector. The vignetting is a radial function which reaches 46% at the midpoint of the side of the IPC; the regions affected by the ribs (which are 4′ wide and roughly 20′ from the center, parallel to the sides; see Harnden et al. 1984 for details) are set to zero exposure. This map was then moved across the sky at the rate determined by the aspect solution and effective exposure time assigned to bins 1 arcmin^2 on the sky accordingly. For convenience, the sky was divided into a set of 6.°5 square bins on 6° centers. No exposure was accumulated during times when the detector was off, or data was not received for other reasons (e.g., telemetry dropout).

4.3. *Source Probabilities*

The Poisson probability of a collection of "source" photons arising by chance inside a source region centered on the percolation centroid can be calculated given a local background. Source counts were derived by taking all counts within a 6′ on a side box centered on the centroid given by the percolation algorithm. Background was estimated from two "square annuli" of inner side 6′, outer side 12′, and inner side 12′, outer side 30′ (background regions 1 and 2). The mean exposure times in the source and the background regions were derived by averaging the 1′ bins of the exposure map. In the case where there were no background counts, we calculated the probabili-

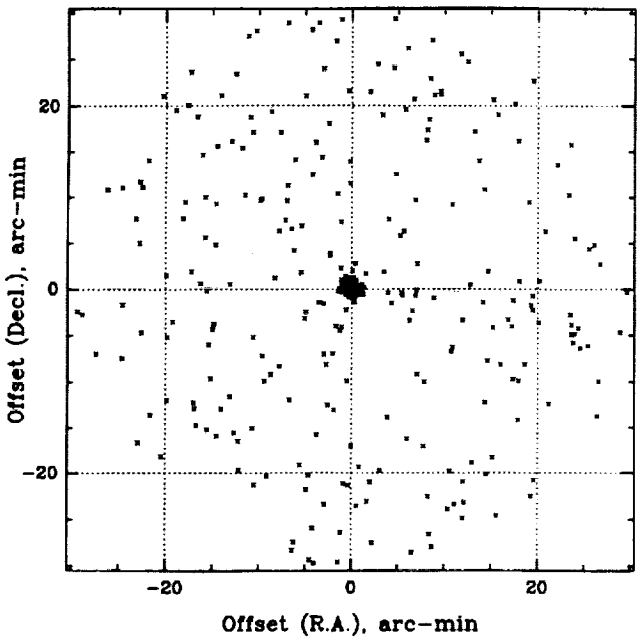

FIG. 7*a*

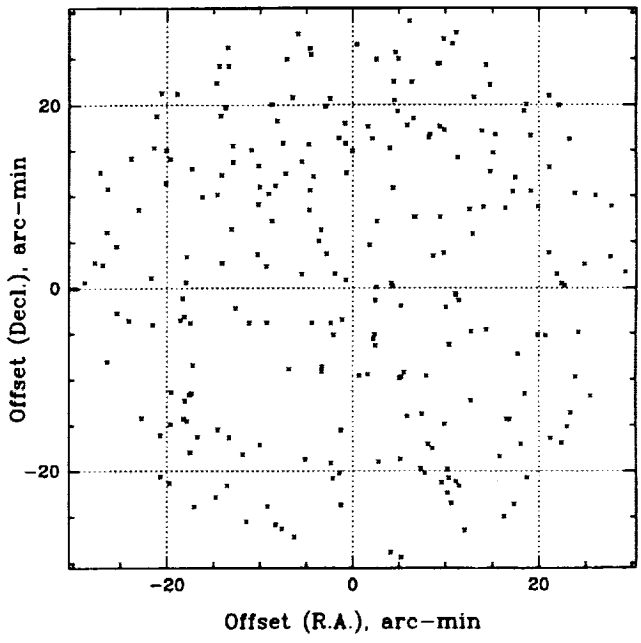

FIG. 7*b*

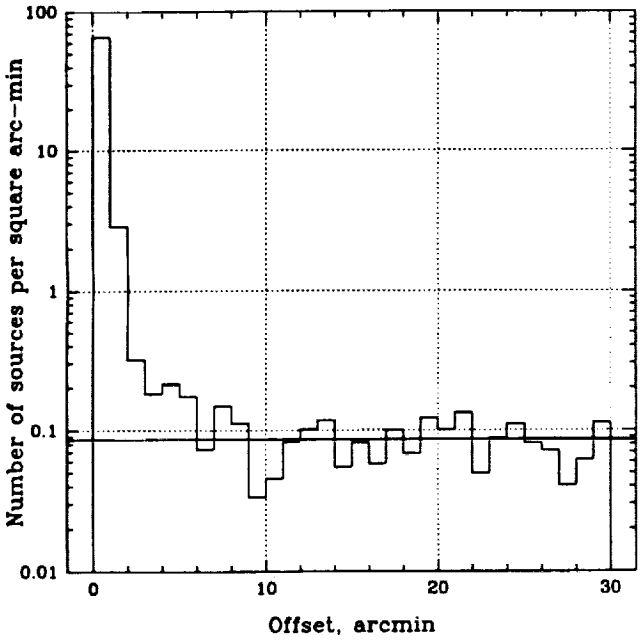

FIG. 7*c*

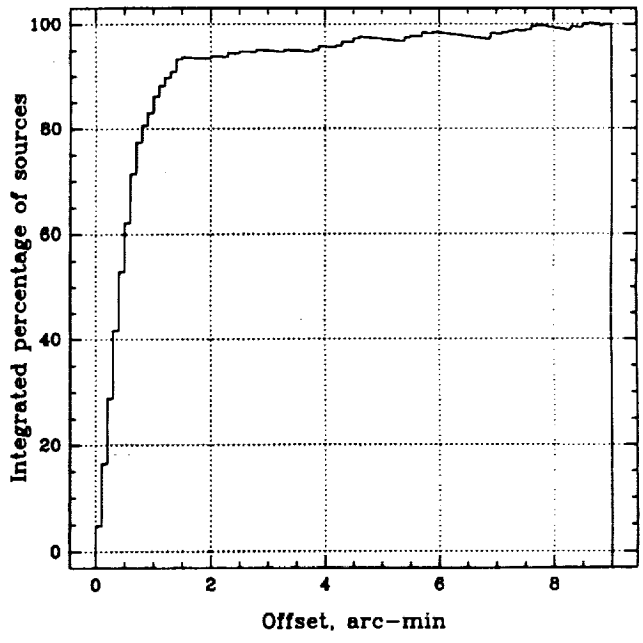

FIG. 7*d*

FIG. 7.—(*a*) Offsets of Slew source positions from Bright Star Catalog identifications, in R.A. and decl., after all aspect corrections are applied. (*b*) Offsets as in (*a*) but for an artificial set of Slew Survey sources created by shifting the real Slew Survey source by 1° in R.A.. This shows the background rate of identifications due to accidental matches of position. (*c*) Radial version of (*a*) with a heavy line marking the false identification background rate from (*b*). (*d*) Integrated histogram of (*a*) with the background from (*b*) subtracted.

ties by assuming one background count. Otherwise, we used background region 2 for background subtraction. The probability, $P_{\rm rand}$, was determined for each candidate source. (On the CD-ROM, $P_{\rm rand}$ is called Prob2; Prob1, the same probability using the background region 1, was also calculated and is listed on the CD-ROM.) The values of $P_{\rm rand}$ order the candidate sources according to their likely reality (small probabilities being more likely real). $P_{\rm rand}$ does not by itself tell us which sources to accept. For this we must define a threshold value of $P_{\rm rand}$.

4.4. *Estimating the False Source Rate*

4.4.1. *Relation between Probability Thresholds and Photon Number*

The false source rate is a function of the threshold probability and the number of counts in a source. We can estimate the

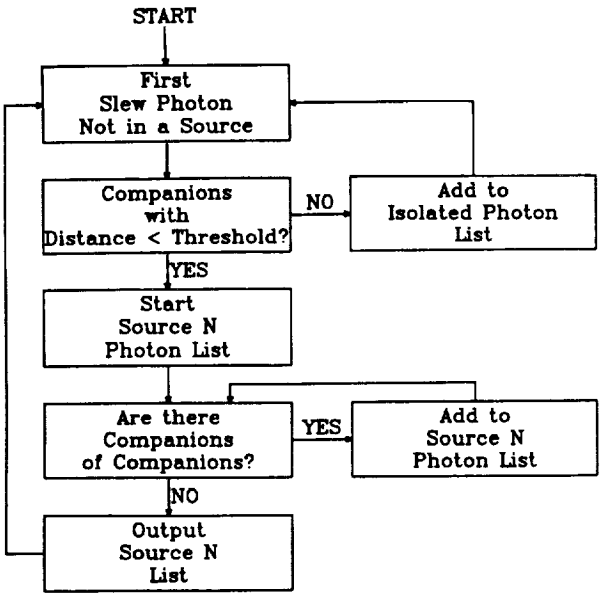

FIG. 8.—Percolation algorithm flowchart

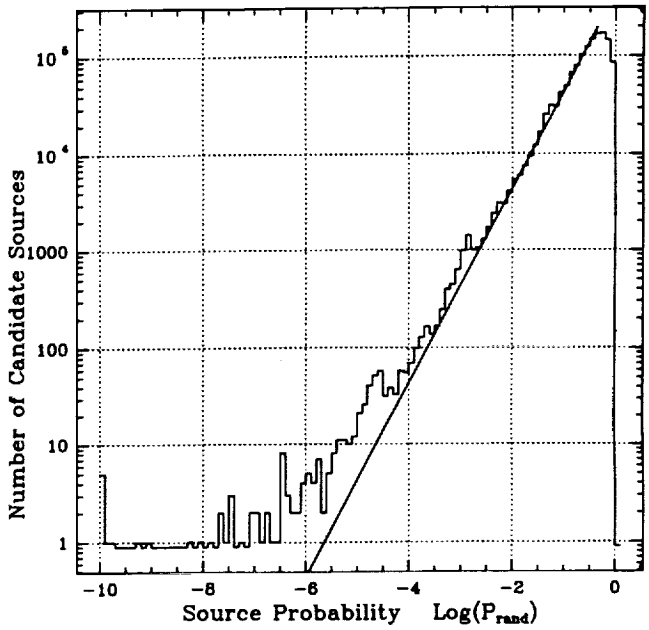

FIG. 10.—Number of candidate sources with 1 photon detected by the percolation algorithm vs. Poisson probability, P_{rand}. The solid line shows the number expected assuming there are no real sources in the data. This is a reasonable approximation for three decades of P_{rand}.

fraction of false sources from global properties of the Slew Survey. For example, Figure 10 shows a histogram of the number of single photon candidates (sources most likely to be false) as a function of P_{rand}. The histogram peaks at a probability of 0.5 where the number of "source" photons equals the number of background photons, which is the most likely case. (Above a probability of 0.5 our sample will necessarily always be incomplete because the percolation algorithm cannot include candidates with zero counts in the source box.) If the probability calculation is appropriate to the data, then we should find that the number of candidate sources drops linearly with the probability. We show a straight line of slope 1 in Figure 10 which was normalized by setting the area under the line equal to the area under the histogram up to a probability of 0.5. This normalization assures that the line intersects the histogram at $P_{rand} \sim 0.5$. Since the line fits the data well for about four decades in probability, we conclude that the Poisson probability is a good description of the data. This is a conservative approach because we are assuming that the percentage of "true" sources within the total sample is essentially zero, whereas some single-photon "sources" will indeed be real sources.

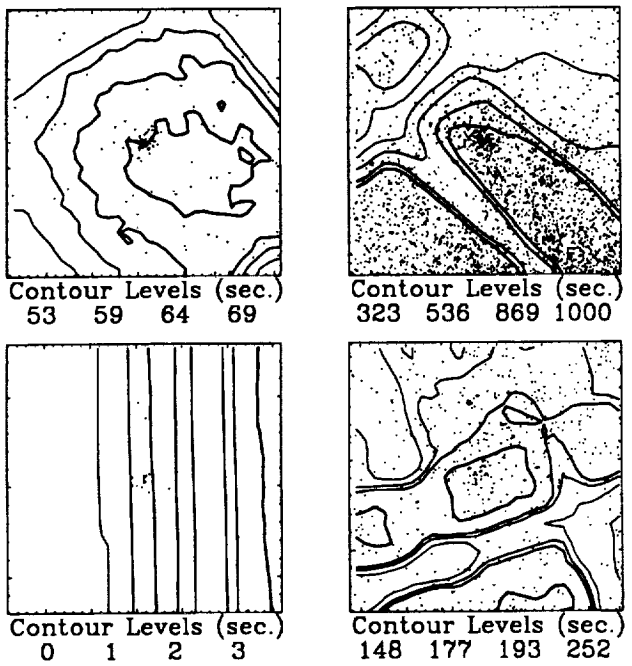

FIG. 9.—Four typical regions of the Slew Survey exposure map. Each region is 30′ on a side, the size of background region 2, and is centered on a Slew source. The Slew Survey names are, clockwise from the upper left, 1ES 1340-611, 1ES 2031-411, 1ES 1142+198, and 1ES 1746-370.

We generated diagrams similar to Figure 10 for cases of two to 10 source counts, since in our experience this range of counts have appreciable (10%–20%) contamination by false sources. The *fraction of false sources accepted* for a given threshold probability (P_{th}) is the normalized area lying below the straight line and with $P_{rand} \leq P_{th}$. Similarly, the *fraction of real sources rejected* is the area above the straight line and with $P_{rand} > P_{th}$. Figure 11*a* shows the two fractions for $\log(P_{rand}) = -3.95$, and Figure 11*b* shows them for $\log(P_{rand}) = -5$. For $\geq$ 3 photons, the curves change only slightly if $\log(P_{rand})$ is reduced to -6. We find that for a given P_{rand} value, the false source rate is a strong function of the number of photons for $\leq$ 8 photons. Therefore, it is misleading to quote merely an average false source rate (integrated over all numbers of source counts), given the large number of few-count sources. We take the more conservative approach of demanding a maximum false source rate for each number of counts individually.

We chose a false source rate of 2% for the Slew Survey, to guarantee high reliability of the source list. To determine the corresponding threshold probability as a function of the number of counts, we determined, for each value of probability (in 0.25 $\log P_{rand}$ steps) in the range $-6 < \log(P_{rand}) < -3.95$, the

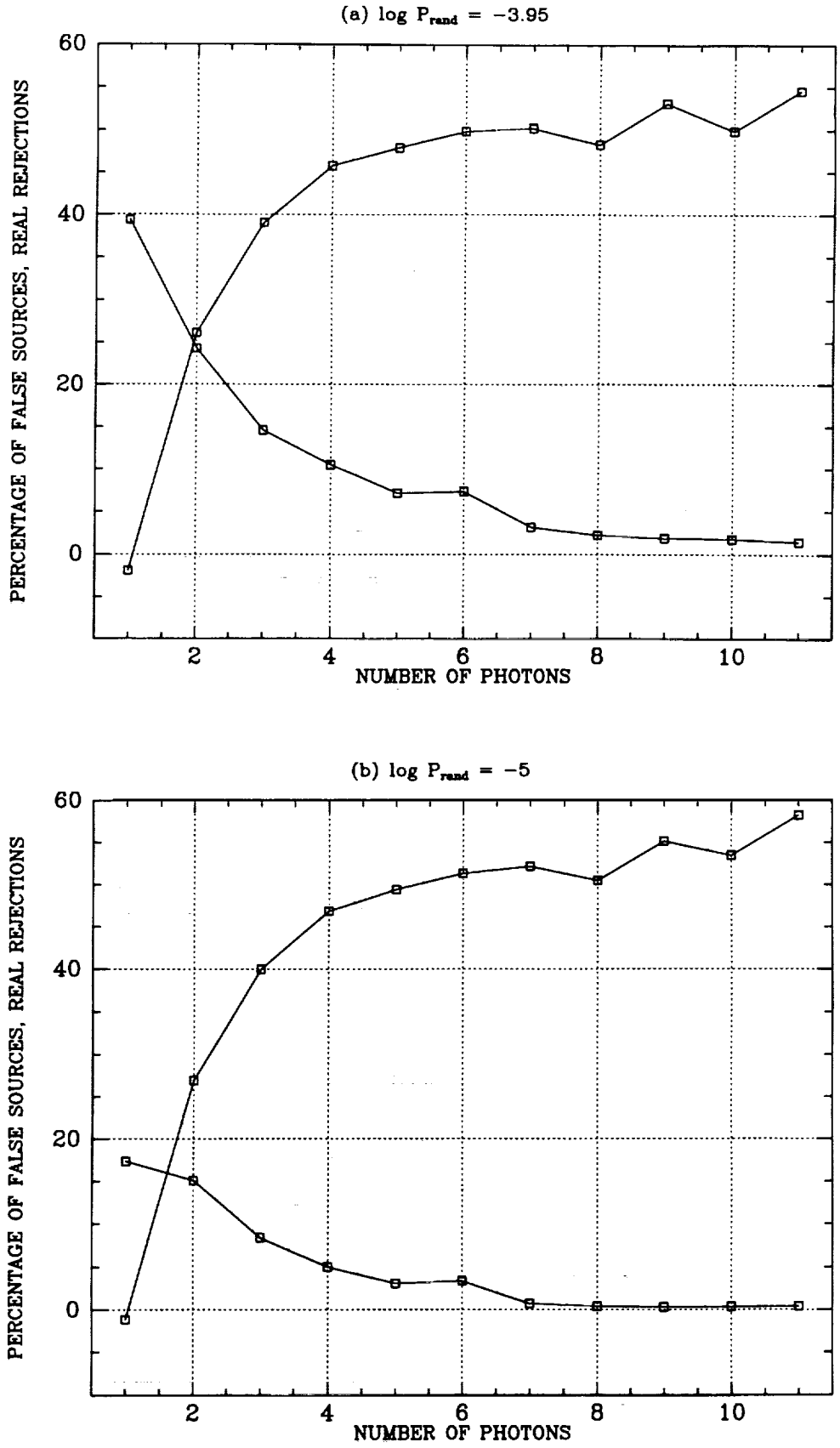

FIG. 11.—The percentage of false Slew Survey sources accepted (*lower curve*) and percentage of real sources rejected (*upper curve*) are shown as a function of the number of counts for two different probability thresholds. We show the cases of log (P_{rand}) = −3.95 (*a*) and log (P_{rand}) = −5 (*b*).

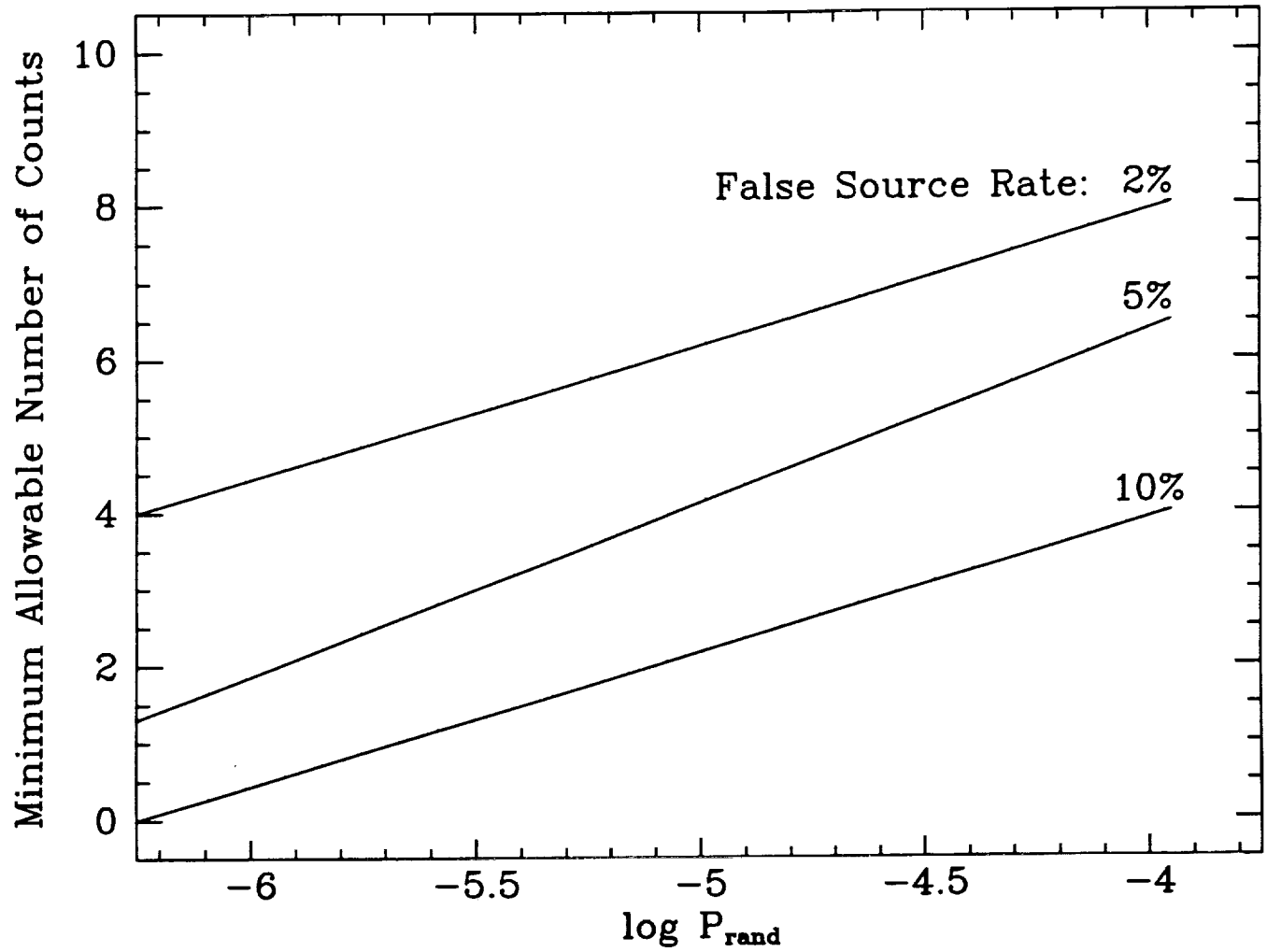

FIG. 12.—The dependence of the minimum allowable number of counts on log (P_{rand}) is shown for three different false source rates: 2%, 5%, and 10%. A false source rate of 2% and log (P_{rand}) ≤ −3.95 were adopted for the Slew Survey catalog.

minimum allowable number of counts. The minimum number, for example at log (P_{rand}) = −5, is six counts for 2% false sources. For higher false source rates, lower photon thresholds apply: four for 5%, and two for 10%. In other words, for ≤ 2% false sources and log (P_{rand}) > −5, all detected sources with five counts or fewer must be rejected. In a plot of log (P_{rand}) versus number of counts, a given false source rate is well approximated by a straight line interpolated from the integer values. We show the 2%, 5%, and 10% lines in Figure 12; other values of false source rate can be estimated from the figure.

4.4.2. *A Global Probability Threshold*

We also performed an independent test to establish a global threshold probability for real sources. We made identifications of all the candidates with ≥3 photons against two catalogs of known X-ray sources that have positions known to better than 1′—the *Einstein* IPC Catalog (2E; Harris et al. 1991) and the *HEAO* A-3 Catalog (Remillard et al. 1991). Figure 13 shows the offset of the Slew position from the known position in arcminutes for sources matched in this way against the probability of the source being a chance congregation of photons, P_{rand}. Extended sources (clusters of galaxies, supernova remnants, and all other IPC sources with "extent parameter" > 3′) were excluded from this comparison.

It is clear from Figure 13 that for small probabilities ($P_{rand} < 10^{-6}$) almost all the sources must be real since they are clustered at offsets of order the aspect accuracy derived from individual slews. Similarly at large probabilities ($P_{rand} > 10^{-3}$), there are a great number of false sources since they are distributed nearly uniformly in offset. Based on this diagram, we imposed an additional log (P_{rand}) = −3.95 threshold, regardless of the number of photons in the source. Our threshold P_{rand} for accepting a candidate source as real is clearly at a level where the fraction of identified sources lying within 2′ of the optical position begins to decrease rapidly (Fig. 14).

The criteria of 2% false sources and log (P_{rand}) ≤ −3.95 yields a list of 819 prospective sources with 16 false sources expected to be included.[1] If the statistics were Gaussian, the probability

[1] The source list on the CD-ROM was created with the condition log (P_{rand}) ≤ −3.95, but without the 2% false source cut. As a result, many more sources (1067) were reported to be real. Only those sources with log (P_{rand}) ≤ −3.95 and lying above the 2% curve in Fig. 12 are accepted for our analysis here, giving a final number of 819.

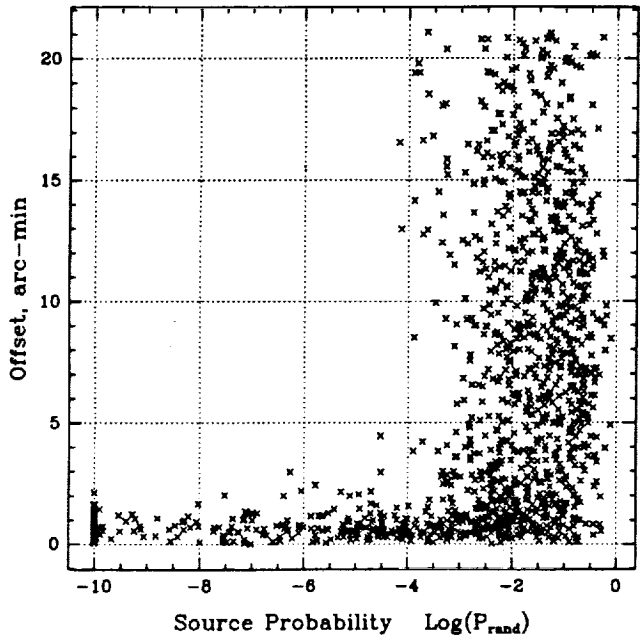

FIG. 13.—Offset in arcminutes between the Slew source positions and the accurate positions of known X-ray sources (for objects in Remillard et al. 1991 and nonextended objects in the 2E catalog) vs. probability of a source arising by chance.

constraint would correspond to a 3.3 σ threshold. However, as demonstrated in the foregoing analysis, the highly asymmetric nature of the Poisson distribution for such small numbers of counts makes the detections more significant that common experience with 3 σ results would suggest.

The estimate of threshold P_{rand} is based solely on known sources (i.e., large numbers of counts) and is therefore conservative. Sources on the 2% curve in Figure 12 and with log $P_{rand} > -3.95$ may in fact be real. Some of these sources may be extractable by searching the original Slew Survey data at a predefined set of positions such as those of an optical catalog. This is possible given the software and data on the CD-ROM (Plummer et al. 1991). The source list (see § 6) gives the values of P_{rand} for each source so that readers may set more stringent thresholds if they wish.

As a final check, two of us (M. E. and J. S.) visually inspected each of the proposed sources for cases of dubious detections. A total of 10 sources were eliminated in this manner. Of these eight were rejected because photons from the outer fringes of a bright source caused a spurious second detection; two were rejected because the exposure gradients across the region were extreme and an isolated region of high exposure led to a "source." A reliability index (1, 2, 3; 3 best) was compiled based on the visual inspection (see § 6).

In Figure 14, the fraction of objects within 2′ of the correct position is plotted against the probability of a source arising by chance. Note that the figure contains an excess of sources near to zero offset even at $P_{rand} > 10^{-3}$, which is consistent with Figure 12. This again implies that other real sources exist in the data. Searches of the Slew Survey data base at given positions, defined a priori by, e.g., an optical catalog may give significant detections even if no source appears in this catalog. (Since the number of trials is small, a lower significance threshold can be used.)

4.5. *High Background and Extended Sources*

As noted above, in regions of high exposure the percolation algorithm did not produce sensible results because the mean distance between background photons became similar to the

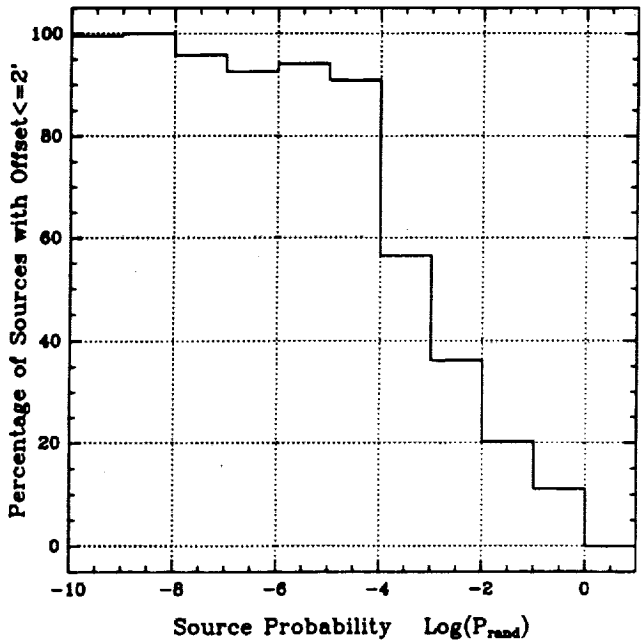

FIG. 14.—Fraction of Slew sources lying within 2′ of the position of a known X-ray source (for objects in Remillard et al. 1991 and nonextended objects in the 2E catalog) vs. probability of a source arising by chance.

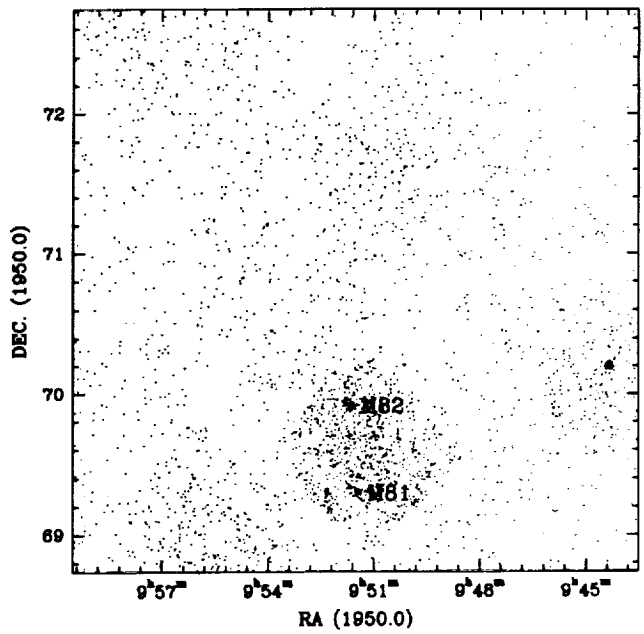

FIG. 15.—The M81/M82 region showing how the high density of background photons confuses the percolation algorithm with the standard percolation radius of 2′.

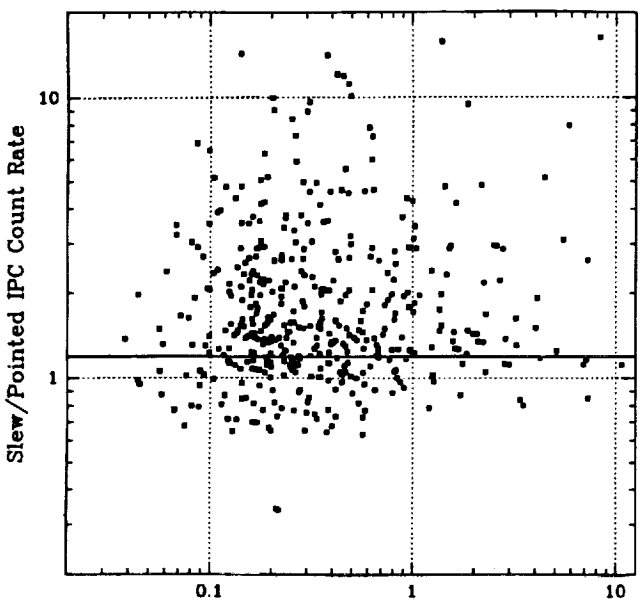

FIG. 16a

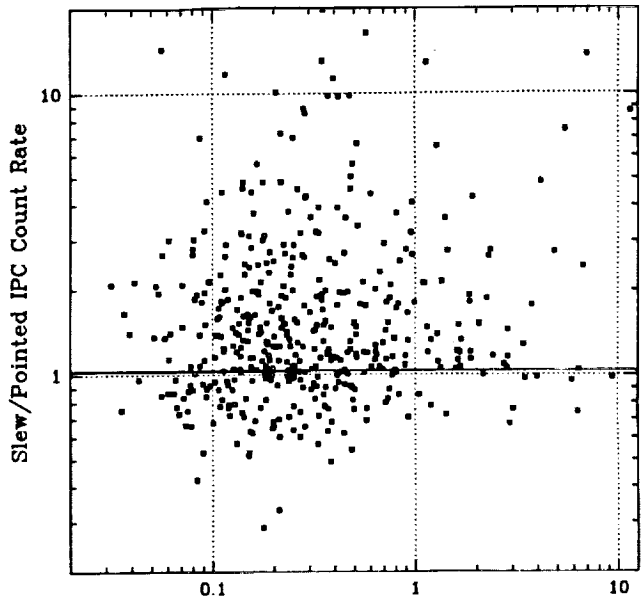

FIG. 16b

FIG. 16.—(*a*) Slew Survey count rate vs. ratio of Slew/Pointed IPC count rate ("2E"). (*b*) Slew Survey count rate restricted to PI 2-10 vs. ratio of Slew/Pointed IPC count rate ("2E").

percolation length. Thus large areas of background were included with sources, leading to large extended "sources." This tends to merge sources together and leads to their systematic undercounting in these regions. We dealt with this problem by selecting all sources with a maximum photon distance from the percolation centroid of >9′. We then reran the percolation algorithm with a smaller percolation length, which normally resolved the problem. Figure 15 shows how the galaxies M81 and M82 were initially included in a single source, but were resolved by using a shorter percolation length.

We found that when Prob1/Prob2 (defined in § 4.3) is large ($>10^3$), the source is extended, or that there are multiple sources within 15′. A visual inspection of all cases with Prob1/Prob2 > 10^3 was made (M. E. and J. S.). For all such sources an "Image Code" was assigned which notes extended sources larger than ~15′(E), regions with multiple sources within 15′ (M), and sources which are a part of a larger extended source (P). Sources with acceptable Prob1/Prob2 are assigned the code "A."

Some sources are truly extended on this scale. Each extended source was inspected visually, which we found to be an effective, but unfortunately subjective, means of discriminating real sources from confusion with background. This procedure added 33 sources and improved the positions of 78. A more automatic means of changing the percolation length with the exposure to match the mean free path between background photons needs to be developed. Some few sources have extent of order degrees (e.g., the Cygnus Loop, Puppis A). Although these are not included in our source catalog, the data are on the CD-ROM. These sources will be treated fully in a later paper (Schachter et al. 1991; see also § 7).

5. SOURCE PROPERTIES

Having produced a list of reliable sources, we need to determine their properties. The IPC gives information on positions, count rates, structure, and pulse height (energy).

The reliability of the positions was established using known X-ray sources, as described above (§ 3; Fig. 7*c*).

Count rates were derived from the 6′ diameter box used for the probability calculation with background from background region 2 (see § 4.3).

For extended sources (e.g., clusters of galaxies, supernova remnants, and those labeled "E" in the source table), the count rates will clearly not be accurate. For most of these, a better count rate can be derived using the counts and exposure in the 6′–12′ "square annulus" surrounding the central detection cell (background region 1). This information is available on the CD-ROM version of the Slew Survey (see "lists/unix/readme.txt," "lists/vms/readme.txt.," etc.).

The count rates were checked for accuracy by comparing the Slew Survey rates with those derived from the pointed IPC data for sources in common. In Figure 16a we plot the Slew Survey count rates as listed in this catalog versus the pointed IPC count rates from the 2E catalog (Harris et al. 1991). There is a strong correlation with a slight offset (a factor 1.19) toward higher count rates in the Slew Survey. This is due primarily to our use of all 15 PI bins in the Slew Survey, compared with the standard two to 10 used in pointed data. (The restricted range for pointed data is used to minimize background, which is unnecessary in the Slew Survey.) When we restrict the Slew Survey source count rates to the same PI bins, the offset is reduced to a factor 1.03, as shown in Figure 16*b*. The source of

TABLE 5

IDENTIFIED SOURCES TO DATE

Class	Number of New X-Ray Sources	Total Number of Identifications	% Survey Detected	% Survey Predicted (MS)
AGNs	9	124	19	30
BL Lacs	0	31	5	10
Clusters	11	78	12	20
CVs	0	22	3	6
Stars:	92	242	38	20
Known Active	2	46	...	...
Binaries	4	19	...	...
Wind candidates (OBA)	11	32	...	...
Coronal candidates (≥F)	68	127	...	...
Unknown, peculiar	7	18	...	...
X-ray binaries and pulsars	0	39	6	6
Other:	21	101	16	8
Galaxies	17	37	...	...
SN Remnants	0	28	...	...
White dwarfs	1	6	...	...
2E sources	0	23	...	...
SIMBAD sources	3	6	...	...
EXOSAT sources	0	2	...	...

this residual offset is still under investigation. The errors on these count rates are nontrivial to determine since both the background and the source counts are not in the Gaussian limit and so do not add in quadrature. The problem of calculating these uncertainties in the Poisson case has recently been investigated by Kraft, Burrows, & Nousele (1991), and we have used their methods with software routines which they kindly supplied to us. (Note that the uncertainties on the CD-ROM assumed Gaussian statistics. Updated values can be obtained using *einline;* Harris et al. 1991).

Several measures of source extent were attempted. Large sources, >9′ diameter, are readily selected using the maximum distance of a source photon from the percolation centroid. Smaller extended sources are clearly seen on the maps but are not so easily characterized. We are continuing a search for an objective means of classifying the size of sources.

The mean pulse height bin for each source was calculated from the photons in the 6′ box. The "pulse height–invariant" (PI) bins were used since they have a first order correction to remove the effects of the variable gain of the IPC (Harnden et al. 1984). (This variation changes the mapping of photon energy to pulse height bin.) That an extreme ultraviolet source from the Wide Field Camera on *ROSAT* (1ES 1631+781) has a mean PI bin of 2 (on a scale from 1, low energy, to 15, high energy) shows that the PI data carry useful information.

6. SOURCE LIST

The Slew Survey source catalog contains 819 sources. Table 5 gives a summary of the identifications made.

6.1. *Table of Objects*

Table 6 is the Slew Survey source catalog. The identifications suggested in Table 6 are discussed in the next section (§ 7). Table 6 has the following entries.

Column (1).—Source name. "1ES" stands for first *Einstein* Slew Survey source. Coordinate names are based on the B1950.0 position constructed from hours, minutes ± degrees, tenths of degrees, truncated according to the IAU convention.

Columns (2) and (3).—Position. These are given in B1950.0 coordinates, based on the percolation algorithm centroid. Where noted, positions have been refined by changing the percolation length as discussed in § 4.5. Errors on position are primarily systematic, arising from the aspect solution. A 90% error radius of 1.2 and a 95% radius of 2.0 are estimated from Figure 7*d*.

Column (4).—Count rate. Mean count rate in all PI bins (1–15). This is on average a factor 1.19 larger than the standard IPC "broad-band" count rate (based on PI channels 2–10) used in the 2E catalog (see § 5). Counts are taken from a box 6′ on a side centered on the percolation algorithm centroid. Background counts scaled for exposure and area from a box 30′ on a side (background region 2) have been subtracted. Errors represent a 1 σ confidence interval. When total source plus background in the source box had ≤100 counts, the error bars are based on a Poisson probability, distribution as computed in Kraft et al. (1991), which gives asymmetric error bars. For sources with a larger number of photons, a Gaussian approximation was used.

Column (5).—Number of photons (NP) in the box which is 6′ on a side and *number of slews* (NS) that contribute photons to the object. Other slews may have passed over the source positions but yielded no photons.

Column (6).—Probability, $P_{\rm rand}$. Probability of finding the number of photons listed in column (5) relative to background region 2. Small numbers indicate a higher chance that the source is real. Values of $P_{\rm rand} < 1 \times 10^{-10}$ are listed as equal to 1×10^{-10}. To generate the list of accepted sources, we used thresholds as in § 4.5.

Column (7).—Exposure. Total Slew Survey exposure time averaged over the box which is 6′ on a side used in column (3).

TABLE 6

THE FIRST *Einstein* SLEW SURVEY CATALOG

Slew Desig.	RA 1950	DEC 1950	IPC Rate (cts s^{-1})	NP/NS	P_{rand}	Exp. (s)	PI	QI	EOS # EMSS	Δ2E (′)	A3 EXO	Δ1H (′)	Cat.	Class.: Type/z	Name	ΔC (′)
1ES0003+158	00 03 23	+15 52 55	$0.09^{+0.03}_{-0.03}$	20/3	7.03E−05	145.0	6	3A	12	0.6	...	...	HB	AGN:0.112	PHL 658	0.5
1ES0003+199	00 03 48	+19 55 15	$1.63^{+0.35}_{-0.31}$	26/3	1.00E−10	15.4	4	3A	...	...	x1H0003+200	0.8	HB	AGN:0.025	MRK 335	0.7
1ES0004+287	00 04 04	+28 44 18	$0.29^{+0.07}_{-0.06}$	26/4	1.00E−10	77.2	5	3A	m15	0.4	...	...	WLY	S:K0V	WLY 5	0.8
1ES0005+159	00 05 17	+15 59 01	$0.12^{+0.05}_{-0.04}$	13/5	4.26E−05	79.8	11	3A	...	...	...	...	...	...	...	...
1ES0008+107	00 08 00	+10 42 03	$0.57^{+0.08}_{-0.07}$	63/4	1.00E−10	102.9	6	3A	29	0.5	x1H0014+111	0.8	HB	AGN:0.089	III ZW 2	0.8
1ES0008−025	00 08 46	−02 35 02	$0.29^{+0.14}_{-0.11}$	7/3	2.17E−05	21.1	6	3A	...	...	...	...	...	...	...	...
1ES0013+195	00 13 37	+19 35 38	$0.28^{+0.13}_{-0.11}$	7/5	1.04E−05	22.6	6	3A	...	...	...	...	SBD	S:M4	G 32 -6°	0.0
1ES0021−723	00 21 39	−72 21 40	$0.09^{+0.03}_{-0.03}$	19/5	7.46E−06	143.6	5	3A	82	0.9	...	...	SBD	P	47 TUC	1.3
1ES0022+638	00 22 26	+63 52 03	$9.91^{+0.65}_{-0.66}$	236/9	1.00E−10	23.5	7	3A	83	2.3	x1H0022+638	1.6	A3	SNR	TYCHO	1.7
1ES0033+595	00 33 04	+59 33 23	$0.59^{+0.22}_{-0.18}$	10/5	1.00E−10	16.2	7	3A	...	...	...	...	...	...	...	...
1ES0037+405	00 37 30	+40 33 19	$0.06^{+0.02}_{-0.02}$	29/4	1.92E−05	301.7	6	3A	113	0.2	...	...	2E	...	5C3 76	0.2
1ES0037+293	00 37 43	+29 18 26	$0.23^{+0.10}_{-0.08}$	10/3	5.14E−06	36.6	10	3A	m118	2.2	...	...	MS	CG:0.069	A77	2.2
1ES0039−095	00 39 19	−09 34 43	$0.96^{+0.12}_{-0.11}$	83/8	1.00E−10	79.6	7	3A	136	0.4	...	...	2E	CG:0.052	A85	0.7
1ES0039+400	00 39 36	+40 03 04	$0.09^{+0.02}_{-0.02}$	48/6	1.00E−10	370.5	7	3E	141	1.0	...	...	VV	AGN:0.102	IV ZW 29	0.7
1ES0039+409	00 39 58	+40 59 48	$0.41^{+0.05}_{-0.05}$	90/6	1.00E−10	197.5	5	3E	147	0.2	x1H0039+408	0.4	UGC	GAL:-0.001	M 31	0.4
1ES0041−182	00 41 09	−18 15 26	$0.88^{+0.15}_{-0.14}$	40/4	1.00E−10	43.4	4	3A	163	0.8	...	...	WLY	S:K0III	WLY 31	1.0
1ES0041+402	00 41 57	+40 16 51	$0.08^{+0.03}_{-0.03}$	19/5	6.12E−05	160.3	6	3A	...	...	...	...	...	...	...	...
1ES0043+413	00 43 00	+41 23 27	$0.07^{+0.02}_{-0.01}$	49/2	1.47E−09	464.5	5	3A	169	0.3	...	...	SBD	...	P SKHB 307	0.2
1ES0044−211	00 44 31	−21 06 21	$0.14^{+0.05}_{-0.04}$	26/3	3.87E−06	119.2	7	3A	179	2.8	...	...	2E	GAL	2E	2.5
1ES0044+239	00 44 40	+23 59 27	$0.65^{+0.09}_{-0.09}$	63/6	1.00E−10	90.8	5	3A	181	0.3	...	...	SAO	AC:K1II	ζ AND	0.4
1ES0045−255	00 45 07	−25 33 58	$0.16^{+0.03}_{-0.03}$	37/4	1.00E−10	191.9	5	3A	184	0.3	...	...	RNG	GAL:0.001	NGC 253	0.6
1ES0045+311	00 45 41	+31 09 34	$0.12^{+0.06}_{-0.05}$	8/3	4.86E−05	55.7	9	3A	...	...	...	...	...	...	...	...
1ES0048+291	00 48 50	+29 07 15	$0.20^{+0.09}_{-0.07}$	10/1	8.34E−05	39.6	7	3A	m198	0.8	1H0043+294	0.9	VV	AGN:0.036	VV	0.9
1ES0050+124	00 50 58	+12 25 09	$0.39^{+0.09}_{-0.08}$	27/3	1.00E−10	64.2	5	3A	209	0.2	...	...	VV	AGN:0.061	I ZW 1	0.2
1ES0051−749	00 51 26	−74 55 33	$0.30^{+0.06}_{-0.06}$	36/5	1.00E−10	101.1	6	3A	214	0.2	...	...	SAO	AC:G0	CV TUC	0.1
1ES0052+251	00 52 09	+25 09 35	$0.27^{+0.08}_{-0.07}$	16/5	3.06E−10	52.5	5	3A	217	0.5	x1H0048+250	0.6	VV	AGN:0.154	PG	0.5
1ES0053+604	00 53 42	+60 27 09	$2.05^{+0.33}_{-0.30}$	45/8	1.00E−10	21.4	6	3A	...	...	x1H0053+604	0.4	A3	XRB-Be	γ CAS	0.4
1ES0054+231	00 54 32	+23 09 18	$0.20^{+0.06}_{-0.05}$	25/2	2.83E−08	93.5	4	3A	232	0.2	...	...	SAO	AC:G8IIIb	SAO 074388	0.3
1ES0054+145	00 54 38	+14 30 45	$0.15^{+0.05}_{-0.05}$	15/4	2.93E−06	78.5	6	3A	233	1.3	x	...	VV	AGN:0.171	PHL 909	1.7
1ES0055+227	00 55 17	+22 45 02	$0.17^{+0.07}_{-0.06}$	12/3	1.08E−04	53.7	4	3A	...	...	...	...	...	...	...	...
1ES0057+315	00 57 06	+31 33 45	$0.91^{+0.12}_{-0.11}$	69/8	1.00E−10	72.2	5	3A	244	0.7	x1H0106+324	0.7	VV	AGN:0.015	MRK 352	0.7
1ES0100+405	01 00 56	+40 35 02	$0.22^{+0.07}_{-0.06}$	17/3	4.77E−09	64.0	5	3A	254	0.9	...	...	SBD	S	G 132 -50A*	1.3
1ES0101+410	01 01 48	+41 02 52	$0.23^{+0.10}_{-0.08}$	10/2	2.16E−05	35.6	7	3A	260	1.0	...	...	GCV	S:PEC(UG)	RX AND	1.0

TABLE 6—*Continued*

Slew Desig.	RA 1950	DEC 1950	IPC Rate (cts s^{-1})	NP/NS	P_{rand}	Exp. (s)	PI	QI	EOS # EMSS	Δ2E (′)	A3 EXO	Δ1H (′)	Cat.	Class.: Type/z	Name	ΔC (′)
1ES0102−722	01 02 25	−72 17 50	$0.82^{+0.09}_{-0.09}$	106/9	1.00E−10	117.7	6	3A	261	0.4	x	...	2E	SNR	SMC	1.7
1ES0103−726	01 03 32	−72 38 01	$0.18^{+0.05}_{-0.05}$	25/9	1.03E−07	101.7	5	3A	267	1.3	x	...	GCV	S	SZ TUC	2.2
1ES0107−580	01 07 55	−58 02 07	$0.55^{+0.33}_{-0.24}$	4/1	3.39E−07	7.2	6	3A	...	...	...	...	...	...	...	...
1ES0108+174	01 08 25	+17 24 40	$0.06^{+0.02}_{-0.02}$	23/5	6.18E−05	230.5	7	3A	311	1.5	...	...	ABL	CG:0.066	A154	1.8
1ES0114−027	01 14 06	−02 46 03	$1.85^{+0.17}_{-0.17}$	128/3	1.00E−10	67.7	4	3A	339	0.6	...	...	BSC	AC:G5IIIe	AY CET	0.5
1ES0114+065	01 14 18	+06 33 35	$0.25^{+0.08}_{-0.07}$	15/2	5.01E−09	51.5	5	3A	340	0.6	x	...	SAO	S:G5	UV PSC	0.7
1ES0115+634	01 15 17	+63 28 26	$1.52^{+0.29}_{-0.26}$	33/5	1.00E−10	20.9	9	3A	345	0.6	1H0115+635	0.4	A3	XRB-Be	V635 CAS	0.4
1ES0115−737	01 15 45	−73 42 18	$0.18^{+0.04}_{-0.04}$	39/7	1.00E−10	160.0	7	3A	350	0.4	x1H0115−737	0.1	A3	XRB	SMC X-1	0.1
1ES0115−272	01 15 50	−27 14 37	$0.26^{+0.10}_{-0.08}$	11/3	4.64E−07	36.8	8	3A	349	0.8	...	...	ABL	CG	A2895	2.3
1ES0119−286	01 19 31	−28 36 22	$0.61^{+0.21}_{-0.18}$	11/4	1.00E−10	17.0	4	3A	....	...	x1H0122−281.B	0.3	HB	AGN:0.117	GD 1339	0.3
1ES0120+004	01 20 16	+00 26 50	$0.34^{+0.15}_{-0.12}$	8/5	2.23E−06	21.1	5	3A	...	...	...	...	SAO	S:G0	HD 8358*	0.5
1ES0120+340	01 20 20	+34 05 43	$1.01^{+0.18}_{-0.16}$	40/2	1.00E−10	37.7	7	3A	369	1.0	...	...	2E	...	...	...
1ES0121−590	01 21 53	−59 03 48	$2.29^{+0.18}_{-0.18}$	171/3	1.00E−10	72.9	5	3A	378	0.2	x1H0122−590	0.3	HB	AGN:0.045	FAIR 9	0.3
1ES0122+084A	01 22 29	+08 29 52	$0.17^{+0.06}_{-0.05}$	15/8	6.28E−06	68.6	7	2A	...	...	...	...	SBD	CG:0.045	A193*	2.9
1ES0122+084B	01 22 33	+08 26 23	$0.21^{+0.07}_{-0.06}$	14/7	9.35E−07	55.0	7	3A	...	...	...	...	ABL	CG:0.045	A193*	0.8
1ES0122+190	01 22 52	+19 04 33	$0.12^{+0.06}_{-0.05}$	10/6	5.01E−05	63.8	8	3A	...	...	...	...	...	...	...	...
1ES0124+189	01 24 50	+18 55 36	$0.20^{+0.07}_{-0.06}$	12/2	8.01E−07	50.7	4	3A	390	0.5	...	...	VV	AGN:0.017	MRK 359	0.4
1ES0131+303	01 31 02	+30 23 53	$0.42^{+0.06}_{-0.06}$	72/7	1.00E−10	150.1	7	3A	409	0.5	x1H0129+303	0.9	RNG	GAL:-0.001	NGC 598	0.4
1ES0133+207	01 33 42	+20 43 05	$0.14^{+0.04}_{-0.04}$	23/6	3.98E−07	121.4	6	3A	437	0.8	x	...	HB	AGN:0.425	3C47	1.0
1ES0136−182	01 36 30	−18 12 37	$0.18^{+0.03}_{-0.03}$	64/9	1.00E−10	282.3	4	3A	455	0.7	x	...	SBD	S:M5.5V:e	LHS 9	1.2
1ES0138+391	01 38 57	+39 08 58	$0.12^{+0.05}_{-0.04}$	16/7	2.53E−05	93.5	7	2A	...	...	1H0140+393	1.0	VV	AGN:0.060	B2 0138+39B	0.9
1ES0139−189	01 39 05	−18 54 14	$0.42^{+0.18}_{-0.14}$	8/4	1.78E−07	17.6	4	3A	...	...	...	...	...	...	...	...
1ES0139−681	01 39 39	−68 07 54	$1.38^{+0.19}_{-0.18}$	63/9	1.00E−10	43.1	3	3A	469	0.4	x1H0136−681	0.6	A3	CV	BL HYI	0.6
1ES0142+614	01 42 51	+61 29 52	$3.36^{+0.56}_{-0.51}$	41/7	1.00E−10	12.0	7	3A	...	...	x1H0132+607	0.3	A3	XRB	X0142+614	0.4
1ES0143−253	01 43 17	−25 18 04	$0.30^{+0.12}_{-0.10}$	9/6	6.80E−08	27.3	4	3A	...	...	...	...	BSC	S:F1V	ϵ SCL	0.2
1ES0149+229	01 49 27	+22 57 36	$0.22^{+0.10}_{-0.08}$	8/5	2.23E−06	32.6	11	3A	...	...	...	...	...	...	...	...
1ES0149+358	01 49 42	+35 53 33	$0.29^{+0.07}_{-0.06}$	33/3	1.00E−10	90.0	7	3E	493	2.1	...	...	ABL	CG:0.016	A262	2.5
1ES0150+293	01 50 12	+29 19 29	$0.33^{+0.06}_{-0.06}$	39/5	1.00E−10	106.3	4	3A	495	0.7	...	...	WLY	S:F6IV	WLY 9062	0.7
1ES0152+022	01 52 51	+02 13 43	$0.31^{+0.13}_{-0.10}$	9/4	1.04E−06	26.2	5	3A	...	...	...	...	...	...	...	...
1ES0154−518	01 54 00	−51 51 25	$0.45^{+0.20}_{-0.16}$	8/4	1.17E−06	16.2	3	3A	...	...	...	...	WLY	S:G5IV+	WLY 81AB	0.2
1ES0157+706	01 57 50	+70 39 01	$0.24^{+0.12}_{-0.09}$	8/6	7.39E−05	27.7	6	3A	...	...	...	...	BSC	S:A3IV	SAO 4554	0.9
1ES0158−365	01 58 00	−36 33 06	$0.19^{+0.09}_{-0.07}$	9/7	5.44E−05	38.2	6	3A	...	...	...	...	...	...	...	...
1ES0158+003	01 58 32	+00 19 29	$0.51^{+0.10}_{-0.09}$	34/5	1.00E−10	59.6	5	3A	m513	0.5	...	...	2E	...	MS	0.5

TABLE 6—*Continued*

Slew Desig.	RA 1950	DEC 1950	IPC Rate (cts s^{-1})	NP/NS	P_{read}	Exp. (s)	PI	QI	EOS # EMSS	Δ2E (′)	A3 EXO	Δ1H (′)	Cat.	Class.: Type/z	Name	ΔC (′)
1ES0203+158	02 03 36	+15 51 15	$0.12^{+0.05}_{-0.04}$	17/3	3.43E−05	95.0	6	3A	...	...	...	...	...	...	...	...
1ES0204+150	02 04 11	+15 03 29	$0.53^{+0.06}_{-0.06}$	105/7	1.00E−10	180.3	7	3A	m522	0.3	x1H0157+142	0.3	A3	CV	TT ARI	0.3
1ES0205+024	02 05 14	+02 29 43	$0.20^{+0.07}_{-0.06}$	15/3	4.83E−07	61.3	6	3A	526	1.0	...	...	HB	AGN:0.155	MRK 586	1.0
1ES0206+522	02 06 19	+52 12 18	$0.61^{+0.20}_{-0.17}$	12/6	1.00E−10	18.6	6	3A	534	0.3	1H0203+513	0.6	VV	AGN:0.049	GPX 002	0.7
1ES0209+300	02 09 29	+30 04 50	$0.46^{+0.10}_{-0.09}$	30/3	1.00E−10	60.7	5	3A	544	0.7	...	...	BSC	AC:G5III+F5V	ζ TRI	0.6
1ES0212−010	02 12 00	−01 00 09	$1.02^{+0.12}_{-0.12}$	78/4	1.00E−10	73.9	6	3A	548	0.3	x1H0215−007	0.2	VV	AGN:0.027	MRK 590	0.2
1ES0212+735	02 12 54	+73 33 32	$0.17^{+0.07}_{-0.06}$	10/2	8.90E−07	50.0	7	3A	549	2.2	...	...	HB	AGN:2.367	S5 0212+735	2.2
1ES0215−021	02 15 02	−02 08 16	$0.27^{+0.13}_{-0.10}$	7/2	1.97E−05	22.8	10	3A	...	...	...	...	...	...	...	...
1ES0219+428	02 19 30	+42 48 27	$0.29^{+0.03}_{-0.03}$	156/11	1.00E−10	453.8	6	3A	558	0.2	x	...	VV	BL:0.444	3C 66A	0.1
1ES0221+323	02 21 55	+32 20 21	$0.23^{+0.11}_{-0.09}$	8/4	9.39E−05	28.7	10	3A	...	...	...	...	...	...	...	...
1ES0224+307	02 24 32	+30 45 04	$0.45^{+0.08}_{-0.07}$	43/3	1.00E−10	88.2	5	3A	569	0.2	x	...	SBD	S	BD+30 397AB	1.1
1ES0225+310	02 25 18	+31 05 29	$0.35^{+0.07}_{-0.06}$	36/4	1.00E−10	96.5	8	3A	573	0.1	x1H0218+304	0.7	VV	AGN:0.016	MRK 1040	0.4
1ES0226−615	02 26 54	−61 32 41	$0.58^{+0.23}_{-0.19}$	9/5	3.07E−08	14.4	4	3A	...	...	...	...	SAO	S:F8	SAO 248569	1.1
1ES0229+200	02 29 58	+20 04 18	$0.51^{+0.16}_{-0.14}$	14/5	1.00E−10	25.9	7	3A	...	...	...	...	...	...	...	...
1ES0232−090	02 32 10	−09 00 53	$0.66^{+0.11}_{-0.10}$	44/5	1.00E−10	62.6	6	3A	590	0.6	x1H0227−094	0.5	VV	AGN:0.043	NGC 985	0.5
1ES0232−440	02 32 25	−44 01 08	$1.47^{+0.50}_{-0.42}$	11/4	1.00E−10	7.3	5	3A	592	1.1	x1H0226−448	0.8	SBD	AC:M0Vp	HD 16157	0.7
1ES0235+016	02 35 48	+01 40 50	$0.64^{+0.30}_{-0.24}$	7/4	1.03E−05	9.9	6	3A	617	1.0	...	...	VV	AGN:0.024	NGC 1019	1.3
1ES0235+164	02 35 54	+16 24 15	$0.04^{+0.01}_{-0.01}$	35/6	7.97E−06	450.4	7	3E	618	0.2	...	...	HB	BL:0.940	OD 160	0.4
1ES0236+610	02 36 46	+61 00 07	$0.26^{+0.10}_{-0.09}$	12/4	7.25E−06	37.1	7	3A	627	1.1	x	...	GCV	S:B1EIB:	LS I +61 303	1.0
1ES0236−002	02 36 51	−00 14 19	$0.18^{+0.07}_{-0.06}$	11/5	3.02E−07	51.8	6	3A	628	0.8	...	...	2E	...	...	...
1ES0237−531	02 37 05	−53 10 24	$0.64^{+0.24}_{-0.20}$	10/4	2.40E−09	14.5	4	3A	...	...	x	...	SBD	S:F8IV/V+	HD 16699*	0.4
1ES0238−009	02 38 43	−00 54 23	$0.26^{+0.12}_{-0.10}$	9/3	1.39E−05	29.0	3	3A	...	...	x	...	SAO	S:F7IV	SAO 130055	0.6
1ES0238+057	02 38 52	+05 45 46	$0.21^{+0.10}_{-0.08}$	8/6	5.01E−05	31.3	5	3A	...	...	...	...	SBD	S:M	BD+05 378	1.4
1ES0238+069	02 38 55	+06 58 40	$0.17^{+0.04}_{-0.04}$	29/5	1.00E−10	134.7	8	3A	645	0.3	...	...	VV	AGN:0.028	MRK 595	0.3
1ES0240−002	02 40 08	−00 13 50	$0.53^{+0.06}_{-0.06}$	85/4	1.00E−10	148.8	5	3A	649	0.5	x1H0244+001	0.4	VV	AGN:0.003	NGC 1068	0.4
1ES0241+622	02 41 02	+62 15 37	$0.19^{+0.07}_{-0.06}$	13/2	2.65E−06	53.9	8	3A	653	0.1	x1H0240+621	0.2	VV	AGN:0.044	4U 0241+61	0.2
1ES0241−381	02 41 26	−38 06 21	$2.22^{+1.17}_{-0.91}$	5/2	1.57E−07	2.2	2	2A	...	...	1H0247−370	2.0	SBD	AC:G6V+	SAO 193879	2.0
1ES0242−675	02 42 29	−67 33 30	$0.36^{+0.16}_{-0.13}$	8/4	1.48E−05	19.4	7	3A	...	...	...	...	...	...	...	...
1ES0244+694	02 44 21	+69 26 27	$0.62^{+0.23}_{-0.20}$	10/3	8.78E−09	14.9	5	3A	663	0.9	...	...	SAO	S:A3V	SAO 012445	0.7
1ES0244+191	02 44 38	+19 09 57	$0.29^{+0.10}_{-0.09}$	13/3	7.30E−08	39.0	6	3A	664	0.1	...	...	SAO	S:G0	SAO 093105	0.1
1ES0245+309	02 45 42	+30 54 16	$0.96^{+0.19}_{-0.17}$	32/5	1.00E−10	31.6	5	3A	669	0.4	...	...	WLY	S:G9	VY ARI	0.3
1ES0247−253	02 47 16	−25 20 03	$0.18^{+0.08}_{-0.07}$	7/1	1.04E−05	35.5	8	3A	...	...	...	...	...	...	...	...
1ES0249−251	02 49 09	−25 08 09	$0.18^{+0.06}_{-0.05}$	14/4	7.24E−08	67.0	6	3A	673	1.0	...	...	ABL	CG:0.116	A389	1.3

TABLE 6—*Continued*

Slew Desig.	RA 1950	DEC 1950	IPC Rate (cts s^{-1})	NP/NS	P_{rand}	Exp. (s)	PI	QI	EOS # EMSS	Δ2E (′)	A3 EXO	Δ1H (′)	Cat.	Class.: Type/z	Name	ΔC (′)
1ES0250−129	02 50 06	−12 58 07	$0.17^{+0.07}_{-0.06}$	13/2	1.06E−05	57.9	4	3A	674	0.9	...	...	BSC	S:K2V	HD 17925	0.0
1ES0250−618	02 50 41	−61 50 01	$0.35^{+0.14}_{-0.12}$	9/5	2.98E−07	23.1	4	3A	...	...	1H0256−617	0.6	SBD	AC:K1Vp	SAO 248669	0.6
1ES0255+139	02 55 06	+13 56 13	$0.16^{+0.08}_{-0.06}$	8/2	9.40E−05	40.9	8	2A	...	...	...	...	...	...	...	...
1ES0255+128	02 55 08	+12 50 34	$0.26^{+0.04}_{-0.04}$	75/3	1.00E−10	235.2	7	3A	682	0.3	...	...	ABL	CG:0.072	A399*	1.8
1ES0256+133	02 56 06	+13 21 56	$0.26^{+0.07}_{-0.06}$	28/3	1.00E−10	85.2	8	3E	687	1.6	1H0253+138	1.9	ABL	CG:0.075	A401	1.8
1ES0257+442	02 57 22	+44 15 24	$0.74^{+0.37}_{-0.29}$	6/4	8.04E−06	7.5	6	3A	...	...	...	...	UGC	GAL	U02468	1.5
1ES0303+067	03 03 35	+06 44 59	$0.30^{+0.14}_{-0.12}$	7/4	1.79E−05	20.8	10	3A	...	...	...	...	...	...	...	...
1ES0304+407	03 04 56	+40 45 05	$2.67^{+0.69}_{-0.60}$	18/3	1.00E−10	6.6	5	3A	724	0.8	x	...	BSC	S:B8V	β PER	0.9
1ES0305−284	03 05 50	−28 24 24	$0.33^{+0.15}_{-0.12}$	9/3	2.62E−05	22.8	7	3A	...	...	...	...	SBD	S:K7V	CD-28 1030*	0.2
1ES0309−291	03 09 58	−29 11 02	$1.02^{+0.24}_{-0.22}$	22/6	1.00E−10	20.5	4	3A	...	...	...	...	WLY	S:F8IV+	WLY 127AB	0.2
1ES0310−568	03 10 04	−56 49 43	$0.23^{+0.10}_{-0.08}$	9/9	2.29E−05	32.7	7	2A	...	...	...	...	...	...	...	...
1ES0310−640	03 10 10	−64 05 01	$0.23^{+0.09}_{-0.07}$	11/9	3.88E−07	41.0	6	2A	...	...	...	...	...	...	...	...
1ES0311−227	03 11 59	−22 46 44	$1.27^{+0.13}_{-0.13}$	108/7	1.00E−10	82.1	5	3A	740	0.3	x1H0311−227	0.2	A3	CV	EF ERI	0.2
1ES0313−770	03 13 00	−77 03 18	$0.14^{+0.05}_{-0.04}$	17/2	4.47E−06	89.2	6	3A	746	0.3	...	...	HB	AGN:0.223	PKS	0.4
1ES0316−444	03 16 11	−44 24 39	$0.97^{+0.45}_{-0.36}$	7/4	1.15E−06	6.7	7	3A	...	...	x1H0315−445	0.4	ABL	CG:0.070	A3112	0.4
1ES0316+413	03 16 31	+41 19 48	$7.25^{+0.16}_{-0.16}$	2420/6	1.00E−10	316.4	7	3A	751	0.2	x1H0316+413.AB	0.3	A3	CG:0.018	A426*	0.3
1ES0316+031	03 16 44	+03 11 20	$0.25^{+0.10}_{-0.09}$	11/4	1.20E−05	36.1	4	3A	752	0.8	x	...	WLY	S:G5V	WLY 137	0.0
1ES0323+285	03 23 32	+28 32 16	$3.50^{+0.22}_{-0.23}$	252/4	1.00E−10	70.7	5	3A	770	0.2	x1H0334+291	0.3	SBD	AC:G5IV+K0	UX ARI	0.3
1ES0323+022	03 23 39	+02 14 37	$0.80^{+0.24}_{-0.21}$	15/6	1.00E−10	17.6	7	3A	771	0.3	x1H0323+022	0.2	VV	BL:0.147	H 0323+022	0.3
1ES0324+095	03 24 26	+09 33 42	$0.54^{+0.21}_{-0.17}$	9/4	9.51E−09	15.7	7	3A	...	...	...	...	BSC	S:B9Vn	HD 21364	0.3
1ES0325+042	03 25 17	+04 13 13	$0.29^{+0.12}_{-0.10}$	10/5	2.85E−06	29.4	6	3A	...	...	...	...	...	...	...	...
1ES0327−242	03 27 11	−24 16 15	$0.19^{+0.06}_{-0.05}$	22/3	8.24E−08	87.5	3	3A	m783	0.7	...	...	SAO	S:K5	SAO 168581	0.4
1ES0328+054	03 28 14	+05 27 48	$0.46^{+0.17}_{-0.14}$	12/5	8.52E−08	23.0	6	3A	...	...	...	...	...	...	...	...
1ES0330−621	03 30 08	−62 07 17	$0.42^{+0.20}_{-0.16}$	8/5	3.76E−05	16.2	7	3A	...	...	...	...	...	...	...	...
1ES0334+004	03 34 14	+00 25 24	$4.02^{+0.11}_{-0.11}$	1349/9	1.00E−10	331.8	4	3A	804	0.3	x1H0327+000	0.2	SBD	AC:G9V	V711 TAU	0.3
1ES0339−214	03 39 52	−21 24 12	$0.75^{+0.12}_{-0.11}$	46/4	1.00E−10	57.9	6	3A	m826	0.1	...	...	MS	AGN:0.015	MS	0.2
1ES0341−538	03 41 40	−53 49 14	$0.37^{+0.16}_{-0.13}$	9/4	1.92E−05	20.6	7	3A	845	1.9	1H0341−537	1.3	ABL	CG:0.059	A3158	1.3
1ES0347−121	03 47 02	−12 08 33	$1.47^{+0.27}_{-0.25}$	34/7	1.00E−10	22.4	5	3A	...	...	...	...	...	...	...	...
1ES0347+170	03 47 33	+17 05 31	$0.47^{+0.09}_{-0.08}$	38/3	1.00E−10	75.9	5	3A	894	0.3	x	...	MCS	WD:DA2	BD+16 516	0.9
1ES0352+308	03 52 14	+30 53 54	$2.07^{+0.37}_{-0.34}$	36/5	1.00E−10	16.9	8	3A	906	0.5	x1H0352+308	0.2	A3	XRB-Be	ζ PER	0.3
1ES0352−686	03 52 52	−68 40 15	$0.49^{+0.12}_{-0.11}$	22/14	1.00E−10	40.9	6	3A	...	...	...	...	...	...	...	...
1ES0353−741	03 53 23	−74 10 07	$0.20^{+0.07}_{-0.06}$	17/3	5.17E−06	64.3	7	3A	m908	0.6	1H0350−735	1.7	A3	CG:0.127	MS	1.7
1ES0355−612	03 55 19	−61 12 55	$0.33^{+0.10}_{-0.09}$	18/12	2.85E−09	45.9	6	3A	...	...	...	...	...	...	...	...

TABLE 6—*Continued*

Slew Desig.	RA 1950	DEC 1950	IPC Rate (cts s^{-1})	NP/NS	P_{rand}	Exp. (s)	PI	QI	EOS # EMSS	Δ2E (′)	A3 EXO	Δ1H (′)	Cat.	Class.: Type/z	Name	ΔC (′)
1ES0357−400	03 57 56	−40 01 50	$0.30^{+0.12}_{-0.10}$	10/6	6.64E−06	28.1	6	3A	...	...	...	...	SBD	S:K0	HD 25300	1.2
1ES0403−373	04 03 13	−37 19 12	$0.42^{+0.15}_{-0.13}$	12/6	3.97E−08	25.1	6	3A	...	...	...	...	SBD	GAL:0.055	ESO 359- 19	0.2
1ES0405−123	04 05 25	−12 20 06	$0.36^{+0.09}_{-0.08}$	24/1	1.00E−10	58.3	7	3A	938	0.9	1H0413−116	0.8	VV	AGN:0.574	MS	0.8
1ES0407−080	04 07 17	−08 01 52	$1.98^{+0.32}_{-0.29}$	46/2	1.00E−10	22.5	5	3A	943	0.5	1H0409−078	0.5	A3	AC	SAO 130994	0.6
1ES0408−587	04 08 20	−58 47 54	$0.37^{+0.17}_{-0.14}$	7/6	2.48E−06	17.4	9	2A	...	...	...	...	...	...	...	...
1ES0410+103	04 10 37	+10 19 34	$0.79^{+0.17}_{-0.15}$	29/7	1.00E−10	34.5	6	3A	949	1.1	x1H0409+102	2.3	ABL	CG:0.090	A478	1.5
1ES0411+261	04 11 30	+26 09 35	$0.14^{+0.07}_{-0.06}$	8/2	9.65E−05	46.4	5	3A	952	0.7	...	...	SAO	S:G5	SAO 076514	1.6
1ES0412−382	04 12 09	−38 12 03	$0.64^{+0.30}_{-0.24}$	7/3	1.17E−06	10.1	6	3A	...	...	...	...	EXC	GAL:0.050	ESO(B) 303R	1.5
1ES0412+060	04 12 48	+06 04 15	$0.16^{+0.03}_{-0.03}$	41/5	1.00E−10	206.9	4	3A	956	0.2	...	...	BSC	S:G0IV	HD26923	0.5
1ES0413−625	04 13 36	−62 34 55	$0.15^{+0.05}_{-0.05}$	17/7	2.27E−06	83.6	5	3A	m958	1.2	...	...	BSC	S:G8II-III	HD27256	1.6
1ES0414+009	04 14 19	+00 57 36	$1.61^{+0.66}_{-0.54}$	8/2	7.74E−10	4.8	6	3A	959	0.8	x1H0414+009	0.6	HB	BL:0.287	1H	0.6
1ES0414+365	04 14 49	+36 35 19	$0.30^{+0.16}_{-0.12}$	5/4	5.86E−07	16.0	9	3A	...	...	...	...	...	...	...	...
1ES0414+379	04 14 58	+37 54 33	$0.41^{+0.12}_{-0.10}$	18/4	1.00E−10	38.6	7	3A	963	0.7	1H0414+380	0.6	VV	AGN:0.048	3C 111.0	0.6
1ES0415+231	04 15 06	+23 09 27	$0.35^{+0.15}_{-0.12}$	8/4	7.50E−07	21.1	6	3A	...	...	...	...	SBD	S:K0	HD 284303	1.2
1ES0415+283	04 15 24	+28 19 50	$0.26^{+0.09}_{-0.08}$	13/5	4.34E−07	42.5	6	3A	...	...	x	...	GCV	S:K3E-K7E	V410 TAU	0.3
1ES0418+281	04 18 51	+28 10 32	$0.26^{+0.11}_{-0.09}$	9/3	1.52E−05	29.5	6	3A	987	0.8	1H0419+280.A	0.7	SBD	AC:G2III	SAO 076567	0.6
1ES0418−550	04 18 52	−55 03 02	$0.34^{+0.07}_{-0.06}$	39/6	1.00E−10	101.2	6	3A	988	0.5	x1H0414−551	0.4	VV	AGN:0.005	NGC 1566	0.4
1ES0419+148	04 19 36	+14 48 40	$0.07^{+0.03}_{-0.02}$	22/12	1.33E−05	197.1	6	3M	...	...	...	...	SBD	S:F8	HD 285758	2.2
1ES0419+149	04 19 57	+14 56 42	$0.09^{+0.03}_{-0.02}$	31/12	4.15E−08	240.4	5	3M	1000	0.7	...	...	SAO	S:G0	SAO 093896	0.7
1ES0421+146	04 21 22	+14 38 46	$0.17^{+0.03}_{-0.03}$	47/16	1.00E−10	221.0	5	3A	1020	0.2	...	...	SAO	S:G0	SAO 093910	0.3
1ES0423+154	04 23 29	+15 29 54	$0.25^{+0.05}_{-0.04}$	42/13	1.00E−10	143.8	5	3A	1034	0.5	x	...	BSC	S:F0V	HD28052	0.5
1ES0423+146	04 23 51	+14 36 12	$0.11^{+0.04}_{-0.03}$	17/10	1.58E−05	112.8	10	1A	...	...	...	...	SAO	S:G7III	SAO 093935	0.9
1ES0424+177	04 24 18	+17 44 42	$0.16^{+0.07}_{-0.06}$	11/5	2.64E−05	54.6	6	3A	1043	0.4	...	...	2E	...	...	...
1ES0424+099	04 24 48	+09 54 13	$0.14^{+0.05}_{-0.04}$	15/9	5.61E−06	80.3	8	2A	...	...	...	...	...	...	...	...
1ES0425−573	04 25 03	−57 18 41	$0.67^{+0.20}_{-0.17}$	17/6	1.00E−10	22.7	5	3A	...	...	1H0419−577	0.1	A3	AGN	1H	0.1
1ES0426−131	04 26 43	−13 07 07	$0.12^{+0.05}_{-0.04}$	11/3	4.96E−05	72.1	6	3A	...	...	...	...	BSC	S:B1Vne	DU ERI	2.6
1ES0429−537	04 29 33	−53 43 18	$0.69^{+0.22}_{-0.19}$	14/8	1.10E−10	18.5	4	3A	...	...	1H0435−531	0.4	VV	AGN:0.040	FAIR 303	0.3
1ES0429+130	04 29 36	+13 00 09	$0.20^{+0.09}_{-0.07}$	9/5	1.16E−05	38.0	4	3A	...	...	...	...	SBD	S:F8	HD 286840*	2.7
1ES0430+052	04 30 32	+05 14 57	$0.68^{+0.03}_{-0.03}$	834/32	1.00E−10	1153.3	7	3A	1087	0.1	x1H0426+051	0.1	VV	AGN:0.033	3C 120	0.1
1ES0430+179	04 30 36	+17 54 34	$0.12^{+0.04}_{-0.03}$	23/4	3.48E−07	134.1	6	3A	m1089	0.2	1H0427+177	0.3	BSC	S:B9IVn	HD28867	0.3
1ES0430−615	04 30 47	−61 31 22	$0.38^{+0.06}_{-0.05}$	75/7	1.00E−10	162.6	6	3E	1090	1.8	...	...	SBD	CG:0.055	ESO 118- 30	2.7
1ES0431−133	04 31 21	−13 22 00	$1.00^{+0.08}_{-0.06}$	315/7	1.00E−10	292.3	6	3A	1092	0.5	x1H0430−133	0.7	ABL	CG:0.032	A496	1.2
1ES0433+270	04 33 42	+27 02 15	$0.73^{+0.10}_{-0.09}$	69/3	1.00E−10	90.5	4	3A	1103	0.4	...	...	SAO	S:K2	SAO 076672	0.2

TABLE 6—*Continued*

Slew Desig.	RA 1950	DEC 1950	IPC Rate (cts s^{-1})	NP/NS	P_{rand}	Exp. (s)	PI	QI	EOS # EMSS	Δ2E (′)	A3 EXO	Δ1H (′)	Cat.	Class.: Type/z	Name	ΔC (′)
1ES0435−472	04 35 54	−47 17 14	$0.50^{+0.23}_{-0.18}$	8/5	5.27E−06	14.1	4	3A	...	...	...	...	...	...	...	...
1ES0437−046	04 37 02	−04 41 30	$0.50^{+0.16}_{-0.14}$	14/6	1.95E−10	25.3	8	3A	...	...	...	...	GCV	S	BF ERI	0.6
1ES0437+444	04 37 21	+44 25 55	$2.76^{+0.93}_{-0.79}$	11/1	1.00E−10	3.9	10	3A	...	...	...	...	GCV	S	OU PER	1.9
1ES0439−085	04 39 30	−08 32 20	$0.21^{+0.10}_{-0.08}$	8/4	6.02E−05	32.1	5	3A	...	...	...	...	...	...	...	...
1ES0439−682	04 39 56	−68 14 44	$0.20^{+0.08}_{-0.07}$	13/11	1.39E−05	50.8	2	3A	...	...	...	...	...	...	...	...
1ES0441−107	04 41 22	−10 46 31	$0.12^{+0.04}_{-0.04}$	20/4	9.93E−07	117.6	8	3A	1142	0.7	...	...	SAO	S:A5	RZ ERI	0.7
1ES0444−704	04 44 32	−70 24 51	$0.20^{+0.07}_{-0.06}$	11/5	3.26E−08	48.5	3	3A	...	...	...	...	HD	S:K7	HD270712	0.8
1ES0446+449	04 46 12	+44 56 08	$0.15^{+0.05}_{-0.04}$	30/4	2.06E−06	128.1	8	3E	...	...	...	...	...	...	...	...
1ES0447+068	04 47 10	+06 51 40	$0.77^{+0.33}_{-0.27}$	8/1	2.14E−07	9.6	4	3A	...	...	...	...	SAO	S:F6V	SAO 112106	1.0
1ES0452−559	04 52 25	−55 55 54	$0.27^{+0.08}_{-0.07}$	17/3	1.00E−10	55.1	5	3A	1177	1.2	x1H0451−560	1.0	A3	AC	1H	1.0
1ES0453−685	04 53 50	−68 33 40	$0.16^{+0.07}_{-0.06}$	12/8	7.09E−05	54.9	6	3A	1184	0.6	...	...	SBD	SNR	0453-68.5	0.8
1ES0454−220	04 54 00	−22 03 30	$0.17^{+0.07}_{-0.06}$	14/2	5.87E−06	62.1	8	3A	1185	0.3	...	...	HB	AGN:0.534	PKS	0.7
1ES0457+017	04 57 00	+01 42 29	$0.39^{+0.06}_{-0.06}$	50/2	1.00E−10	117.1	5	3A	1191	0.1	x	...	WLY	S:M1EV	WLY 182	0.3
1ES0459+034	04 59 31	+03 27 38	$0.45^{+0.11}_{-0.10}$	24/2	1.00E−10	48.0	7	3A	m1208	0.3	1H0510+031	0.1	VV	AGN:0.016	GHIGO	0.1
1ES0459−753	04 59 47	−75 21 49	$0.44^{+0.16}_{-0.13}$	12/6	2.34E−08	24.0	8	3A	...	...	x1H0502−755	0.8	SBD	AC:K1IIIp	HD32918	0.9
1ES0501+589	05 01 50	+58 57 06	$0.35^{+0.11}_{-0.09}$	16/3	1.00E−10	41.0	6	3A	1213	0.3	1H0501+592	0.2	A3	AC	BM CAM	0.2
1ES0504−575	05 04 40	−57 32 10	$0.77^{+0.26}_{-0.22}$	12/7	1.00E−10	14.7	4	3A	...	...	...	...	WLY	S:F8V	WLY 189	0.3
1ES0505−054	05 05 01	−05 28 03	$0.35^{+0.07}_{-0.07}$	33/5	1.00E−10	82.4	8	3A	m1220	0.1	...	...	MS	AC	MS	1.1
1ES0505−679	05 05 48	−67 56 28	$0.71^{+0.16}_{-0.14}$	28/9	1.00E−10	35.6	5	3A	1222	0.3	...	...	2E	SNR	DEM 17	0.8
1ES0505−546	05 05 58	−54 38 09	$0.47^{+0.20}_{-0.16}$	8/6	6.29E−08	16.0	6	3A	...	...	...	...	...	...	...	...
1ES0506−680	05 06 11	−68 05 36	$0.28^{+0.11}_{-0.09}$	15/7	2.18E−05	39.6	7	3M	1223	0.7	...	...	2E	SNR	N23 (LMC)	0.9
1ES0507−040	05 07 15	−04 04 52	$0.35^{+0.15}_{-0.12}$	9/5	1.91E−06	22.6	6	3A	...	...	x1H0506−039	1.4	A3	BL	EXO	1.4
1ES0509−687	05 09 15	−68 47 13	$0.81^{+0.11}_{-0.11}$	62/14	1.00E−10	71.6	5	3A	1232	0.2	x	...	2E	SNR	N103B (LMC)	0.5
1ES0509−675	05 09 28	−67 34 54	$0.26^{+0.04}_{-0.04}$	60/7	1.00E−10	185.0	5	3A	1235	1.1	...	...	SBD	SNR	0509-67.5	1.8
1ES0510−119	05 10 00	−11 56 02	$0.31^{+0.11}_{-0.09}$	13/8	2.57E−08	36.5	6	3A	...	...	...	...	SAO	S:B8V	SAO 150223	0.5
1ES0510−162	05 10 42	−16 16 16	$0.07^{+0.03}_{-0.02}$	24/3	8.62E−05	207.0	6	3A	1236	0.6	x	...	SAO	S:A0P	μ LEP	0.4
1ES0513−002	05 13 38	−00 12 51	$0.58^{+0.18}_{-0.14}$	18/1	1.00E−10	28.5	7	3A	1240	0.6	x	...	VV	AGN:0.033	AKN 120	0.6
1ES0518−458	05 18 24	−45 49 42	$0.47^{+0.08}_{-0.07}$	44/5	1.00E−10	85.6	6	3A	1252	0.2	x1H0507−459	1.0	VV	AGN:0.034	PIC A	1.0
1ES0519−690	05 19 55	−69 05 09	$0.68^{+0.07}_{-0.07}$	111/18	1.00E−10	151.7	6	3A	1257	0.1	...	...	2E	SNR	LMC	0.2
1ES0521−720	05 21 17	−72 00 27	$7.27^{+0.24}_{-0.24}$	919/18	1.00E−10	125.1	7	3A	1264	0.1	x1H0521−720	0.1	A3	XRB	LMC X-2	0.1
1ES0523−543	05 23 53	−54 19 13	$0.36^{+0.16}_{-0.13}$	8/4	1.04E−05	19.5	8	3A	...	...	...	...	...	...	...	...
1ES0524−711	05 24 50	−71 11 13	$0.12^{+0.04}_{-0.03}$	27/11	1.94E−06	144.8	6	3A	1276	1.2	...	...	SBD	S:Be	BI 156	2.2
1ES0525−660	05 25 22	−66 02 01	$0.34^{+0.08}_{-0.07}$	33/18	1.00E−10	79.1	5	3M	1277	0.4	x	...	2E	SNR	N49B (LMC)	0.3

TABLE 6—*Continued*

Slew Desig.	RA 1950	DEC 1950	IPC Rate (cts s^{-1})	NP/NS	P_{rand}	Exp. (s)	PI	QI	EOS # EMSS	Δ2E (′)	A3 EXO	Δ1H (′)	Cat.	Class.: Type/z	Name	ΔC (′)
1ES0526−661	05 26 03	−66 07 35	$0.85^{+0.11}_{-0.10}$	78/30	1.00E−10	85.9	6	3A	1279	0.8	x	...	2E	SNR	N49 (LMC)	0.8
1ES0527+111	05 27 10	+11 11 38	$0.93^{+0.24}_{-0.21}$	29/2	1.69E−10	23.9	4	2A	...	...	...	...	...	...	...	...
1ES0527−328	05 27 37	−32 51 21	$0.14^{+0.05}_{-0.04}$	17/1	7.81E−06	86.5	9	3A	1286	0.4	x1H0527−328	0.6	A3	CV	TV COL	0.6
1ES0528−654	05 28 32	−65 29 15	$2.17^{+0.18}_{-0.18}$	150/30	1.00E−10	66.7	5	3A	1290	0.6	x	...	SAO	S:K1IIIp	SAO 249286	0.5
1ES0529−003	05 29 26	−00 19 55	$0.59^{+0.07}_{-0.07}$	84/4	1.00E−10	131.4	4	3A	1293	0.3	...	...	BSC	S:B0III+O9	δ ORI	0.3
1ES0529+097	05 29 30	+09 47 32	$0.28^{+0.08}_{-0.07}$	18/1	1.00E−10	55.1	5	3A	1294	0.3	...	...	GCV	S:M4VE	V 998ORI	0.2
1ES0531+100	05 31 48	+10 05 18	$0.18^{+0.05}_{-0.05}$	22/2	2.87E−08	95.4	5	3A	1315	0.1	...	...	SBD	S	HD 245059	0.3
1ES0532+215	05 32 12	+21 34 35	$3.94^{+1.36}_{-1.17}$	14/1	7.97E−08	3.0	7	2M	...	...	...	...	...	...	...	...
1ES0532−664	05 32 49	−66 24 19	$0.44^{+0.08}_{-0.07}$	41/16	1.00E−10	83.5	6	3A	1368	0.2	x1H0534−667	0.2	A3	XRB	LMC X-4	0.2
1ES0532−054	05 32 50	−05 25 07	$1.24^{+0.06}_{-0.06}$	455/7	1.00E−10	338.6	7	3A	1366	0.1	x	...	SAO	S:OE5	ORI STARS	0.2
1ES0532−059	05 32 57	−05 56 16	$0.44^{+0.05}_{-0.05}$	106/8	1.00E−10	212.1	4	3A	1377	0.7	x	...	BSC	S:O9III	HD 37043	0.5
1ES0533+215	05 33 04	+21 31 54	$1.91^{+0.46}_{-0.41}$	25/1	1.00E−10	11.6	7	2M	...	...	...	...	...	...	...	...
1ES0534−580	05 34 02	−58 03 53	$0.47^{+0.08}_{-0.07}$	44/5	1.00E−10	86.9	4	3A	1425	0.5	x1H0538−577	0.4	A3	CV	TW PIC	0.4
1ES0534−077	05 34 16	−07 42 00	$0.24^{+0.10}_{-0.08}$	9/6	3.92E−07	34.4	7	3A	...	...	...	...	SBD	...	KMS 66	1.9
1ES0534−699	05 34 27	−69 57 16	$0.06^{+0.02}_{-0.02}$	55/16	2.01E−05	437.0	5	3A	1436	0.9	...	...	2E	SNR	DEM 238	0.7
1ES0535−660	05 35 40	−66 03 59	$2.83^{+0.16}_{-0.16}$	321/30	1.00E−10	111.6	6	3A	1461	0.2	x	...	2E	SNR	N63A (LMC)	0.1
1ES0536−580	05 36 36	−58 02 39	$0.13^{+0.06}_{-0.05}$	11/4	6.25E−05	66.7	9	3A	...	...	...	...	...	...	...	...
1ES0538−691A	05 38 05	−69 11 48	$0.12^{+0.02}_{-0.02}$	128/27	1.00E−10	518.9	7	3A	1499	0.6	x	...	2E	SNR	N157B (LMC)	0.6
1ES0538−019	05 38 14	−01 58 54	$0.73^{+0.31}_{-0.25}$	8/2	6.83E−08	10.3	5	3A	1500	1.0	...	...	SBD	S:O9Iab:	HD 37742*	0.9
1ES0538−641	05 38 40	−64 06 42	$16.97^{+0.58}_{-0.56}$	945/26	1.00E−10	55.3	7	3A	...	...	1H0538−641	0.2	A3	XRB	LMC X-3	0.1
1ES0538+037	05 38 46	+03 45 20	$0.20^{+0.07}_{-0.06}$	14/1	2.28E−06	55.7	5	3A	1507	0.6	...	...	SAO	S:G5	SAO 113040	0.9
1ES0538−691B	05 38 52	−69 06 32	$0.08^{+0.02}_{-0.02}$	97/22	3.86E−06	467.4	6	1M	1513	1.4	x	...	2E	SNR	2E	1.4
1ES0540−697	05 40 06	−69 46 09	$10.71^{+0.10}_{-0.10}$	11654/44	1.00E−10	1077.1	7	3A	1522	0.2	x1H0540−697	0.1	A3	XRB	LMC X-1	0.1
1ES0540−693	05 40 37	−69 21 35	$0.48^{+0.03}_{-0.03}$	553/42	1.00E−10	947.5	7	3A	1525	0.2	x	...	2E	P	2E	0.4
1ES0543−555	05 43 02	−55 34 09	$0.40^{+0.18}_{-0.15}$	8/5	1.87E−05	17.2	5	3A	...	...	...	...	RNG	GAL:0.015	NGC 2087	3.0
1ES0543−683	05 43 39	−68 23 17	$0.22^{+0.06}_{-0.06}$	23/7	6.01E−10	82.4	5	3A	1550	1.0	x	...	2E	S	2E	0.9
1ES0545−336	05 45 12	−33 38 50	$0.40^{+0.15}_{-0.13}$	10/4	1.76E−08	23.1	4	3A	...	...	...	...	...	...	...	...
1ES0546−642	05 46 30	−64 15 18	$0.17^{+0.07}_{-0.06}$	12/11	1.21E−05	56.5	5	3A	...	...	...	...	...	...	...	...
1ES0547−697	05 47 35	−69 42 44	$0.04^{+0.01}_{-0.01}$	114/18	3.81E−07	1018.2	6	3A	1570	0.8	...	...	2E	SNR	N135 (LMC)	0.5
1ES0548−322	05 48 50	−32 16 54	$2.22^{+0.16}_{-0.16}$	194/3	1.00E−10	85.7	5	3A	1574	0.2	x1H0548−322	0.3	HB	BL:0.069	PKS	0.1
1ES0552−641	05 52 04	−64 06 06	$0.17^{+0.07}_{-0.06}$	13/9	5.06E−05	56.1	7	3A	...	...	...	...	...	...	...	...
1ES0556−532	05 56 57	−53 16 07	$0.34^{+0.15}_{-0.12}$	8/4	4.66E−06	20.8	6	2A	...	...	...	...	...	...	...	...
1ES0558−504	05 58 33	−50 27 29	$2.00^{+0.46}_{-0.41}$	22/6	1.00E−10	10.9	4	3A	...	...	x1H0557−503	0.6	HB	AGN:0.137	PKS	0.6

TABLE 6—*Continued*

Slew Desig.	RA 1950	DEC 1950	IPC Rate (cts s^{-1})	NP/NS	P_{read}	Exp. (s)	PI	QI	EOS # EMSS	Δ2E (′)	A3 EXO	Δ1H (′)	Cat.	Class.: Type/z	Name	ΔC (′)
1ES0559−399	05 59 51	−39 56 35	$0.07^{+0.03}_{-0.02}$	32/4	8.98E−05	247.8	6	3A	...	...	...	...	EXC	GAL	GAL 0559-3959	2.7
1ES0602−482	06 02 48	−48 17 36	$0.60^{+0.28}_{-0.23}$	8/4	2.33E−05	11.4	5	3M	...	...	...	...	...	...	...	...
1ES0603−484	06 03 27	−48 27 25	$0.84^{+0.32}_{-0.27}$	10/4	5.37E−08	10.8	3	3M	...	...	...	...	SAO	S:G5	SAO 217708	0.5
1ES0613+227	06 13 52	+22 46 40	$0.98^{+0.33}_{-0.29}$	15/3	1.08E−07	12.7	7	3E	...	...	...	...	...	...	...	...
1ES0614+227	06 14 20	+22 45 29	$1.11^{+0.44}_{-0.37}$	12/2	1.02E−05	8.6	7	3E	...	...	...	...	HD	S:K2	HD254475	1.4
1ES0614−584	06 14 57	−58 24 41	$0.41^{+0.10}_{-0.09}$	24/9	1.00E−10	51.9	4	3A	...	...	...	...	...	...	...	...
1ES0615−655	06 15 27	−65 32 01	$0.22^{+0.10}_{-0.08}$	9/7	9.47E−05	33.3	5	3A	...	...	...	...	...	...	...	...
1ES0618−580	06 18 25	−58 02 05	$0.33^{+0.10}_{-0.08}$	19/9	1.49E−10	48.9	5	3A	...	...	...	...	SAO	S:K2V	SAO 234448	0.2
1ES0620−666	06 20 13	−66 40 21	$0.20^{+0.09}_{-0.08}$	9/8	4.87E−05	36.3	6	3A	...	...	...	...	...	...	...	...
1ES0622−526	06 22 50	−52 40 19	$0.13^{+0.04}_{-0.03}$	29/7	3.47E−07	150.4	6	3A	1642	0.3	...	x	BSC	S:F0II	HD 45348	0.2
1ES0623+187	06 23 15	+18 47 57	$0.23^{+0.06}_{-0.06}$	20/2	1.00E−10	76.5	5	3A	1646	0.7	...	...	SAO	S:K3V+	WLY 233AB	0.6
1ES0625−536	06 25 16	−53 40 34	$0.13^{+0.04}_{-0.04}$	29/9	4.06E−07	145.3	6	3E	1656	2.0	...	...	ABL	CG:0.053	A3391	1.7
1ES0625−600	06 25 27	−60 01 12	$0.19^{+0.08}_{-0.07}$	11/5	3.82E−05	45.9	6	3A	...	...	...	...	...	...	...	...
1ES0626−544	06 26 31	−54 24 00	$0.07^{+0.02}_{-0.02}$	46/6	6.78E−05	311.0	5	3E	...	...	1H0623−539	2.0	ABL	CG:0.050	A3395	2.0
1ES0627−018	06 27 17	−01 48 36	$0.49^{+0.22}_{-0.16}$	7/5	1.32E−07	13.6	6	3A	...	...	...	...	...	...	...	...
1ES0629+068	06 29 07	+06 49 03	$0.16^{+0.06}_{-0.05}$	16/7	3.29E−05	71.2	4	3A	1678	0.6	...	...	SAO	S:G3IV	SAO 114005	0.5
1ES0629+049	06 29 31	+04 57 17	$0.09^{+0.03}_{-0.03}$	28/6	1.00E−05	199.6	6	3E	1684	1.7	...	...	2E	SNR	MON. NEBULA	1.5
1ES0630−540	06 30 59	−54 03 30	$0.15^{+0.04}_{-0.04}$	25/10	1.02E−07	119.1	6	3A	1695	1.0	...	...	2E	...	...	...
1ES0630+178	06 30 59	+17 48 41	$0.14^{+0.03}_{-0.03}$	40/8	1.00E−10	215.7	3	3A	1697	0.4	...	x	SBD	S	2CG 195 +04	0.1
1ES0635−747	06 35 08	−74 44 13	$0.23^{+0.09}_{-0.08}$	13/6	1.15E−05	43.0	5	3A	1718	2.1	...	...	2E	...	...	...
1ES0635−206	06 35 23	−20 39 27	$0.14^{+0.06}_{-0.05}$	10/2	6.54E−05	57.1	6	3A	...	...	...	...	...	...	...	...
1ES0635−698	06 35 30	−69 49 44	$0.21^{+0.07}_{-0.06}$	18/11	7.73E−09	69.8	6	3A	...	...	...	...	SBD	S:G3V	HD 47875	2.2
1ES0637−752	06 37 23	−75 14 09	$0.16^{+0.06}_{-0.05}$	23/5	6.82E−06	95.0	5	3A	1720	0.6	x1H0633−752	0.5	VV	AGN:0.651	PKS	0.5
1ES0637−614	06 37 26	−61 29 16	$0.56^{+0.15}_{-0.13}$	19/9	1.00E−10	30.7	4	3A	...	...	...	...	BSC	S:G1-2V	HD48189	0.3
1ES0638+099	06 38 12	+09 57 27	$0.18^{+0.04}_{-0.04}$	29/4	1.00E−10	129.1	4	3A	1723	0.8	...	x	BSC	S:O7Ve	MON. STARS	0.9
1ES0638+094	06 38 22	+09 29 07	$0.11^{+0.03}_{-0.03}$	31/4	1.26E−07	191.5	5	3A	1724	1.3	...	x	SAO	S:B3	MON. STARS	2.0
1ES0639−756	06 39 36	−75 36 11	$0.14^{+0.06}_{-0.05}$	16/7	1.06E−04	75.3	7	2A	1725	0.4	...	...	2E	...	...	...
1ES0640+059	06 40 47	+05 54 03	$0.10^{+0.04}_{-0.03}$	18/4	1.05E−05	122.0	9	3A	1726	0.4	...	...	SAO	S:G5III	SAO 114321	0.1
1ES0642−166	06 42 56	−16 39 08	$0.83^{+0.13}_{-0.12}$	50/3	1.00E−10	56.1	2	3A	1730	0.5	...	x	MCS	WD:DA2	α CMA B	0.3
1ES0643−167	06 43 04	−16 47 50	$0.21^{+0.08}_{-0.07}$	19/3	4.89E−05	59.0	8	3M	1731	0.6	...	x	2E	CV	HL CMA	0.6
1ES0644−541	06 44 30	−54 10 18	$0.27^{+0.09}_{-0.08}$	13/10	2.52E−08	42.7	5	3A	...	...	...	...	ABL	CG	A3404	1.3
1ES0646−515	06 46 00	−51 32 09	$0.32^{+0.10}_{-0.09}$	16/7	2.52E−09	43.2	5	3A	...	...	...	...	...	...	...	...
1ES0647+250	06 47 40	+25 05 34	$0.96^{+0.39}_{-0.32}$	8/2	1.59E−10	8.1	6	3A	...	...	...	...	...	...	...	...

TABLE 6—*Continued*

Slew Desig.	RA 1950	DEC 1950	IPC Rate (cts s^{-1})	NP/NS	P_{rand}	Exp. (s)	PI	QI	EOS # EMSS	Δ2E (′)	A3 EXO	Δ1H (′)	Cat.	Class.: Type/z	Name	ΔC (′)
1ES0655+542	06 55 30	+54 15 20	$0.23^{+0.10}_{-0.08}$	9/1	2.25E−06	35.0	5	3A	1750	1.1	x	...	VV	AGN:0.044	MRK 374	0.9
1ES0657−558	06 57 28	−55 52 28	$0.22^{+0.06}_{-0.05}$	26/7	1.00E−10	96.6	6	3A	1759	0.2	...	...	2E	...	...	
1ES0702+646	07 02 27	+64 40 45	$0.17^{+0.07}_{-0.06}$	10/7	5.28E−05	46.6	4	3A	...	...	...	...	VV	AGN:0.079	VII ZW 118*	0.3
1ES0702−241	07 02 56	−24 07 24	$0.60^{+0.30}_{-0.23}$	6/2	3.00E−06	9.4	10	3A	...	...	...	...	...	...	...	...
1ES0712−363	07 12 23	−36 21 17	$0.45^{+0.20}_{-0.17}$	8/5	1.86E−05	15.5	7	3A	...	...	...	...	SAO	S:F6-7V	SAO 197732	1.3
1ES0715−810	07 15 44	−81 03 11	$0.33^{+0.16}_{-0.13}$	7/5	8.03E−06	19.1	11	3A	...	...	...	...	...	...	...	...
1ES0715−703	07 15 45	−70 19 10	$0.21^{+0.09}_{-0.08}$	10/8	3.36E−05	38.6	4	3A	...	...	...	...	...	...	...	...
1ES0715−259	07 15 56	−25 59 24	$0.13^{+0.06}_{-0.05}$	12/7	1.04E−04	66.9	7	2A	...	...	...	...	...	...	...	...
1ES0716−248	07 16 38	−24 51 32	$0.06^{+0.02}_{-0.02}$	37/11	1.51E−06	373.3	6	3A	1804	0.1	...	...	SBD	S:O9Ib	HD 57061*	0.2
1ES0717+558	07 17 24	+55 52 47	$0.31^{+0.05}_{-0.05}$	53/2	1.00E−10	147.6	6	3A	1805	1.0	1H0712+558	2.8	ABL	CG:0.038	A576	2.9
1ES0717−572	07 17 29	−57 14 55	$0.48^{+0.16}_{-0.14}$	14/9	9.27E−09	25.5	5	3A	...	...	...	...	SAO	S:G0IV-V	SAO 235087	0.9
1ES0718−313	07 18 29	−31 20 02	$0.39^{+0.17}_{-0.14}$	9/5	4.95E−06	19.8	2	3A	...	...	x	...	...	...	...	...
1ES0730+074	07 30 06	+07 29 48	$0.38^{+0.17}_{-0.14}$	8/3	5.90E−06	18.8	9	3A	...	...	...	...	...	...	...	...
1ES0731+319	07 31 27	+31 58 41	$0.90^{+0.11}_{-0.10}$	79/5	1.00E−10	82.3	5	3A	1827	0.4	x1H0729+316	0.2	A3	AC	YY GEM	0.2
1ES0735+178	07 35 12	+17 48 54	$0.04^{+0.01}_{-0.01}$	44/14	6.70E−05	463.2	6	3A	1843	0.6	x	...	HB	BL:0.424	PKS	0.6
1ES0736+053	07 36 35	+05 21 25	$1.44^{+0.58}_{-0.48}$	8/1	1.25E−10	5.4	2	3A	1849	1.4	x	...	WLY	S:F5IV	α CMI A	1.5
1ES0737+395	07 37 08	+39 30 04	$0.35^{+0.17}_{-0.14}$	7/4	9.29E−06	17.8	9	3A	...	...	...	...	...	...	...	...
1ES0737+746	07 37 46	+74 40 58	$0.30^{+0.14}_{-0.11}$	7/3	2.95E−06	21.2	7	3A	m1855	0.6	...	...	MS	BL:0.315	MS	0.6
1ES0738+612	07 38 30	+61 15 37	$0.86^{+0.33}_{-0.27}$	9/2	1.00E−10	10.2	5	3A	...	...	...	...	SAO	S:K0	SAO 014296	1.1
1ES0740+290	07 40 11	+29 00 15	$2.09^{+0.15}_{-0.15}$	197/5	1.00E−10	92.0	5	3A	1861	0.2	x1H0741+289	0.1	A3	AC	σ Gem	0.2
1ES0740+228	07 40 38	+22 50 08	$0.42^{+0.19}_{-0.15}$	8/4	9.35E−06	16.7	6	3A	...	...	...	...	SAO	S:K0	SAO 079647	0.2
1ES0742+036	07 42 03	+03 40 27	$0.39^{+0.04}_{-0.04}$	115/5	1.00E−10	261.5	4	3A	1871	0.1	x1H0743+037	0.1	A3	AC	YZ CMI	0.1
1ES0752+393	07 52 06	+39 19 30	$0.26^{+0.07}_{-0.06}$	22/1	1.00E−10	71.0	5	3A	1888	0.4	x	...	VV	AGN:0.034	MRK 382	0.6
1ES0758+574	07 58 29	+57 24 49	$0.25^{+0.06}_{-0.06}$	26/3	1.00E−10	85.8	5	3A	1900	0.3	...	...	BSC	AC:F8V	HD65626	0.5
1ES0801−398	08 01 50	−39 52 06	$0.34^{+0.09}_{-0.08}$	21/4	1.31E−10	52.3	5	3A	1910	0.4	x	...	BSC	S:O5Iaf	HD66811	0.4
1ES0801+242	08 01 51	+24 16 07	$0.91^{+0.49}_{-0.37}$	5/1	1.57E−06	5.3	9	3A	...	...	...	...	...	...	...	...
1ES0804+761	08 04 50	+76 11 34	$0.59^{+0.22}_{-0.18}$	11/3	6.73E−09	16.9	5	3A	1919	0.7	x1H0758+762	0.9	A3	AGN:0.099	PG	0.9
1ES0807−471	08 07 59	−47 11 03	$0.18^{+0.05}_{-0.04}$	26/5	1.00E−10	114.7	6	3A	1936	0.3	...	...	BSC	S:WC8+O7.5e	γ VEL	0.2
1ES0808+627	08 08 06	+62 45 39	$0.57^{+0.07}_{-0.06}$	92/6	1.00E−10	151.6	5	3A	1938	0.4	x1H0811+625	0.3	A3	CV	SU UMA	0.3
1ES0811−570	08 11 30	−57 04 44	$0.39^{+0.13}_{-0.11}$	15/5	5.44E−08	32.0	8	3A	1955	0.5	...	...	2E	...	...	...
1ES0812−188	08 12 49	−18 53 36	$2.78^{+0.40}_{-0.37}$	56/4	1.00E−10	19.7	3	3A	1959	1.1	x	...	SHA	CV	VV PUP	0.9
1ES0814−073	08 14 58	−07 21 47	$0.64^{+0.05}_{-0.05}$	215/12	1.00E−10	307.8	7	3E	1961	0.5	...	...	2E	CG:0.071	A644	0.5
1ES0815−480	08 15 49	−48 03 22	$0.23^{+0.10}_{-0.08}$	9/4	1.07E−05	33.5	10	3A	...	...	...	...	...	...	...	...

TABLE 6—*Continued*

Slew Desig.	RA 1950	DEC 1950	IPC Rate (cts s^{-1})	NP/NS	P_{rand}	Exp. (s)	PI	QI	EOS # EMSS	Δ2E (′)	A3 EXO	Δ1H (′)	Cat.	Class.: Type/z	Name	ΔC (′)
1ES0818+544	08 18 51	+54 28 16	$0.16^{+0.07}_{-0.06}$	10/3	6.33E−05	48.9	4	3A	m1971	0.3	...	...	MS	AGN:0.086	MS	0.5
1ES0821−426	08 21 26	−42 41 34	$4.34^{+0.25}_{-0.25}$	1120/11	1.00E−10	135.0	5	2A	...	...	...	...	...	...	...	...
1ES0824+662	08 24 10	+66 12 23	$0.20^{+0.08}_{-0.07}$	12/2	2.31E−05	46.2	5	3A	1987	0.3	...	...	2E	...	...	...
1ES0826−703	08 26 20	−70 21 37	$0.23^{+0.10}_{-0.08}$	11/8	6.10E−05	37.5	5	3A	...	...	...	...	...	...	...	...
1ES0826+660	08 26 34	+66 01 51	$0.15^{+0.06}_{-0.05}$	12/1	9.17E−05	61.1	6	3A	1995	1.1	...	...	2E	CG:0.181	A665	1.2
1ES0827−687	08 27 35	−68 43 09	$0.15^{+0.07}_{-0.06}$	9/7	1.02E−04	48.5	8	3A	...	...	...	...	...	...	...	...
1ES0829+237	08 29 11	+23 47 10	$0.32^{+0.15}_{-0.12}$	8/1	9.54E−06	21.7	11	3A	...	...	...	...	...	...	...	...
1ES0829+159	08 29 41	+15 59 17	$0.56^{+0.25}_{-0.20}$	8/3	7.11E−06	12.7	6	3A	...	...	...	...	SAO	S	SAO 097895	2.4
1ES0832−421	08 32 16	−42 10 50	$0.36^{+0.12}_{-0.11}$	24/2	9.11E−06	43.5	3	3E	...	...	...	...	...	...	...	...
1ES0833−450	08 33 38	−45 00 33	$1.36^{+0.20}_{-0.18}$	91/7	1.00E−10	51.0	6	3A	2014	0.4	x	...	2E	P	HU VEL	0.5
1ES0834+651	08 34 52	+65 11 10	$0.35^{+0.16}_{-0.13}$	8/2	5.60E−06	20.1	3	3A	2018	0.8	x1H0833+654	0.8	A3	AC	π^1 UMA	0.8
1ES0836+319	08 36 01	+31 57 35	$0.14^{+0.06}_{-0.05}$	9/2	3.22E−05	52.3	7	3A	2022	0.8	...	...	SAO	AC:K2III+K4I	RZ CNC	1.1
1ES0836+710	08 36 20	+71 03 33	$0.33^{+0.13}_{-0.11}$	9/6	1.80E−08	25.6	8	3A	...	...	...	...	VV	AGN:2.160	4C 71.07	0.8
1ES0837−425	08 37 05	−42 31 35	$0.48^{+0.17}_{-0.15}$	31/4	6.44E−05	35.4	3	3M	...	...	...	...	...	...	...	...
1ES0837−430	08 37 12	−43 01 00	$1.40^{+0.39}_{-0.34}$	36/4	8.64E−08	16.6	4	3M	2027	2.5	...	...	2E	...	...	...
1ES0839−446	08 39 04	−44 39 13	$0.46^{+0.12}_{-0.11}$	38/3	4.66E−08	53.5	4	3E	...	...	...	...	...	...	...	...
1ES0839−445	08 39 19	−44 31 20	$0.71^{+0.14}_{-0.13}$	50/4	1.00E−10	52.2	4	3A	...	...	...	...	HD	S:A0	HD74209	2.5
1ES0840−420	08 40 03	−42 05 45	$0.31^{+0.11}_{-0.10}$	19/2	1.20E−05	42.4	4	3A	...	...	...	...	...	...	...	...
1ES0841−436	08 41 50	−43 39 23	$0.21^{+0.07}_{-0.06}$	56/3	3.76E−05	119.5	3	1A	...	...	...	...	...	...	...	...
1ES0842−425	08 42 21	−42 35 06	$0.49^{+0.16}_{-0.14}$	32/2	1.40E−05	37.8	3	1A	...	...	...	...	...	...	...	...
1ES0844+349	08 44 35	+34 56 17	$0.13^{+0.06}_{-0.05}$	12/4	3.48E−05	69.9	5	3A	2048	0.3	x	...	VV	AGN:0.064	PG	0.3
1ES0847+267	08 47 42	+26 44 00	$0.19^{+0.09}_{-0.07}$	8/5	4.74E−05	36.0	6	3A	...	...	...	...	...	...	...	...
1ES0849+080	08 49 34	+08 04 57	$0.48^{+0.07}_{-0.07}$	58/3	1.00E−10	107.4	5	3A	m2060	0.3	x	...	VV	AGN:0.063	1E	0.7
1ES0851+392	08 51 05	+39 17 20	$0.53^{+0.18}_{-0.16}$	12/1	5.39E−09	20.6	3	3A	...	...	...	...	...	...	...	...
1ES0851+203	08 51 57	+20 18 07	$0.45^{+0.03}_{-0.03}$	243/17	1.00E−10	489.7	5	3A	2076	0.1	x	...	HB	BL:0.306	OJ 287	0.2
1ES0853−445	08 53 20	−44 32 51	$0.58^{+0.17}_{-0.15}$	28/1	1.07E−07	33.7	2	3E	...	...	...	...	...	...	...	...
1ES0853−448	08 53 58	−44 52 30	$0.69^{+0.21}_{-0.19}$	27/2	6.15E−07	26.4	3	3E	...	...	...	...	...	...	...	...
1ES0856+369	08 56 56	+36 58 04	$0.11^{+0.04}_{-0.04}$	15/5	2.78E−05	97.2	4	3A	2084	0.7	...	...	SBD	S:Fe	SAO 61189	2.8
1ES0906−094A	09 06 20	−09 26 19	$0.25^{+0.07}_{-0.07}$	27/3	9.36E−08	75.5	6	3M	2100	2.6	1H0906−095	1.4	ABL	CG:0.053	A754	1.0
1ES0906−094B	09 06 45	−09 28 30	$0.49^{+0.09}_{-0.09}$	43/3	1.00E−10	73.9	7	3M	2103	1.2	x	...	2E	CG:0.053	A754	1.2
1ES0914+519	09 14 28	+51 55 48	$0.22^{+0.10}_{-0.08}$	8/6	3.54E−05	31.4	6	3A	...	...	...	...	ABL	CG:0.197	A773	0.9
1ES0915+165	09 15 40	+16 30 26	$0.47^{+0.08}_{-0.07}$	43/3	1.00E−10	85.3	7	3A	2116	0.6	...	...	VV	AGN:0.029	MRK 704	0.6
1ES0915−118	09 15 41	−11 53 15	$0.81^{+0.21}_{-0.18}$	20/3	1.00E−10	23.3	6	3A	2117	0.4	x1H0917−121	0.2	A3	AGN:0.055	3C218	0.2

TABLE 6—*Continued*

Slew Desig.	RA 1950	DEC 1950	IPC Rate (cts s^{-1})	NP/NS	P_{rand}	Exp. (s)	PI	QI	EOS # EMSS	Δ2E (′)	A3 EXO	Δ1H (′)	Cat.	Class.: Type/z	Name	ΔC (′)
1ES0919−549	09 19 03	−54 59 23	$4.33^{+1.87}_{-1.49}$	7/1	1.00E−10	1.6	6	3A	...	...	x1H0918−548	1.1	A3	XRB	X0918-549	1.1
1ES0919+404	09 19 15	+40 24 41	$0.86^{+0.38}_{-0.31}$	7/2	2.43E−08	7.8	6	3A	...	...	...	...	SAO	S:K2V	SAO 042826	1.0
1ES0920−136	09 20 30	−13 36 51	$0.63^{+0.31}_{-0.24}$	6/1	7.71E−07	9.0	7	3A	...	...	...	...	SAO	S:K0IV	SAO 155136	0.6
1ES0921+143	09 21 25	+14 22 29	$0.13^{+0.05}_{-0.04}$	16/2	1.19E−05	93.0	7	1A	2131	1.5	...	...	ABL	CG:0.136	A795	1.8
1ES0921−630	09 21 28	−63 04 39	$0.50^{+0.13}_{-0.11}$	21/9	1.00E−10	38.7	6	3A	...	...	x1H0920−629	0.4	A3	XRB	2S	0.4
1ES0921+525	09 21 44	+52 30 41	$1.40^{+0.25}_{-0.23}$	39/11	1.00E−10	26.5	5	3A	...	...	...	...	VV	AGN:0.036	MRK 110	0.6
1ES0923+129	09 23 18	+12 56 32	$0.34^{+0.15}_{-0.12}$	8/1	1.85E−06	20.9	5	3A	2139	0.7	x1H0929+122	0.7	VV	AGN:0.028	MRK 705	0.7
1ES0923+392	09 23 56	+39 15 09	$0.12^{+0.04}_{-0.04}$	22/3	1.05E−05	126.0	5	3A	2141	0.2	x	...	VV	AGN:0.698	4C 39.25	0.3
1ES0927+500	09 27 11	+50 04 49	$0.65^{+0.23}_{-0.20}$	11/6	1.84E−09	15.6	5	3A	...	...	...	...	SBD	...	H 0927+50.1	2.6
1ES0929+216	09 29 14	+21 41 48	$0.10^{+0.03}_{-0.03}$	19/4	1.66E−06	140.7	5	3A	2151	2.4	...	...	RNG	GAL:0.002	NGC 2903	1.1
1ES0930+700	09 30 04	+70 03 18	$0.82^{+0.09}_{-0.09}$	88/5	1.00E−10	102.6	5	3A	2153	0.2	...	...	BSC	S:G4III-IV	DK UMA	0.3
1ES0939+759	09 39 18	+75 57 37	$0.37^{+0.18}_{-0.15}$	6/4	4.13E−06	15.1	9	3A	...	...	...	...	...	...	...	...
1ES0942+098	09 42 49	+09 50 03	$0.24^{+0.06}_{-0.06}$	21/4	1.00E−10	77.6	5	3A	m2182	0.4	1H0932+107	0.0	VV	AGN:0.013	VV	0.8
1ES0943−140	09 43 17	−14 05 55	$0.40^{+0.10}_{-0.09}$	25/6	1.00E−10	54.4	8	3A	2183	0.3	x1H0946−144	0.3	VV	AGN:0.008	NGC 2992	0.2
1ES0950+495	09 50 52	+49 30 09	$0.23^{+0.08}_{-0.07}$	15/7	5.10E−07	53.4	5	3A	m2193	0.6	...	...	MS	BL	MS	1.2
1ES0951+693	09 51 24	+69 18 32	$0.19^{+0.03}_{-0.03}$	61/8	1.00E−10	260.6	6	3A	2195	0.4	x1H0950+696.B	0.5	VV	AGN:0.000	M81	0.5
1ES0951+699	09 51 39	+69 54 29	$0.41^{+0.06}_{-0.05}$	74/10	1.00E−10	160.4	6	3A	2197	0.6	x1H0950+696.A	0.5	A3	GAL:0.001	M82	0.5
1ES0953+693	09 53 53	+69 18 37	$0.08^{+0.03}_{-0.03}$	28/4	3.08E−05	203.4	6	3A	2199	0.4	x	...	SBD	GAL:0.175	UGC 5336*	2.6
1ES0957+247	09 57 09	+24 47 35	$0.97^{+0.30}_{-0.26}$	14/3	1.00E−10	13.7	4	3A	...	...	...	...	SAO	AC:K0VE+B:	DH LEO	1.3
1ES1002−559	10 02 09	−55 56 13	$0.43^{+0.17}_{-0.14}$	9/5	1.13E−07	19.2	6	3A	...	...	...	...	SAO	S:K1-2III	SAO 237656	0.7
1ES1003+677	10 03 06	+67 46 59	$0.12^{+0.05}_{-0.04}$	15/4	1.95E−05	92.4	7	3A	2225	1.7	...	...	SHA	CV	CH UMA	0.5
1ES1007+491	10 07 09	+49 08 44	$0.21^{+0.09}_{-0.08}$	10/2	3.91E−05	37.4	5	3A	...	...	...	...	...	...	...	...
1ES1011+496	10 11 52	+49 41 07	$0.63^{+0.21}_{-0.18}$	12/2	1.00E−10	17.7	5	3A	2250	0.7	1H1013+498	0.6	HB	BL	GB 1011+498	0.6
1ES1016+201	10 16 49	+20 07 40	$1.58^{+0.20}_{-0.18}$	74/3	1.00E−10	45.3	4	3A	2259	1.0	x	...	WLY	S:M4EV	AD LEO	1.2
1ES1020+493	10 20 31	+49 20 17	$0.25^{+0.10}_{-0.09}$	11/4	3.36E−06	36.3	7	3A	...	...	...	...	SBD	S:F5	HD 89944	2.9
1ES1020+201	10 20 45	+20 07 31	$0.42^{+0.05}_{-0.05}$	82/7	1.00E−10	175.2	7	3A	2275	0.3	x1H1017+202	0.5	VV	AGN:0.004	NGC 3227	0.6
1ES1022+519	10 22 23	+51 57 09	$0.42^{+0.17}_{-0.14}$	10/4	1.27E−06	20.6	4	3A	2283	2.8	...	...	VV	AGN:0.045	MRK 142	1.3
1ES1023+207	10 23 00	+20 46 25	$0.15^{+0.06}_{-0.05}$	10/5	3.62E−05	54.7	7	3A	...	...	...	...	...	...	...	...
1ES1028+511	10 28 14	+51 08 56	$1.91^{+0.52}_{-0.45}$	16/5	1.00E−10	8.3	4	3A	...	...	...	...	...	...	...	...
1ES1034−272	10 34 18	−27 17 32	$0.28^{+0.08}_{-0.07}$	23/3	2.21E−08	62.8	7	3A	...	...	1H1033−273	2.4	A3	CG:0.012	A1060	2.4
1ES1035−268	10 35 30	−26 51 48	$0.14^{+0.05}_{-0.05}$	14/3	2.10E−05	75.1	7	3A	2300	0.3	...	...	ZCT	GAL:0.010	I2597*	2.7
1ES1039−630	10 39 23	−63 00 21	$0.23^{+0.10}_{-0.08}$	9/8	7.45E−06	33.4	7	3A	...	...	...	...	...	...	...	...
1ES1042−594	10 42 28	−59 27 41	$0.20^{+0.07}_{-0.06}$	27/10	1.03E−04	77.1	6	3M	2313	1.6	...	...	SAO	S:B	SAO 238418	1.7

TABLE 6—*Continued*

Slew Desig.	RA 1950	DEC 1950	IPC Rate (cts s^{-1})	NP/NS	P_{rand}	Exp. (s)	PI	QI	EOS # EMSS	Δ2E (′)	A3 EXO	Δ1H (′)	Cat.	Class.: Type/z	Name	ΔC (′)
1ES1043−594	10 43 16	−59 25 16	$0.32^{+0.09}_{-0.08}$	33/9	4.36E−08	69.8	7	3M	2318	1.1	x1H1045−597	1.1	A3	S:PEC	η CAR	1.2
1ES1044−491	10 44 33	−49 07 58	$0.65^{+0.31}_{-0.24}$	6/5	9.65E−09	9.0	5	3A	2326	1.7	...	...	BSC	S:G5III+G2V	ν VEL	1.4
1ES1044+549	10 44 37	+54 54 35	$0.64^{+0.34}_{-0.27}$	5/2	1.46E−06	7.5	5	3A	...	...	...	...	...	...	...	...
1ES1047+070	10 47 46	+07 00 38	$0.17^{+0.08}_{-0.07}$	9/1	6.42E−05	42.3	8	3A	...	...	...	...	...	...	...	...
1ES1048−596	10 48 04	−59 37 21	$0.16^{+0.06}_{-0.05}$	15/6	8.42E−06	69.6	9	3A	2336	0.5	x	...	2E	P	2E	0.5
1ES1052+607	10 52 33	+60 44 09	$0.57^{+0.10}_{-0.09}$	43/4	1.00E−10	69.2	5	3A	...	...	x1H1051+607	0.4	A3	AC	DM UMA	0.4
1ES1053+072	10 53 58	+07 17 16	$0.17^{+0.07}_{-0.06}$	10/2	8.64E−05	46.8	6	3A	2358	0.8	...	...	GCV	S:M6.5VE	CN LEO	2.8
1ES1055+605	10 55 29	+60 31 47	$0.20^{+0.09}_{-0.07}$	9/4	1.86E−05	37.8	3	3A	...	...	x	...	HB	AGN:0.149	E1055+605	1.8
1ES1055−521	10 55 51	−52 11 24	$0.10^{+0.02}_{-0.02}$	67/10	1.00E−10	477.5	3	3A	2365	0.8	x	...	2E	P	2E	0.7
1ES1100+772	11 00 17	+77 15 01	$0.18^{+0.04}_{-0.04}$	36/5	1.00E−10	161.2	5	3A	2389	0.7	...	...	HB	AGN:0.311	3C249.1	0.6
1ES1101−606	11 01 03	−60 39 02	$0.21^{+0.04}_{-0.03}$	57/10	1.00E−10	218.3	7	3E	...	...	...	...	SAO	S:M0	SAO 251235	0.4
1ES1101−232	11 01 10	−23 12 08	$1.90^{+0.56}_{-0.48}$	14/3	1.00E−10	7.2	6	3A	...	...	1H1100−230	1.2	VV	BL	4U 1057-21	2.3
1ES1101+384	11 01 42	+38 28 26	$3.36^{+0.22}_{-0.22}$	236/4	1.00E−10	69.2	4	3A	2393	0.4	x1H1104+382	0.4	VV	BL:0.031	MRK 421*	0.4
1ES1103+728	11 03 28	+72 50 03	$0.17^{+0.03}_{-0.03}$	45/5	1.00E−10	208.7	7	3A	2395	0.3	x	...	VV	AGN:0.009	NGC 3516	0.5
1ES1105+833	11 05 20	+83 21 54	$0.47^{+0.22}_{-0.18}$	7/3	1.69E−06	13.6	3	3A	...	...	...	...	SAO	S:K0	SAO 001824	1.0
1ES1111−374	11 11 38	−37 24 30	$0.26^{+0.05}_{-0.05}$	39/4	1.00E−10	126.5	5	3A	2424	0.2	...	...	2E	CV	V 436 CEN	0.1
1ES1113+432	11 13 01	+43 15 12	$10.12^{+1.32}_{-1.23}$	64/2	1.00E−10	6.3	3	3A	...	...	...	...	...	...	...	...
1ES1113−369	11 13 06	−36 58 13	$0.11^{+0.05}_{-0.04}$	12/3	9.79E−05	79.7	6	3A	...	...	...	...	...	...	...	...
1ES1115+318	11 15 28	+31 48 49	$2.58^{+0.55}_{-0.49}$	26/4	1.00E−10	9.8	6	3A	2440	0.6	1H1121+309.B	0.7	A3	AC	ξ UMA	0.7
1ES1116+686	11 16 21	+68 41 31	$0.39^{+0.17}_{-0.14}$	8/6	6.34E−07	19.0	5	3A	...	...	...	...	...	...	...	...
1ES1118+424	11 18 01	+42 26 51	$1.16^{+0.30}_{-0.27}$	18/5	1.00E−10	15.0	4	3A	...	...	x	...	EHG	BL	EXO	1.2
1ES1119−603	11 19 02	−60 21 12	$8.32^{+0.45}_{-0.45}$	352/8	1.00E−10	41.8	7	3A	2450	0.4	x1H1118−602	0.2	A3	XRB	CEN X-3	0.2
1ES1121−012	11 21 02	−01 14 51	$0.52^{+0.27}_{-0.21}$	5/3	3.43E−09	9.5	6	3A	...	...	...	...	SBD	GAL	Z 1121.0-0117	2.2
1ES1122−589	11 22 15	−58 59 09	$5.82^{+0.31}_{-0.31}$	371/20	1.00E−10	62.9	6	3A	2460	1.3	x1H1121−591	1.1	A3	SNR	MSH 11-54	1.1
1ES1126−610	11 26 48	−61 00 17	$0.37^{+0.17}_{-0.14}$	8/5	1.75E−05	18.5	7	2A	...	...	...	...	SBD	S:A	HD 306536	0.4
1ES1133+704	11 33 24	+70 26 14	$1.72^{+0.21}_{-0.20}$	79/9	1.00E−10	44.0	4	3A	2487	0.9	x1H1137+699	0.8	VV	BL:0.046	MRK 180	0.7
1ES1136−374	11 36 34	−37 27 54	$0.84^{+0.07}_{-0.07}$	151/6	1.00E−10	171.1	6	3A	2501	0.2	x1H1135−372	0.3	VV	AGN:0.009	NGC 3783	0.3
1ES1136+342	11 36 34	+34 12 42	$0.35^{+0.15}_{-0.12}$	9/2	4.28E−07	22.9	5	3A	m2499	0.6	...	...	VV	AGN:0.033	VV	0.5
1ES1137−651	11 37 06	−65 07 18	$1.29^{+0.39}_{-0.33}$	14/4	1.00E−10	10.5	6	3A	...	...	1H1137−649	0.4	A3	AC	HD101379	0.4
1ES1137+660	11 37 06	+66 03 55	$0.14^{+0.03}_{-0.03}$	41/6	1.00E−10	217.8	5	3A	2503	0.7	x	...	HB	AGN:0.646	3C 263	0.6
1ES1138+522	11 38 05	+52 16 38	$0.17^{+0.07}_{-0.06}$	15/5	1.73E−05	63.0	6	3A	2507	0.2	...	...	GCV	AC:F9+K1IV	RW UMA	0.1
1ES1140+719	11 40 48	+71 58 10	$0.40^{+0.08}_{-0.07}$	38/9	1.00E−10	82.4	6	3A	m2515	0.3	1H1140+719	0.2	A3	CV	YY DRA	0.2
1ES1141+799	11 41 56	+79 57 50	$0.47^{+0.22}_{-0.18}$	7/5	3.87E−06	13.6	6	3A	...	...	...	...	UGC	GAL	UO6728	1.5

TABLE 6—*Continued*

Slew Desig.	RA 1950	DEC 1950	IPC Rate (cts s^{-1})	NP/NS	P_{rand}	Exp. (s)	PI	QI	EOS # EMSS	Δ2E (′)	A3 EXO	Δ1H (′)	Cat.	Class.: Type/z	Name	ΔC (′)
1ES1142+198	11 42 28	+19 52 42	$0.15^{+0.03}_{-0.03}$	65/3	1.13E−10	266.5	6	3E	2521	0.7	x	...	VV	AGN:0.021	NGC 3862	0.5
1ES1143−550	11 43 20	−55 04 04	$0.20^{+0.10}_{-0.08}$	8/5	4.24E−05	33.2	4	3A	...	...	...	...	...	...	...	...
1ES1145+204	11 45 27	+20 29 37	$0.41^{+0.10}_{-0.09}$	23/3	1.00E−10	50.6	5	3A	2534	0.6	...	...	SAO	AC:A7V+G5III	SAO 081998	0.3
1ES1145−619	11 45 35	−61 54 25	$0.38^{+0.14}_{-0.12}$	13/7	1.05E−07	29.1	6	3A	2535	1.2	x1H1144−617.B	1.3	2E	P	V801 CEN	1.3
1ES1147−625	11 47 36	−62 30 24	$0.31^{+0.08}_{-0.07}$	30/6	1.09E−10	74.4	5	3E	2541	0.4	x	...	SBD	S:B9V	HD 102867	1.9
1ES1148−624	11 48 56	−62 24 34	$0.20^{+0.07}_{-0.06}$	21/3	2.57E−05	68.2	5	3E	...	...	...	...	SBD	S:B8	HD 309207	2.7
1ES1148−620	11 48 57	−62 01 35	$0.29^{+0.10}_{-0.09}$	17/7	1.36E−06	44.6	5	3A	2550	1.1	x	...	2E	...	...	...
1ES1149−110	11 49 33	−11 05 21	$0.63^{+0.25}_{-0.20}$	9/6	5.08E−09	13.5	4	3A	...	...	...	...	VV	AGN:0.049	PG	0.6
1ES1155+557	11 55 25	+55 43 51	$0.44^{+0.10}_{-0.09}$	26/2	1.00E−10	51.7	5	3A	2561	0.3	x	...	VV	AGN:0.003	NGC 3998	0.6
1ES1159+583	11 59 37	+58 19 14	$0.09^{+0.03}_{-0.03}$	19/4	9.26E−05	140.0	5	3E	2574	0.4	...	...	2E	CG:0.103	A1446	1.0
1ES1200+448	12 00 35	+44 48 36	$0.94^{+0.08}_{-0.08}$	164/8	1.00E−10	166.2	4	3A	2578	0.3	x1H1205+440	0.2	VV	AGN:0.002	NGC 4051	0.2
1ES1201+021	12 01 54	+02 09 44	$0.47^{+0.21}_{-0.17}$	8/4	1.20E−05	15.0	5	3A	2583	0.7	...	...	2E	CG:0.020	MKW 4	0.8
1ES1202+281	12 02 09	+28 10 35	$0.23^{+0.07}_{-0.07}$	17/2	3.71E−08	60.0	6	3A	2584	0.5	...	...	HB	AGN:0.165	GQ COM	0.3
1ES1204−526	12 04 29	−52 36 04	$0.08^{+0.03}_{-0.03}$	28/14	2.83E−05	198.6	6	3A	...	...	...	...	...	...	...	...
1ES1207−521	12 07 24	−52 09 45	$0.07^{+0.02}_{-0.02}$	44/13	8.12E−05	311.6	6	3A	2599	0.2	...	...	2E	SNR	PKS	0.2
1ES1208+396	12 08 02	+39 41 04	$0.31^{+0.03}_{-0.03}$	158/15	1.00E−10	438.9	6	3A	2603	0.2	x1H1210+393	0.1	VV	AGN:0.003	NGC 4151	0.2
1ES1209−524	12 09 00	−52 26 43	$0.08^{+0.03}_{-0.02}$	67/11	3.63E−05	344.1	4	3E	...	...	...	...	...	...	...	...
1ES1210−646	12 10 36	−64 36 06	$0.55^{+0.10}_{-0.09}$	42/12	1.00E−10	69.5	7	3A	...	...	...	...	...	...	...	...
1ES1211+143	12 11 45	+14 20 02	$1.38^{+0.17}_{-0.16}$	75/2	1.00E−10	52.7	5	3A	2620	0.4	x	...	VV	AGN:0.085	PG	0.2
1ES1212−652	12 12 04	−65 15 40	$0.25^{+0.11}_{-0.09}$	11/8	8.67E−05	33.1	7	3E	...	...	...	...	SBD	S:G0/G1V:	HD 106392	1.7
1ES1212−651	12 12 30	−65 09 31	$0.42^{+0.13}_{-0.11}$	16/9	7.51E−10	33.1	5	3E	...	...	...	...	...	...	...	...
1ES1212+334	12 12 33	+33 28 08	$0.17^{+0.05}_{-0.05}$	19/4	1.23E−07	88.4	7	3A	2626	0.6	...	...	UGC	GAL:0.004	NGC 4203	0.6
1ES1212+078	12 12 36	+07 48 53	$0.25^{+0.11}_{-0.09}$	10/7	3.38E−05	32.4	7	3A	...	...	...	...	SAO	S:K0	SAO 119284	0.9
1ES1213+728	12 13 26	+72 49 32	$0.58^{+0.08}_{-0.08}$	62/9	1.00E−10	99.1	5	3A	2631	0.3	1H1213+718.A	0.4	A3	AC	DK DRA	0.4
1ES1214+328	12 14 32	+32 48 14	$0.15^{+0.06}_{-0.05}$	11/3	2.36E−05	59.6	9	3A	...	...	...	...	...	...	...	...
1ES1215+039	12 15 03	+03 54 51	$0.34^{+0.13}_{-0.11}$	11/4	1.64E−06	27.7	7	3A	...	...	...	...	SBD	GAL:0.075	4C +04.41*	1.6
1ES1215+303	12 15 20	+30 22 34	$0.22^{+0.06}_{-0.06}$	21/4	2.92E−10	78.3	4	3A	2644	1.2	x	...	HB	BL	ON 325	1.1
1ES1215+300	12 15 55	+30 05 24	$0.95^{+0.14}_{-0.13}$	59/5	1.00E−10	58.8	4	3A	m2648	0.4	x1H1219+301.B	0.2	VV	AGN:0.012	MRK 766	0.2
1ES1216+426	12 16 21	+42 39 16	$0.23^{+0.10}_{-0.09}$	8/4	2.01E−05	30.3	8	3A	...	...	...	...	...	...	...	...
1ES1217+023	12 17 40	+02 19 30	$0.26^{+0.05}_{-0.04}$	47/10	1.00E−10	147.3	6	3A	2661	1.1	x	...	HB	AGN:0.240	ON 029	0.9
1ES1218+637	12 18 05	+63 43 44	$0.39^{+0.19}_{-0.15}$	7/2	2.21E−05	16.0	9	3A	...	...	...	...	...	...	...	...
1ES1218−637	12 18 45	−63 47 07	$0.13^{+0.04}_{-0.04}$	18/9	1.67E−06	106.3	5	3A	2671	0.4	...	...	2E	SNR*	1218-63.7	0.1
1ES1218+304	12 18 50	+30 27 12	$2.25^{+0.76}_{-0.63}$	11/2	1.00E−10	4.8	5	3A	...	...	x1H1219+301.A	0.4	VV	BL	3A 1218+303	0.3

TABLE 6—*Continued*

Slew Desig.	RA 1950	DEC 1950	IPC Rate (cts s^{-1})	NP/NS	P_{rand}	Exp. (s)	PI	QI	EOS # EMSS	Δ2E (′)	A3 EXO	Δ1H (′)	Cat.	Class.: Type/z	Name	ΔC (′)
1ES1218+285	12 18 57	+28 30 39	$0.23^{+0.07}_{-0.06}$	19/2	6.13E−09	66.3	7	3A	2673	1.1	...	...	VV	BL:0.102	ON 231	0.9
1ES1219+755	12 19 31	+75 35 29	$0.47^{+0.04}_{-0.04}$	147/13	1.00E−10	281.9	5	3A	m2677	0.2	x1H1211+762	0.3	HB	AGN:0.070	MRK 205	0.3
1ES1219+044	12 19 48	+04 29 32	$0.13^{+0.03}_{-0.03}$	43/6	5.72E−10	220.7	6	3A	2679	0.6	...	...	HB	AGN:0.965	PKS	0.5
1ES1223+132	12 23 37	+13 14 48	$0.30^{+0.08}_{-0.07}$	26/3	2.43E−10	68.1	5	3A	2707	2.2	...	...	UGC	GAL:-0.001	N4406	1.5
1ES1223−628	12 23 57	−62 48 58	$1.16^{+0.28}_{-0.24}$	21/9	1.00E−10	17.7	4	3A	...	...	x	...	SAO	S:B1V+B0.5V	α^2 CRU	1.0
1ES1226+023	12 26 34	+02 19 44	$3.20^{+0.12}_{-0.12}$	712/8	1.00E−10	218.5	5	3A	2729	0.2	x1H1226+022	0.1	VV	AGN:0.158	3C 273.0	0.2
1ES1227+082	12 27 15	+08 16 18	$0.25^{+0.04}_{-0.04}$	70/9	1.00E−10	225.3	6	3A	2735	0.2	1H1228+081	0.2	A3	GAL:0.003	N4472	0.3
1ES1228−465	12 28 08	−46 30 24	$0.45^{+0.20}_{-0.16}$	7/4	4.68E−07	14.7	7	3A	...	...	...	...	SAO	S:F5V	SAO 223481	0.8
1ES1228+126	12 28 17	+12 39 01	$2.50^{+0.51}_{-0.46}$	37/4	1.00E−10	12.6	6	3E	2744	1.0	x1H1226+128	1.0	A3	CG:0.004	VIRGO CL.	1.0
1ES1229+710	12 29 30	+71 00 35	$0.20^{+0.07}_{-0.06}$	18/10	6.35E−08	70.5	5	3A	...	...	...	...	...	...	...	...
1ES1230+176	12 30 13	+17 39 55	$0.21^{+0.10}_{-0.08}$	9/5	4.94E−05	35.4	9	3A	...	...	...	...	...	...	...	...
1ES1231+100	12 31 49	+10 05 13	$0.17^{+0.07}_{-0.06}$	15/8	9.38E−06	64.9	6	3A	...	...	...	...	...	...	...	...
1ES1233−634	12 33 45	−63 27 54	$0.45^{+0.14}_{-0.12}$	15/3	2.36E−09	29.2	6	3A	...	...	...	...	...	...	...	...
1ES1234+223	12 34 01	+22 18 56	$0.16^{+0.06}_{-0.05}$	14/4	4.28E−06	67.7	6	3A	...	...	...	...	...	...	...	...
1ES1234+459	12 34 26	+45 55 22	$0.32^{+0.13}_{-0.11}$	10/4	2.78E−06	26.6	6	3A	...	...	...	...	SBD	GAL	Z 1234.5+4556	0.9
1ES1235+120	12 35 10	+12 05 16	$0.23^{+0.04}_{-0.04}$	47/9	1.00E−10	161.7	6	3A	2801	0.6	...	...	VV	AGN:0.005	NGC 4579	0.6
1ES1235−399	12 35 42	−39 55 37	$0.10^{+0.04}_{-0.03}$	24/5	6.33E−05	150.5	6	3A	...	...	...	...	...	...	...	...
1ES1238−332	12 38 07	−33 17 59	$0.38^{+0.18}_{-0.14}$	7/4	1.56E−05	16.6	7	3A	...	...	...	...	SBD	GAL	ESO 381- 7	0.4
1ES1239−011	12 39 04	−01 10 45	$0.86^{+0.42}_{-0.33}$	6/1	2.07E−07	6.7	4	3A	...	...	...	...	WLY	S:F0V	WLY 482A	0.8
1ES1239+069	12 39 23	+06 54 56	$0.25^{+0.11}_{-0.09}$	10/6	2.43E−05	32.4	7	3A	...	...	...	...	...	...	...	...
1ES1239−627	12 39 50	−62 46 38	$0.26^{+0.08}_{-0.07}$	17/3	3.89E−09	55.9	7	3A	2828	0.3	1H1249−637	0.6	BSC	S:B2pe	HD 110432	0.6
1ES1240+029	12 40 17	+02 57 38	$0.36^{+0.07}_{-0.06}$	46/7	1.00E−10	107.2	5	3A	2829	0.2	...	...	UGC	GAL:0.003	N4636	0.4
1ES1241+275	12 41 06	+27 33 10	$0.32^{+0.15}_{-0.12}$	7/4	6.85E−06	19.7	4	3A	...	...	...	...	ABL	CG:0.241	A1602	1.6
1ES1241+723	12 41 24	+72 18 18	$0.24^{+0.11}_{-0.09}$	8/5	6.08E−05	28.3	7	3A	...	...	...	...	...	...	...	...
1ES1244+026	12 44 02	+02 38 32	$0.39^{+0.07}_{-0.06}$	52/7	1.00E−10	116.3	5	3A	2854	0.4	...	...	VV	AGN:0.048	PG	0.0
1ES1246−410	12 46 00	−41 01 34	$1.04^{+0.09}_{-0.09}$	161/7	1.00E−10	135.7	6	3A	2862	1.0	x1H1244−409	0.7	ABL	CG:0.011	A3526	1.2
1ES1246+085	12 46 03	+08 35 43	$0.08^{+0.03}_{-0.03}$	25/4	1.64E−05	186.8	6	3A	2861	0.7	...	...	2E	...	...	...
1ES1246+605	12 46 30	+60 35 50	$0.19^{+0.05}_{-0.04}$	26/2	1.00E−10	111.6	6	3A	2865	0.3	1H1241+626.B	0.3	A3	AC	HD111456	0.3
1ES1246−588	12 46 39	−58 48 40	$1.91^{+0.40}_{-0.36}$	27/7	1.00E−10	13.7	7	3A	...	...	x1H1244−588	0.5	A3	XRB	X1246-588	0.5
1ES1248−296	12 48 55	−29 39 45	$0.41^{+0.18}_{-0.14}$	8/4	8.54E−07	17.8	8	3E	...	...	...	...	...	...	...	...
1ES1249−296	12 49 06	−29 37 03	$0.35^{+0.17}_{-0.14}$	7/6	1.43E−05	17.6	6	3A	...	...	...	...	...	...	...	...
1ES1249+174	12 49 13	+17 28 11	$0.20^{+0.10}_{-0.08}$	8/4	9.53E−05	32.6	9	3A	...	...	...	...	...	...	...	...
1ES1249+278	12 49 17	+27 48 03	$0.48^{+0.17}_{-0.14}$	12/3	4.00E−10	22.8	4	3A	2874	0.9	x	...	BSC	S:G0IIIp	HD111812	0.8

TABLE 6—*Continued*

Slew Desig.	RA 1950	DEC 1950	IPC Rate (cts s^{-1})	NP/NS	P_{rand}	Exp. (s)	PI	QI	EOS # EMSS	Δ2E (′)	A3 EXO	Δ1H (′)	Cat.	Class.: Type/z	Name	ΔC (′)
1ES1249−131	12 49 36	−13 07 52	$0.45^{+0.20}_{-0.16}$	8/2	2.76E−06	15.9	6	3A	...	...	x	...	VV	AGN:0.014	IRAS 1249-13	0.8
1ES1249−289	12 49 43	−28 58 41	$4.08^{+0.22}_{-0.22}$	354/5	1.00E−10	85.6	6	3A	2876	0.2	x1H1251−291	0.0	A3	CV	EX HYA	0.1
1ES1252−060	12 52 20	−06 03 36	$0.12^{+0.05}_{-0.04}$	16/3	6.42E−05	88.6	7	3A	...	...	...	...	WLY	S:K8V	WLY 9424	0.6
1ES1253+275	12 53 14	+27 31 15	$0.23^{+0.09}_{-0.07}$	15/4	7.19E−06	49.3	5	3A	2896	0.6	...	...	SBD	GAL:0.024	Z 1253.3+2731	1.4
1ES1253−055	12 53 38	−05 31 13	$0.19^{+0.04}_{-0.04}$	31/4	1.00E−10	132.6	6	3A	2900	0.5	x	...	HB	AGN:0.538	3C 279	0.5
1ES1254−690	12 54 27	−69 00 21	$6.97^{+2.04}_{-1.73}$	14/2	1.00E−10	2.0	8	3A	2908	0.8	x1H1254−690	0.9	A3	XRB	X1254-690	1.0
1ES1254−171	12 54 31	−17 08 59	$0.24^{+0.06}_{-0.05}$	32/2	1.00E−10	105.9	6	3A	2909	0.6	...	...	SBD	CG:0.048	A1644	0.8
1ES1254+223	12 54 36	+22 18 06	$0.63^{+0.06}_{-0.06}$	136/12	1.00E−10	200.9	2	3A	2912	0.6	x	...	MCS	WD:DA	EG 187	0.3
1ES1254−172	12 54 51	−17 12 21	$0.12^{+0.04}_{-0.04}$	21/2	6.21E−05	110.2	7	2A	...	...	...	...	EXC	GAL:0.046	GAL 1254-1710*	1.7
1ES1255+244	12 55 06	+24 28 54	$0.36^{+0.12}_{-0.10}$	14/8	1.18E−09	34.2	7	3A	...	...	...	...	...	...	...	...
1ES1255+354	12 55 20	+35 29 16	$0.17^{+0.03}_{-0.03}$	53/6	1.00E−10	243.9	4	3A	m2920	0.7	...	...	WLY	S:M0EV	BF CVN	0.6
1ES1256−014	12 56 08	−01 28 58	$0.58^{+0.09}_{-0.09}$	53/3	1.00E−10	82.6	6	3A	2925	0.5	...	...	ABL	CG:0.084	A1650	1.0
1ES1256−039	12 56 45	−03 54 22	$0.51^{+0.20}_{-0.17}$	10/2	3.89E−07	17.3	6	3A	...	...	...	...	ABL	CG:0.083	A1651	1.0
1ES1257+282	12 57 10	+28 13 02	$0.71^{+0.07}_{-0.07}$	244/4	1.00E−10	235.6	6	3A	2931	0.6	x	...	2E	CG:0.023	COMA CL.	0.6
1ES1257+286	12 57 59	+28 40 41	$0.14^{+0.03}_{-0.03}$	62/4	1.00E−10	268.7	5	3A	2935	0.7	x	...	HB	AGN:0.092	X COM	0.5
1ES1258+126	12 58 19	+12 37 54	$0.33^{+0.10}_{-0.08}$	18/2	1.46E−10	47.8	3	3A	2940	0.7	x	...	WLY	S:M2EV	DT VIR	0.8
1ES1259+289	12 59 07	+28 54 05	$0.12^{+0.04}_{-0.03}$	28/5	8.16E−07	149.8	5	3A	2946	0.7	...	...	GCV	S:G2III	UX COM*	0.3
1ES1259+337	12 59 20	+33 46 07	$0.12^{+0.04}_{-0.03}$	19/5	9.39E−07	122.0	5	3A	...	...	...	...	...	...	...	...
1ES1301−239	13 01 01	−23 57 41	$0.20^{+0.07}_{-0.06}$	15/5	5.83E−07	61.3	7	3A	...	...	...	...	ABL	CG	A1664*	0.7
1ES1301−411	13 01 45	−41 08 10	$0.29^{+0.13}_{-0.11}$	8/5	3.31E−06	24.3	6	3A	...	...	...	...	SBD	S:K0	CD-40 7655	2.7
1ES1303+182	13 03 16	+18 17 28	$0.39^{+0.10}_{-0.09}$	20/6	1.00E−10	46.5	6	3A	2967	0.2	x	...	2E	CV	GP COM	0.5
1ES1304−650	13 04 48	−65 02 09	$0.14^{+0.04}_{-0.04}$	30/7	5.71E−08	146.3	7	3A	2972	0.5	...	...	BSC	S:B0Ia+WC5:	θ MUS	0.5
1ES1306−013	13 06 51	−01 23 19	$0.09^{+0.03}_{-0.03}$	19/5	1.96E−05	140.5	8	2A	m2975	2.2	...	...	2E	...	...	...
1ES1307+086	13 07 19	+08 36 14	$0.35^{+0.09}_{-0.08}$	22/1	1.00E−10	55.7	6	3A	2978	0.8	...	...	HB	AGN:0.155	PG	0.8
1ES1308+326	13 08 07	+32 36 46	$0.16^{+0.04}_{-0.03}$	40/8	1.00E−10	181.7	5	3A	2979	0.5	x	...	HB	BL:0.049	OP 313	0.2
1ES1308+361	13 08 17	+36 11 58	$0.38^{+0.07}_{-0.07}$	39/7	1.00E−10	90.5	4	3A	2980	0.2	x	...	WLY	AC:F4V	RS CVN	0.2
1ES1308−010	13 08 55	−01 04 51	$0.42^{+0.07}_{-0.07}$	47/3	1.00E−10	101.7	6	3A	2986	0.3	...	...	ABL	CG:0.181	A1689	1.7
1ES1309+281	13 09 32	+28 08 12	$0.16^{+0.05}_{-0.04}$	20/2	2.86E−08	97.0	4	3A	2990	0.4	...	...	WLY	S:G0V	WLY 502	0.3
1ES1309+355	13 09 58	+35 31 53	$0.09^{+0.03}_{-0.03}$	20/5	1.38E−05	146.8	6	3A	...	...	...	...	HB	AGN:0.184	TON 1565	0.6
1ES1310−327	13 10 29	−32 42 39	$1.78^{+0.42}_{-0.37}$	23/2	1.00E−10	12.3	3	3A	...	...	...	...	ABL	CG	S724	1.7
1ES1312+347	13 12 02	+34 46 08	$0.31^{+0.09}_{-0.08}$	17/6	2.19E−10	48.0	4	3A	...	...	...	...	...	...	...	...
1ES1312−423	13 12 08	−42 20 33	$0.50^{+0.14}_{-0.12}$	19/8	1.00E−10	33.7	6	3A	m3002	0.4	...	...	MS	BL:0.108	MS	0.6
1ES1314+293	13 14 04	+29 22 09	$5.51^{+0.77}_{-0.71}$	57/7	1.00E−10	10.2	3	3A	3009	0.8	x	...	MCS	WD:DA1	HZ 43A	0.9

TABLE 6—*Continued*

Slew Desig.	RA 1950	DEC 1950	IPC Rate (cts s^{-1})	NP/NS	P_{rand}	Exp. (s)	PI	QI	EOS # EMSS	Δ2E (′)	A3 EXO	Δ1H (′)	Cat.	Class.: Type/z	Name	ΔC (′)
1ES1314+096	13 14 19	+09 41 16	$0.31^{+0.09}_{-0.08}$	17/3	1.11E−10	48.1	5	3A	3010	0.2	x	...	SAO	S:G0V	SAO 119847	0.2
1ES1314+172	13 14 26	+17 16 34	$0.31^{+0.12}_{-0.10}$	11/6	9.96E−07	30.0	6	3A	...	...	...	...	WLY	S:K2V+M2V	WLY 505AB	1.0
1ES1316−424	13 16 40	−42 29 50	$0.19^{+0.07}_{-0.06}$	14/3	5.99E−07	59.8	4	3A	m3018	0.2	...	...	MS	S:M1.5E	MS	0.8
1ES1318+274	13 18 07	+27 27 53	$0.30^{+0.15}_{-0.12}$	6/4	3.73E−06	18.9	4	3A	...	...	...	...	SBD	GAL	G 149 -80	1.3
1ES1318−632	13 18 14	−63 17 50	$0.49^{+0.19}_{-0.16}$	10/6	3.64E−07	18.2	6	3A	...	...	...	...	SBD	S:B	LS 3039	2.1
1ES1319+429	13 19 59	+42 55 32	$0.13^{+0.05}_{-0.04}$	17/4	6.42E−05	89.5	8	3A	...	...	...	...	...	...	...	...
1ES1320+701	13 20 20	+70 09 09	$0.12^{+0.04}_{-0.04}$	32/7	9.34E−05	147.6	6	3A	...	...	...	...	...	...	...	...
1ES1320+084	13 20 23	+08 25 34	$1.44^{+0.68}_{-0.54}$	6/2	9.69E−10	4.1	6	3A	...	...	...	...	VV	AGN:0.050	MRK 1347	0.5
1ES1322−108	13 22 32	−10 53 38	$0.25^{+0.05}_{-0.05}$	33/6	1.00E−10	112.8	3	3A	3039	0.3	...	...	BSC	S:B1III-IV+B	α VIR	0.5
1ES1322−427	13 22 33	−42 45 41	$1.01^{+0.09}_{-0.09}$	130/5	1.00E−10	120.9	10	3A	3038	0.1	1H1323−428	0.3	A3	AGN:0.002	CEN A	0.3
1ES1322−297	13 22 48	−29 46 20	$0.16^{+0.07}_{-0.06}$	11/2	7.64E−05	52.7	8	3A	...	...	...	...	...	...	...	...
1ES1323+717	13 23 32	+71 47 26	$0.27^{+0.11}_{-0.09}$	13/2	2.50E−05	36.6	5	3A	...	...	...	...	EXC	GAL:0.072	GAL 1323+7145	2.8
1ES1324−269	13 24 04	−26 54 37	$0.15^{+0.04}_{-0.04}$	29/4	8.91E−07	129.5	7	3P	...	...	...	...	SBD	GAL:0.046	ESO 509- 9	1.7
1ES1324−268	13 24 48	−26 53 10	$0.15^{+0.05}_{-0.04}$	29/4	8.81E−07	127.2	8	3P	...	...	...	...	SBD	GAL	ESO 509- 14	1.8
1ES1325−261	13 25 07	−26 06 35	$0.17^{+0.08}_{-0.06}$	9/2	6.23E−05	43.5	7	3A	...	...	...	...	SBD	S:K5III	HD 117033	2.7
1ES1325−312	13 25 14	−31 17 14	$0.69^{+0.30}_{-0.24}$	8/4	1.11E−06	10.5	6	3A	...	...	...	...	SAO	S:F5V	SAO 204500	2.7
1ES1326+789	13 26 34	+78 54 04	$0.38^{+0.16}_{-0.13}$	9/7	6.43E−07	21.1	6	3A	...	...	...	...	BSC	S:G2.5IIIb	HD 117566	0.1
1ES1327−313	13 27 12	−31 19 54	$0.17^{+0.07}_{-0.06}$	13/3	7.27E−05	57.8	6	3A	...	...	...	...	SAO	S:K1III	SAO 204527	2.6
1ES1328−547	13 28 08	−54 43 35	$0.20^{+0.08}_{-0.05}$	18/2	3.45E−09	73.5	6	3A	3071	0.8	...	...	SHA	CV	BV CEN	0.6
1ES1328+244	13 28 25	+24 29 31	$0.21^{+0.05}_{-0.05}$	27/4	1.00E−10	104.7	5	3A	3074	0.1	...	...	SAO	S:G5	FK COM	0.4
1ES1330+022	13 30 22	+02 15 15	$0.19^{+0.05}_{-0.05}$	23/4	1.00E−10	98.8	5	3A	3081	0.9	...	...	VV	AGN:0.215	3C287.1	1.0
1ES1330−313	13 30 45	−31 23 58	$0.27^{+0.06}_{-0.06}$	31/7	1.00E−10	96.0	6	3A	3083	0.7	x	...	ABL	CG:0.050	A3562	1.2
1ES1332−080	13 32 05	−08 05 16	$0.16^{+0.05}_{-0.04}$	20/3	2.70E−09	99.6	4	3A	3091	0.6	x	...	WLY	S:K5EV	EQ VIR	0.5
1ES1332+374	13 32 34	+37 25 35	$1.20^{+0.32}_{-0.28}$	19/4	1.00E−10	14.7	4	3A	3098	0.8	1H1332+372	0.7	A3	AC	SAO 063623	0.7
1ES1332−295	13 32 40	−29 35 22	$0.16^{+0.04}_{-0.03}$	35/7	1.00E−10	168.7	7	3A	m3100	0.3	x	...	2E	...	...	...
1ES1333−340	13 33 03	−34 02 33	$1.76^{+0.17}_{-0.17}$	113/10	1.00E−10	62.3	6	3A	3102	0.4	x1H1334−340	0.3	VV	AGN:0.008	MCG-6.30.15	0.3
1ES1333+412	13 33 05	+41 14 57	$0.21^{+0.06}_{-0.05}$	22/5	5.21E−09	84.1	7	3A	3103	1.0	...	...	ABL	CG:0.228	A1763	2.0
1ES1334−296	13 34 19	−29 36 30	$0.10^{+0.02}_{-0.02}$	41/5	5.33E−10	287.9	6	3A	3112	1.2	x	...	RNG	GAL:0.002	NGC 5236	0.4
1ES1336+280	13 36 13	+28 00 36	$0.19^{+0.08}_{-0.07}$	11/5	5.01E−05	44.0	12	3A	...	...	...	...	SBD	GAL:0.036	Z 1336.4+2800	2.3
1ES1339−688	13 39 20	−68 52 06	$0.80^{+0.42}_{-0.33}$	5/2	6.51E−07	6.1	3	3A	...	...	...	...	SAO	S:G2IV-V	SAO 252423	0.7
1ES1340−611	13 40 35	−61 07 02	$0.68^{+0.11}_{-0.10}$	50/3	1.00E−10	69.4	5	3A	3127	0.2	1H1338−604.B	0.1	A3	AC	SAO 0252429	0.1
1ES1344−326	13 44 43	−32 37 09	$1.17^{+0.51}_{-0.41}$	8/3	1.34E−06	6.2	6	3A	...	...	1H1344−326	1.7	ABL	CG:0.040	A3571	1.5
1ES1346−300	13 46 26	−30 03 45	$1.68^{+0.23}_{-0.21}$	64/2	1.00E−10	36.5	7	3A	3141	0.8	x1H1345−300	0.4	VV	AGN:0.014	IC 4329A	0.4

TABLE 6—*Continued*

Slew Desig.	RA 1950	DEC 1950	IPC Rate (cts s^{-1})	NP/NS	P_{rand}	Exp. (s)	PI	QI	EOS # EMSS	Δ2E (′)	A3 EXO	Δ1H (′)	Cat.	Class.: Type/z	Name	ΔC (′)
1ES1346+268	13 46 34	+26 50 07	$1.24^{+0.12}_{-0.12}$	118/3	1.00E−10	90.2	5	3A	3142	0.5	x1H1348+267	0.3	ABL	CG:0.062	A1795	1.8
1ES1351+400	13 51 38	+40 05 24	$0.07^{+0.03}_{-0.02}$	30/5	6.15E−05	232.5	5	3A	m3146	0.5	...	...	MS	AGN:0.062	MS	0.8
1ES1351+695	13 51 57	+69 33 24	$1.36^{+0.17}_{-0.16}$	80/7	1.00E−10	55.4	5	3A	3147	0.2	x1H1350+696	0.5	VV	AGN:0.031	MRK 279*	0.2
1ES1354−314	13 54 42	−31 24 22	$0.65^{+0.31}_{-0.25}$	7/2	5.80E−06	9.7	6	3A	...	...	...	...	SAO	S:K0V	SAO 205032	0.3
1ES1402+042	14 02 16	+04 16 26	$0.08^{+0.03}_{-0.02}$	24/7	6.90E−06	200.3	5	3A	m3177	0.9	x	...	HB	BL	2E	0.9
1ES1404−267	14 04 36	−26 46 33	$0.55^{+0.19}_{-0.16}$	13/4	4.83E−09	21.1	5	3A	...	...	1H1409−267	0.5	ABL	CG:0.021	A3581	0.4
1ES1405−450	14 05 51	−45 03 01	$0.43^{+0.16}_{-0.13}$	11/3	7.59E−08	22.7	5	3A	3194	1.4	x1H1404−450	1.3	A3	CV	1E1405-451	1.3
1ES1410−029	14 10 38	−02 58 28	$0.31^{+0.03}_{-0.03}$	112/8	1.00E−10	309.1	8	3A	3205	0.1	x1H1408−031	0.2	VV	AGN:0.006	NGC 5506	0.3
1ES1410+683	14 10 58	+68 19 20	$0.33^{+0.16}_{-0.13}$	8/5	7.68E−05	20.0	4	3A	...	...	...	...	...	...	...	...
1ES1414+203	14 14 13	+20 21 27	$0.26^{+0.13}_{-0.11}$	8/3	3.50E−05	24.4	3	3A	...	...	...	...	BSC	S:F8V	HD 125040	0.2
1ES1414−197	14 14 42	−19 43 34	$0.26^{+0.10}_{-0.09}$	11/3	4.11E−06	35.6	5	3A	...	...	...	...	SAO	S:A5IV	SAO 158468	0.5
1ES1415+451	14 15 03	+45 10 34	$0.27^{+0.13}_{-0.11}$	8/6	1.04E−04	24.5	3	3A	...	...	...	...	HB	AGN:0.114	PG	0.7
1ES1415−209	14 15 29	−20 57 23	$0.21^{+0.09}_{-0.08}$	9/5	2.40E−05	36.2	8	3A	...	...	...	...	...	...	...	...
1ES1416−129	14 16 23	−12 57 03	$0.21^{+0.04}_{-0.04}$	37/7	1.00E−10	145.4	6	3A	m3238	0.4	x	...	HB	AGN:0.129	PG	0.4
1ES1417−192	14 17 00	−19 14 09	$0.15^{+0.05}_{-0.04}$	17/2	4.72E−07	88.1	5	3A	3244	0.5	...	...	VV	AGN:0.119	PKS	0.8
1ES1421+582	14 21 09	+58 15 09	$0.46^{+0.18}_{-0.15}$	10/6	5.87E−08	19.9	5	3A	...	...	...	...	...	...	...	...
1ES1423+520	14 23 29	+52 04 34	$0.38^{+0.08}_{-0.07}$	33/3	1.00E−10	76.2	5	3A	3265	0.2	...	...	WLY	S:F6V	WLY 549A	0.4
1ES1426−624	14 26 04	−62 27 53	$0.33^{+0.04}_{-0.04}$	78/4	1.00E−10	210.4	4	3A	3278	0.4	x	...	SBD	S:MVE	PM14263-6228	1.7
1ES1426+015	14 26 33	+01 30 31	$0.34^{+0.08}_{-0.07}$	28/6	1.00E−10	69.7	5	3A	m3280	0.5	x1H1427+013	0.3	VV	AGN:0.086	MRK 1383	0.2
1ES1426+428	14 26 38	+42 53 41	$2.55^{+0.67}_{-0.58}$	17/3	1.00E−10	6.6	4	3A	...	...	x1H1430+423	0.3	A3	BL	H1426+427	0.4
1ES1435−067	14 35 37	−06 45 18	$0.22^{+0.08}_{-0.07}$	14/2	3.30E−06	50.6	5	3A	3305	0.2	...	...	HB	AGN:0.129	PG	0.1
1ES1435−606	14 35 48	−60 37 09	$0.76^{+0.16}_{-0.14}$	29/2	1.00E−10	36.5	2	3A	3308	1.3	...	...	SBD	S:G2V	α CEN AB	2.9
1ES1436−624	14 36 38	−62 26 07	$1.49^{+0.34}_{-0.30}$	28/1	1.00E−10	16.7	5	2A	...	...	x	...	SAO	S:A0	SAO 252841	1.6
1ES1437−252	14 37 52	−25 17 43	$0.82^{+0.44}_{-0.34}$	5/3	1.14E−06	5.9	10	3A	...	...	...	...	SBD	S:F0/F2V	HD 129009	2.9
1ES1440+122	14 40 22	+12 13 16	$0.52^{+0.19}_{-0.16}$	11/6	1.23E−08	19.1	5	3A	...	...	...	...	...	...	...	...
1ES1449+193	14 49 07	+19 18 17	$0.79^{+0.12}_{-0.11}$	54/5	1.00E−10	63.9	4	3A	3337	0.3	1H1450+190.B	0.5	SAO	S:G8V+K4V	HD131156AB	0.2
1ES1450+679	14 50 07	+67 56 10	$0.10^{+0.04}_{-0.03}$	16/4	3.02E−05	114.6	8	3A	3340	3.0	...	...	2E	...	...	...
1ES1452+188	14 52 14	+18 50 24	$0.29^{+0.06}_{-0.05}$	45/7	1.00E−10	130.2	5	3A	3350	0.3	1H1450+190.A	0.9	ABL	CG:0.059	A1991	0.6
1ES1454+225	14 54 58	+22 32 09	$0.32^{+0.12}_{-0.10}$	11/4	1.75E−07	30.5	6	3A	m3356	0.6	...	...	MS	CG:0.259	MS	0.6
1ES1456+648	14 56 02	+64 51 52	$0.24^{+0.12}_{-0.09}$	7/4	2.73E−05	25.4	8	3A	...	...	...	...	...	...	...	...
1ES1456−400	14 56 32	−40 01 14	$0.75^{+0.37}_{-0.30}$	6/1	4.56E−06	7.5	9	3A	...	...	...	...	SBD	S:F7/F8V	HD 132349	2.3
1ES1457+033	14 57 17	+03 18 23	$0.40^{+0.20}_{-0.16}$	6/3	3.61E−06	13.9	6	3A	...	...	...	...	...	...	...	...
1ES1458+215	14 58 02	+21 33 12	$0.24^{+0.07}_{-0.07}$	19/2	9.75E−09	63.0	8	3E	3363	0.7	1H1457+214.	1.3	ABL	CG:0.153	A2009	0.9

TABLE 6—*Continued*

Slew Desig.	RA 1950	DEC 1950	IPC Rate (cts s^{-1})	NP/NS	P_{rand}	Exp. (s)	PI	QI	EOS # EMSS	Δ2E (′)	A3 EXO	Δ1H (′)	Cat.	Class.: Type/z	Name	ΔC (′)
1ES1500−415	15 00 17	−41 35 59	$0.49^{+0.06}_{-0.06}$	136/1	1.00E−10	204.3	5	3E	...	...	...	...	...	...	...	...
1ES1501+663	15 01 25	+66 23 56	$2.05^{+0.27}_{-0.25}$	65/13	1.00E−10	30.8	3	3A	...	...	x	...	MCS	WD	WD1501+664	0.3
1ES1501+106	15 01 35	+10 38 06	$0.57^{+0.10}_{-0.10}$	39/2	1.00E−10	63.1	5	3A	3372	0.5	x	...	VV	AGN:0.036	MRK 841	0.4
1ES1502+478	15 02 07	+47 50 55	$2.23^{+0.51}_{-0.45}$	23/7	1.00E−10	10.0	4	3A	3373	0.2	x1H1504+473	0.2	A3	AC	ZZ BOO	0.2
1ES1503+017	15 03 57	+01 47 59	$0.14^{+0.04}_{-0.04}$	21/3	1.81E−06	109.8	5	3A	3380	0.2	...	...	RNG	GAL:0.006	NGC 5846*	0.4
1ES1508+337	15 08 06	+33 42 30	$0.40^{+0.18}_{-0.14}$	9/5	1.32E−07	20.4	6	3A	...	...	1H1510+335	1.9	ABL	CG:0.151	A2034	1.3
1ES1508+059	15 08 26	+05 55 55	$1.54^{+0.27}_{-0.25}$	39/3	1.00E−10	24.3	6	3A	3385	0.4	1H1508+060	1.6	ABL	CG:0.077	A2029	1.5
1ES1509+763	15 09 01	+76 22 44	$0.44^{+0.19}_{-0.16}$	8/3	1.91E−06	16.4	5	3A	...	...	...	...	SAO	S:G5	SAO 008175	1.1
1ES1509−589	15 09 48	−58 56 14	$0.89^{+0.19}_{-0.17}$	31/1	1.00E−10	30.4	8	3A	3389	1.6	x	...	2E	P	MSH 11-52	1.6
1ES1509−588	15 09 49	−58 49 42	$0.43^{+0.15}_{-0.13}$	17/1	2.76E−06	29.7	6	3M	3388	0.6	x	...	2E	SNR	MSH 15-52	2.0
1ES1513+002	15 13 47	+00 16 17	$0.15^{+0.05}_{-0.04}$	24/4	8.18E−07	112.6	8	3A	3404	0.8	...	...	ABL	CG:0.118	A2050	0.8
1ES1514+072	15 14 18	+07 12 15	$0.94^{+0.15}_{-0.14}$	46/2	1.00E−10	46.1	6	3A	3407	0.2	x1H1514+072	0.7	ABL	CG:0.035	A2052	1.3
1ES1517+656	15 17 07	+65 36 26	$0.91^{+0.29}_{-0.24}$	13/7	1.00E−10	13.7	5	3A	...	...	1H1515+660	0.2	A3	BL	H1517+656	0.2
1ES1518−071	15 18 13	−07 10 36	$0.23^{+0.11}_{-0.09}$	8/1	2.03E−05	29.3	9	2A	...	...	...	...	...	...	...	...
1ES1518+593	15 18 13	+59 18 51	$0.36^{+0.14}_{-0.12}$	11/7	1.72E−06	26.0	3	2A	...	...	...	...	VV	AGN:0.079	SBS1518+593	0.4
1ES1519+078	15 19 22	+07 52 48	$0.41^{+0.13}_{-0.11}$	15/7	1.59E−09	31.7	6	3A	3419	1.1	...	...	2E	CG:0.045	MKW 3S	0.5
1ES1520+278	15 20 20	+27 53 12	$0.33^{+0.07}_{-0.07}$	29/3	1.00E−10	76.1	7	3E	3426	0.7	...	...	2E	CG:0.072	A2065	0.8
1ES1520+087	15 20 36	+08 47 08	$0.61^{+0.10}_{-0.09}$	51/6	1.00E−10	74.2	8	3A	3427	0.7	1H1521+083	2.3	ABL	CG:0.034	A2063	1.9
1ES1522+300	15 22 13	+30 00 54	$0.18^{+0.06}_{-0.05}$	17/3	5.43E−07	71.7	5	3A	m3432	3.0	...	...	2E	CG:0.115	A2069	2.8
1ES1527+714	15 27 21	+71 24 15	$0.13^{+0.05}_{-0.04}$	14/5	8.60E−05	79.2	5	2A	...	...	...	...	...	...	...	...
1ES1533+535	15 33 36	+53 30 00	$0.49^{+0.18}_{-0.15}$	11/6	1.18E−09	20.7	6	3A	...	...	...	...	...	...	...	...
1ES1536+515	15 36 48	+51 34 02	$0.32^{+0.15}_{-0.12}$	7/3	1.74E−05	19.4	5	3A	...	...	...	...	...	...	...	...
1ES1539+187	15 39 57	+18 44 48	$0.24^{+0.11}_{-0.09}$	9/6	1.84E−05	31.7	8	3A	...	...	...	...	...	...	...	...
1ES1543+362	15 43 12	+36 13 11	$0.12^{+0.05}_{-0.04}$	16/5	2.53E−05	94.9	6	3E	...	...	1H1544+360	1.6	ABL	CG:0.065	A2124	1.2
1ES1544+820	15 44 08	+82 04 32	$0.53^{+0.14}_{-0.12}$	19/12	1.00E−10	33.1	5	3A	...	...	...	...	...	...	...	...
1ES1545+210	15 45 32	+21 01 17	$0.19^{+0.02}_{-0.02}$	112/11	1.00E−10	474.4	6	3A	3500	0.3	...	...	VV	AGN:0.264	3C 323.1	0.2
1ES1546+104	15 46 40	+10 25 38	$0.25^{+0.11}_{-0.09}$	8/5	4.58E−06	28.8	9	3A	...	...	...	...	...	...	...	...
1ES1547+262	15 47 31	+26 13 14	$0.20^{+0.07}_{-0.06}$	14/7	2.56E−07	58.3	4	3A	3507	0.1	...	...	BSC	S:G3.5III-IV	HD 141714	0.2
1ES1548+114	15 48 21	+11 29 11	$0.09^{+0.03}_{-0.03}$	21/6	6.88E−06	152.1	7	3A	3508	0.6	...	...	HB	AGN:0.436	MC	0.6
1ES1549+203	15 49 50	+20 22 27	$0.10^{+0.03}_{-0.03}$	25/5	1.67E−07	179.4	5	3A	m3513	0.4	...	...	VV	AGN:0.250	LB 906*	0.5
1ES1550+191	15 50 31	+19 06 01	$1.21^{+0.30}_{-0.27}$	20/2	1.00E−10	15.8	3	3A	...	...	x	...	SHA	CV	MR SER	0.9
1ES1552+203	15 52 14	+20 20 22	$0.21^{+0.06}_{-0.05}$	24/4	1.47E−10	93.1	7	3A	m3523	0.6	...	...	2E	...	...	...
1ES1553+113	15 53 19	+11 20 20	$1.61^{+0.18}_{-0.17}$	94/3	1.00E−10	56.1	4	3A	3529	0.3	...	...	HB	BL:0.360	PG	0.5

TABLE 6—*Continued*

Slew Desig.	RA 1950	DEC 1950	IPC Rate (cts s^{-1})	NP/NS	P_{rand}	Exp. (s)	PI	QI	EOS # EMSS	Δ2E (′)	A3 EXO	Δ1H (′)	Cat.	Class.: Type/z	Name	ΔC (′)
1ES1556+273	15 56 15	+27 22 33	$1.01^{+0.12}_{-0.11}$	87/8	1.00E−10	81.8	6	3A	3541	0.3	x1H1556+273	0.3	ABL	CG:0.090	A2142	0.9
1ES1556+257	15 56 38	+25 42 23	$0.30^{+0.15}_{-0.12}$	7/3	2.75E−05	20.4	6	3A	3543	0.3	...	...	SAO	S:K2V	SAO 084114	0.7
1ES1559+161	15 59 58	+16 08 16	$0.11^{+0.03}_{-0.03}$	53/6	2.54E−06	249.6	6	3E	3565	2.0	...	...	2E	CG:0.035	A2147	2.0
1ES1601+160	16 01 24	+16 02 11	$0.16^{+0.06}_{-0.05}$	22/7	2.88E−05	90.3	6	3A	3572	0.6	...	...	ZCT	GAL:0.100	1601+1602	1.5
1ES1601+669	16 01 36	+66 57 09	$0.17^{+0.04}_{-0.04}$	42/10	1.00E−10	179.2	3	3A	3573	1.5	x	...	SBD	S:K0	AG DRA	1.5
1ES1602+178	16 02 23	+17 51 57	$0.18^{+0.03}_{-0.03}$	78/17	1.00E−10	322.2	5	3A	3577	0.5	...	...	UGC	GAL:0.042	U10170*	1.5
1ES1602+240	16 02 42	+24 03 52	$0.14^{+0.05}_{-0.04}$	19/7	4.99E−07	101.1	7	3A	3581	1.6	...	...	2E	CG:0.042	AWM 4	1.6
1ES1606+218	16 06 54	+21 53 30	$0.16^{+0.07}_{-0.06}$	10/6	7.16E−05	50.4	8	3A	...	...	...	...	SBD	S:K2	AG+21 1576	2.7
1ES1607+621	16 07 31	+62 06 10	$0.18^{+0.08}_{-0.07}$	10/6	1.12E−04	42.3	10	2A	...	...	...	...	...	...	...	...
1ES1609−522	16 09 01	−52 17 31	$7.35^{+1.75}_{-1.54}$	21/1	1.00E−10	2.8	8	3A	...	...	x1H1608−522	1.4	A3	XRB	QX NOR	1.4
1ES1610+669	16 10 08	+66 59 45	$0.15^{+0.05}_{-0.05}$	23/5	2.82E−05	96.7	5	3A	...	...	...	...	...	...	...	...
1ES1612+261	16 12 09	+26 11 52	$0.27^{+0.07}_{-0.06}$	22/9	1.00E−10	69.9	6	3A	3617	0.1	x	...	HB	AGN:0.131	TON 256	0.1
1ES1612+339	16 12 47	+33 59 14	$2.27^{+0.20}_{-0.21}$	129/12	1.00E−10	55.2	5	3A	3618	0.2	x	...	WLY	AC:F6V+G1V	WLY 9550AB	0.3
1ES1613+658	16 13 34	+65 50 53	$0.20^{+0.04}_{-0.04}$	35/10	1.00E−10	140.9	4	3A	3624	0.5	x1H1615+655	0.4	VV	AGN:0.129	MRK 876	0.3
1ES1613−509	16 13 56	−50 57 19	$4.43^{+0.31}_{-0.32}$	209/2	1.00E−10	46.1	6	3A	3626	0.6	x	...	2E	SNR	RCW 103	0.8
1ES1614+446	16 14 08	+44 40 38	$0.36^{+0.10}_{-0.09}$	18/12	1.00E−10	44.8	6	3A	...	...	...	...	SAO	S:G0	SAO 045997	0.4
1ES1615+061	16 15 19	+06 11 11	$0.27^{+0.07}_{-0.06}$	27/5	2.10E−10	77.6	7	3A	3634	0.2	x	...	VV	AGN:0.038	H 1613+06	0.2
1ES1615+553	16 15 57	+55 22 47	$0.24^{+0.05}_{-0.04}$	37/8	1.00E−10	127.9	4	3A	3641	0.9	...	...	WLY	S:M1EV	WLY 9552	1.1
1ES1616+436	16 16 53	+43 36 54	$0.28^{+0.14}_{-0.11}$	8/6	1.08E−04	23.4	8	2A	...	...	...	...	...	...	...	...
1ES1618+411	16 18 11	+41 06 09	$0.14^{+0.04}_{-0.04}$	25/2	3.33E−08	131.1	5	3A	3650	0.1	...	...	2E	...	...	...
1ES1621+274	16 21 35	+27 26 56	$0.14^{+0.06}_{-0.05}$	12/5	2.31E−05	66.2	8	2A	3658	2.6	...	...	2E	...	...	...
1ES1622+261	16 22 06	+26 11 41	$0.09^{+0.03}_{-0.03}$	19/6	6.61E−05	144.0	7	3A	...	...	x	...	EHG	AGN	EXO	0.8
1ES1625+261	16 25 01	+26 08 59	$0.10^{+0.04}_{-0.03}$	22/7	3.39E−05	137.0	8	2A	...	...	...	...	...	...	...	...
1ES1626+279	16 26 33	+27 58 54	$0.35^{+0.16}_{-0.13}$	8/6	2.09E−05	19.5	9	3A	...	...	...	...	...	...	...	...
1ES1626+396	16 26 54	+39 39 54	$1.63^{+0.09}_{-0.09}$	346/8	1.00E−10	199.5	6	3A	3705	0.4	x1H1631+394	1.7	ABL	CG:0.030	A2199	1.9
1ES1626+554	16 26 54	+55 29 53	$0.33^{+0.12}_{-0.10}$	12/6	1.02E−07	31.4	4	3A	...	...	...	...	VV	AGN:0.132	PG	0.9
1ES1627+402	16 27 22	+40 13 05	$0.19^{+0.06}_{-0.05}$	23/7	3.80E−09	93.1	4	3A	...	...	x	...	EHG	AGN	EXO	1.0
1ES1631+781	16 31 31	+78 11 18	$0.61^{+0.17}_{-0.15}$	17/10	1.00E−10	26.0	2	3A	...	...	...	...	WFC	WD:DA	RE1629+781	1.0
1ES1634−104	16 34 22	−10 27 43	$0.10^{+0.04}_{-0.04}$	14/3	1.00E−04	95.1	5	3A	3732	1.0	...	...	BSC	S:O9.5Vn	ζ OPH	0.6
1ES1635+663	16 35 39	+66 18 55	$0.16^{+0.04}_{-0.04}$	28/11	2.84E−09	130.6	8	3A	3739	0.1	...	...	ABL	CG:0.171	A2218	0.3
1ES1638+608	16 38 23	+60 48 15	$0.35^{+0.09}_{-0.08}$	24/16	1.00E−10	57.7	6	3A	3742	0.5	...	...	SAO	S:G0V	WW DRA	0.3
1ES1638+634	16 38 45	+63 29 33	$0.14^{+0.06}_{-0.05}$	13/10	2.66E−05	72.4	9	3A	...	...	...	...	...	...	...	...
1ES1641+399	16 41 18	+39 54 01	$0.23^{+0.04}_{-0.04}$	59/8	1.00E−10	200.5	5	3A	3752	0.3	...	...	VV	AGN:0.594	3C345.0	0.2

TABLE 6—*Continued*

Slew Desig.	RA 1950	DEC 1950	IPC Rate (cts s^{-1})	NP/NS	P_{read}	Exp. (s)	PI	QI	EOS # EMSS	Δ2E (′)	A3 EXO	Δ1H (′)	Cat.	Class.: Type/z	Name	ΔC (′)
1ES1649−403	16 49 07	−40 20 24	$0.18^{+0.08}_{-0.07}$	9/2	3.42E−05	40.6	7	3A	...	...	...	...	...	...	...	...
1ES1649+758	16 49 34	+75 49 13	$0.18^{+0.06}_{-0.07}$	10/9	4.90E−05	43.5	7	3A	...	...	...	...	...	...	...	...
1ES1650−417	16 50 22	−41 47 30	$0.12^{+0.04}_{-0.04}$	20/2	2.95E−05	114.9	8	3A	...	...	...	...	SAO	S:B	SAO 227370	1.1
1ES1652+398	16 52 12	+39 50 25	$3.24^{+0.13}_{-0.13}$	616/11	1.00E−10	186.8	5	3A	3780	0.1	x1H1651+398	0.3	VV	BL:0.034	MRK 501	0.1
1ES1652−082	16 52 49	−08 15 17	$0.57^{+0.10}_{-0.10}$	39/1	1.00E−10	63.2	4	3A	3783	0.5	x1H1653−083	0.6	A3	AC	V1054 OPH	0.6
1ES1653+795	16 53 08	+79 35 09	$0.18^{+0.07}_{-0.06}$	13/8	2.21E−06	58.2	6	3A	...	...	...	...	...	...	...	...
1ES1656+354	16 56 02	+35 25 12	$0.48^{+0.07}_{-0.06}$	70/6	1.00E−10	131.2	5	3A	3791	0.1	x1H1656+354	0.2	A3	XRB	HER X-1	0.1
1ES1659+341	16 59 12	+34 07 20	$0.16^{+0.07}_{-0.06}$	12/4	3.56E−05	57.5	7	3A	3805	1.2	...	...	2E	...	...	...
1ES1659+572	16 59 50	+57 17 07	$0.20^{+0.10}_{-0.08}$	8/8	8.22E−05	32.6	8	2A	...	...	...	...	...	...	...	...
1ES1700+341	17 00 52	+34 08 27	$0.49^{+0.16}_{-0.14}$	15/5	7.29E−10	26.8	6	3A	3809	0.8	1H1702+336	0.8	ABL	CG:0.097	A2244	1.5
1ES1701−369	17 01 38	−36 59 40	$0.14^{+0.04}_{-0.04}$	25/2	1.30E−06	121.8	8	2M	...	...	...	...	...	...	...	...
1ES1702+457	17 02 02	+45 44 26	$0.30^{+0.14}_{-0.11}$	9/5	2.53E−05	24.6	5	3A	...	...	...	...	SAO	S:F8	SAO 046462*	1.3
1ES1702−369	17 02 23	−36 58 24	$0.22^{+0.07}_{-0.07}$	19/2	3.31E−06	62.8	7	2A	...	...	...	...	SBD	...	IRAS 17023-3659	1.4
1ES1702+482	17 02 58	+48 12 50	$0.22^{+0.10}_{-0.08}$	8/5	8.63E−05	30.7	5	2A	...	...	...	...	...	...	...	...
1ES1704+545	17 04 10	+54 32 33	$0.18^{+0.07}_{-0.06}$	13/6	1.49E−05	54.5	4	3A	m3830	1.1	...	...	WLY	S:F6V	WLY 9584*	1.1
1ES1704+607	17 04 13	+60 47 56	$0.04^{+0.01}_{-0.01}$	67/22	5.66E−05	704.3	6	3A	3828	1.2	1H1704+605	1.3	HB	AGN:0.371	3C351	1.3
1ES1704+736	17 04 16	+73 36 28	$0.17^{+0.07}_{-0.06}$	12/9	1.75E−05	54.2	10	3A	...	...	...	...	...	...	...	...
1ES1704+240	17 04 31	+24 02 14	$0.68^{+0.09}_{-0.08}$	73/3	1.00E−10	100.3	7	3A	3831	0.4	x1H1706+241	0.2	SAO	S:M0	SAO 084844	0.3
1ES1706+787	17 06 58	+78 43 49	$0.38^{+0.04}_{-0.04}$	126/20	1.00E−10	280.5	7	3A	3842	0.8	...	...	UGC	GAL	U10726*	1.8
1ES1711−547	17 11 29	−54 47 08	$0.40^{+0.16}_{-0.13}$	10/1	2.57E−07	22.2	8	3A	...	...	...	...	SAO	S:F0IV-V	SAO 244557	1.4
1ES1711+657	17 11 48	+65 45 50	$0.16^{+0.07}_{-0.06}$	13/9	4.10E−05	59.4	9	3A	...	...	...	...	...	...	...	...
1ES1712+641	17 12 25	+64 06 28	$0.25^{+0.04}_{-0.04}$	54/14	1.00E−10	172.2	7	3A	3866	1.3	...	...	2E	CG:0.081	A2255	1.2
1ES1714+574	17 14 27	+57 27 19	$0.27^{+0.08}_{-0.07}$	17/10	6.09E−10	54.7	7	3A	...	...	...	...	RNG	GAL:0.028	NGC 6338*	1.3
1ES1716+551	17 16 16	+55 08 14	$0.21^{+0.09}_{-0.08}$	10/7	7.11E−05	37.9	9	3A	...	...	...	...	SAO	S:K0	SAO 030326	2.8
1ES1717+265	17 17 57	+26 32 18	$0.19^{+0.07}_{-0.06}$	14/1	1.06E−05	56.1	4	3A	m3884	0.6	...	...	MS	S:M4V+M5V	WLY 669AB	0.9
1ES1718+266	17 18 12	+26 40 44	$0.28^{+0.08}_{-0.07}$	21/2	1.00E−10	63.6	6	3A	3885	0.4	1H1720+269.B	0.6	2E	CG:0.164	2E	0.3
1ES1718+650	17 18 12	+65 01 48	$0.13^{+0.05}_{-0.04}$	15/5	6.83E−05	83.8	6	3A	...	...	...	...	...	...	...	...
1ES1720+309	17 20 46	+30 55 30	$0.35^{+0.08}_{-0.07}$	25/2	1.00E−10	63.3	5	3A	3893	0.2	x1H1727+308	0.1	VV	AGN:0.043	MRK 506	0.2
1ES1721+343	17 21 32	+34 20 34	$0.57^{+0.07}_{-0.07}$	83/7	1.00E−10	134.9	5	3A	3896	0.3	...	...	HB	AGN:0.206	4C 34.47	0.1
1ES1727+502	17 27 05	+50 15 14	$0.77^{+0.03}_{-0.03}$	571/21	1.00E−10	701.9	5	3A	3909	0.5	x1H1730+500	0.3	VV	BL:0.055	I ZW 187	0.3
1ES1727−214	17 27 40	−21 27 52	$2.99^{+0.32}_{-0.30}$	100/2	1.00E−10	32.6	5	3A	3911	1.4	x1H1728−213	1.0	A3	SNR	KEPLER	1.0
1ES1727+590	17 27 52	+59 04 13	$0.45^{+0.19}_{-0.15}$	8/6	1.74E−07	16.7	5	3A	...	...	...	...	SAO	S:G0	SAO 030416	0.9
1ES1728−169	17 28 49	−16 55 25	$67.92^{+3.52}_{-3.54}$	376/1	1.00E−10	5.5	6	3A	...	...	x1H1728−169	0.4	A3	XRB	GX9+9	0.3

TABLE 6—*Continued*

Slew Desig.	RA 1950	DEC 1950	IPC Rate (cts s^{-1})	NP/NS	P_{rand}	Exp. (s)	PI	QI	EOS # EMSS	Δ2E (′)	A3 EXO	Δ1H (′)	Cat.	Class.: Type/z	Name	ΔC (′)
1ES1731−325	17 31 26	−32 32 53	$0.18^{+0.06}_{-0.05}$	20/2	1.03E−08	86.5	6	3A	3920	0.1	x	...	2E	XRB	TERZ 1*	0.6
1ES1734+742	17 34 10	+74 15 50	$0.80^{+0.12}_{-0.11}$	57/24	1.00E−10	65.8	5	3A	...	...	1H1739+744	0.5	A3	AC	SAO 008842	0.5
1ES1734+686	17 34 25	+68 40 36	$0.24^{+0.10}_{-0.08}$	9/6	2.85E−06	32.6	8	3A	...	...	...	...	...	...	...	...
1ES1735−269	17 35 09	−26 57 40	$0.91^{+0.23}_{-0.21}$	22/1	1.00E−10	21.7	7	3A	...	...	...	...	SBD	S	IRAS 17345-2656	1.0
1ES1735−444	17 35 19	−44 25 09	$39.02^{+1.78}_{-1.79}$	483/5	1.00E−10	12.3	7	3A	...	...	x1H1735−444	0.2	A3	XRB	V926 SCO	0.2
1ES1737+612	17 37 58	+61 16 44	$0.23^{+0.10}_{-0.08}$	9/6	4.48E−06	33.9	5	3A	...	...	...	...	SBD	S:M	HD 160934	2.0
1ES1739+518	17 39 19	+51 51 44	$0.15^{+0.06}_{-0.05}$	15/7	9.30E−05	67.1	5	3A	3934	0.7	...	...	VV	AGN:0.061	E 1739+518	0.6
1ES1741+196	17 41 46	+19 36 16	$0.54^{+0.23}_{-0.19}$	9/4	1.72E−06	14.8	7	3A	...	...	...	...	...	...	...	...
1ES1742−294	17 42 55	−29 29 56	$1.86^{+0.25}_{-0.23}$	65/2	1.00E−10	33.4	9	3A	3943	1.8	x1H1744−293	0.3	A3	XRB	X1742-294	0.3
1ES1743+480	17 43 48	+48 03 41	$0.31^{+0.14}_{-0.12}$	8/5	9.12E−06	22.5	7	3A	...	...	...	...	...	...	...	...
1ES1745+720	17 45 10	+72 04 24	$0.17^{+0.06}_{-0.05}$	17/13	7.99E−07	79.3	7	3A	...	...	...	...	...	...	...	...
1ES1745+504	17 45 13	+50 29 16	$0.24^{+0.11}_{-0.09}$	9/5	5.61E−05	30.1	6	3A	...	...	...	...	...	...	...	...
1ES1746+748	17 46 29	+74 53 38	$0.19^{+0.07}_{-0.06}$	12/9	5.88E−06	51.4	4	3A	...	...	...	...	SAO	S:K0	SAO 008910	0.2
1ES1746−370	17 46 47	−37 02 11	$8.65^{+2.45}_{-2.14}$	15/1	1.00E−10	1.7	8	3A	...	...	x1H1746−370	0.4	A3	XRB	NGC 6441	0.3
1ES1750+707	17 50 59	+70 47 52	$0.17^{+0.07}_{-0.06}$	16/9	3.00E−05	66.7	7	3A	m3969	1.3	x	...	2E	S	2E	1.6
1ES1755−338	17 55 07	−33 49 47	$5.18^{+2.11}_{-1.72}$	8/1	1.50E−10	1.5	10	3A	...	...	...	...	BMC	XRB	4U1755-338	3.0
1ES1757−233	17 57 29	−23 20 25	$0.31^{+0.10}_{-0.09}$	23/2	3.59E−07	53.4	7	2E	...	...	...	...	...	...	...	...
1ES1758−250	17 58 02	−25 04 40	$56.86^{+1.98}_{-1.98}$	837/2	1.00E−10	14.6	9	3A	...	...	x1H1758−250	0.2	A3	XRB	GX5-1	0.3
1ES1758−257	17 58 06	−25 44 04	$2.64^{+0.50}_{-0.45}$	34/3	1.00E−10	12.4	8	3A	...	...	x	...	...	...	...	...
1ES1802+025	18 02 52	+02 30 28	$0.35^{+0.09}_{-0.08}$	25/1	1.00E−10	62.0	4	3A	4004	1.2	...	...	WLY	S:K0V+K5V	WLY 702AB	1.0
1ES1805−118	18 05 09	−11 53 00	$0.79^{+0.33}_{-0.27}$	8/2	7.98E−09	9.6	8	3A	...	...	...	...	...	...	...	...
1ES1807+698	18 07 11	+69 48 47	$0.08^{+0.02}_{-0.02}$	51/14	1.96E−08	394.2	6	3A	4023	0.9	x1H1803+696	0.7	VV	BL:0.051	3C 371.0	0.7
1ES1808−579	18 08 18	−57 57 43	$0.81^{+0.39}_{-0.31}$	6/2	7.57E−08	7.2	6	3A	...	...	...	...	...	...	...	...
1ES1810+696	18 10 23	+69 40 53	$0.06^{+0.02}_{-0.01}$	52/14	1.37E−06	482.2	5	2A	m4039	0.6	x	...	SAO	S:K2	SAO 017800	0.8
1ES1811−171	18 11 34	−17 10 26	$18.99^{+2.68}_{-2.50}$	56/1	1.00E−10	2.9	8	3A	...	...	x1H1811−171	0.7	A3	XRB	GX13+1	0.8
1ES1814+782	18 14 38	+78 12 34	$0.13^{+0.05}_{-0.04}$	15/7	7.11E−05	81.1	5	3A	...	...	...	...	...	...	...	...
1ES1814+498	18 14 58	+49 50 29	$0.63^{+0.09}_{-0.08}$	69/7	1.00E−10	102.5	3	3A	4051	0.5	x1H1814+498	0.5	A3	CV	AM HER	0.5
1ES1817+537	18 17 10	+53 42 59	$0.55^{+0.19}_{-0.16}$	11/5	1.87E−10	18.9	4	3A	...	...	...	...	...	...	...	...
1ES1820−303	18 20 29	−30 23 23	$99.31^{+5.66}_{-5.69}$	309/1	1.00E−10	3.1	7	3A	...	...	x1H1820−303	0.2	A3	XRB	NGC 6624	0.3
1ES1821+643	18 21 43	+64 19 13	$1.08^{+0.23}_{-0.21}$	28/10	1.00E−10	24.3	6	3A	4066	0.3	x1H1820+643	0.3	HB	AGN:0.297	KUV 1821+64*	0.3
1ES1824+151	18 24 38	+15 07 03	$1.18^{+0.47}_{-0.39}$	8/1	1.00E−10	6.7	7	3A	...	...	...	...	SAO	S:K0	SAO 103722	1.2
1ES1827+206	18 27 48	+20 41 56	$0.14^{+0.06}_{-0.05}$	10/1	7.03E−05	58.3	8	2A	...	...	...	...	...	...	...	...
1ES1832+516	18 32 43	+51 40 04	$1.02^{+0.30}_{-0.26}$	15/5	1.00E−10	14.0	5	3A	4094	0.9	x	...	WLY	AC:M0EV	BY DRA	1.0

TABLE 6—*Continued*

Slew Desig.	RA 1950	DEC 1950	IPC Rate (cts s^{-1})	NP/NS	P_{rend}	Exp. (s)	PI	QI	EOS # EMSS	Δ2E (′)	A3 EXO	Δ1H (′)	Cat.	Class.: Type/z	Name	ΔC (′)
1ES1833+326	18 33 11	+32 38 41	$0.49^{+0.10}_{-0.09}$	35/3	1.00E−10	65.4	7	3A	4097	0.7	x1H1835+326	0.6	VV	AGN:0.059	3C382.0	0.7
1ES1833+169	18 33 40	+16 56 41	$0.17^{+0.06}_{-0.05}$	18/5	7.53E−07	78.6	5	3A	...	...	...	...	BSC	S:G2V+G2V	HD 171746	0.6
1ES1841−044	18 41 55	−04 27 10	$0.42^{+0.20}_{-0.16}$	7/2	2.22E−05	14.9	3	3A	...	...	...	...	GCV	S	FT SCT	1.6
1ES1845+797	18 45 41	+79 43 04	$0.20^{+0.02}_{-0.02}$	156/24	1.00E−10	618.8	7	3A	4136	0.2	x1H1858+797	0.2	VV	AGN:0.057	3C 390.3	0.2
1ES1846+005	18 46 22	+00 31 37	$0.22^{+0.08}_{-0.07}$	12/2	7.32E−08	48.3	6	3A	4138	0.2	x	...	SHA	CV	V603 AQL	0.2
1ES1846−238	18 46 45	−23 53 05	$0.43^{+0.13}_{-0.11}$	17/2	1.00E−10	35.4	3	3A	4140	0.6	...	...	WLY	S:M4EV	WLY 729	0.4
1ES1846−009	18 46 56	−00 59 03	$0.24^{+0.11}_{-0.09}$	8/1	1.03E−05	29.6	8	3A	...	...	...	...	...	...	...	...
1ES1850+005	18 50 04	+00 34 51	$0.23^{+0.06}_{-0.05}$	26/3	1.00E−10	93.7	6	3A	4150	1.5	...	...	SBD	SNR	4C .70	2.9
1ES1850−087	18 50 20	−08 45 58	$4.21^{+0.26}_{-0.27}$	260/3	1.00E−10	60.9	7	3A	4151	0.2	x1H1850−087	0.3	A3	XRB	NGC6712	0.3
1ES1851−312	18 51 51	−31 13 27	$0.94^{+0.27}_{-0.23}$	16/3	1.00E−10	16.1	7	3A	...	...	x1H1853−312	0.5	A3	CV	V1223 SGR	0.5
1ES1853−379	18 53 13	−37 58 25	$0.86^{+0.31}_{-0.26}$	10/5	1.00E−10	11.2	3	3A	...	...	...	...	...	...	...	...
1ES1853+012	18 53 23	+01 16 13	$0.78^{+0.29}_{-0.25}$	11/2	1.76E−07	12.4	7	3A	...	...	1H1852+015	2.5	A3	SNR	G34.7-0	2.5
1ES1853+671	18 53 56	+67 09 44	$0.15^{+0.06}_{-0.05}$	12/8	5.48E−05	59.6	6	3A	...	...	...	...	...	...	...	...
1ES1900+699	19 00 52	+69 54 36	$0.15^{+0.05}_{-0.04}$	18/5	1.12E−06	92.1	7	3A	...	...	...	...	ABL	CG:0.094	A2315	2.3
1ES1902−524	19 02 22	−52 25 05	$1.12^{+0.60}_{-0.46}$	5/2	8.97E−07	4.3	7	3A	...	...	...	...	BSC	S:F7V	ρ TEL	0.2
1ES1905+070	19 05 08	+07 04 27	$0.45^{+0.21}_{-0.17}$	7/3	1.63E−05	14.0	6	2A	...	...	...	...	SBD	...	HSNH 111	0.7
1ES1905+000	19 05 51	+00 05 23	$3.85^{+0.67}_{-0.61}$	38/4	1.00E−10	9.7	8	3A	...	...	x1H1905+000	0.7	A3	XRB	X1905+000	0.8
1ES1907+523	19 07 14	+52 20 45	$0.81^{+0.26}_{-0.22}$	13/5	1.00E−10	15.1	4	3A	4195	0.2	...	...	BSC	AC:K1IV	HD179094	0.3
1ES1907+097	19 07 15	+09 44 48	$0.53^{+0.10}_{-0.09}$	38/6	1.00E−10	67.0	9	3A	...	...	x1H1909+096	0.1	A3	XRB-Be	X1907+097	0.1
1ES1908+090	19 08 44	+09 02 12	$0.25^{+0.08}_{-0.07}$	15/5	2.38E−08	50.1	7	3A	4203	0.7	...	...	2E	SNR	W49B	0.8
1ES1908+005	19 08 45	+00 30 30	$3.42^{+0.61}_{-0.55}$	39/2	1.00E−10	10.8	8	3A	...	...	...	...	BMC	XRB	AQL X-1	0.6
1ES1909+048	19 09 21	+04 53 45	$0.87^{+0.04}_{-0.04}$	437/21	1.00E−10	476.6	7	3A	4204	0.2	x1H1908+047	0.2	A3	SNR	SS433	0.2
1ES1914+092	19 14 38	+09 15 09	$0.14^{+0.05}_{-0.04}$	18/2	4.16E−06	93.6	6	2A	...	...	...	...	SAO	S:K2II	SAO 124465*	1.2
1ES1916−053	19 16 07	−05 19 54	$7.13^{+0.37}_{-0.37}$	382/6	1.00E−10	53.0	7	3A	4222	0.1	x1H1916−053	0.3	SHA	CV	V1336 AQL	1.5
1ES1916+195	19 16 39	+19 30 53	$0.28^{+0.12}_{-0.10}$	8/5	5.69E−06	25.3	8	3A	4225	0.6	...	...	SAO	S:B8III+K	U SGE	0.3
1ES1920+223	19 20 44	+22 23 02	$0.53^{+0.28}_{-0.22}$	5/4	1.99E−06	9.1	7	3A	...	...	...	...	SBD	S:A2	HD 344230	1.9
1ES1921−293	19 21 45	−29 20 31	$0.07^{+0.03}_{-0.02}$	29/4	3.57E−05	222.2	7	3A	4245	0.6	x	...	HB	AGN:0.352	OV 236	0.6
1ES1927+654	19 27 00	+65 28 02	$0.93^{+0.17}_{-0.15}$	37/17	1.00E−10	37.9	5	3A	...	...	...	...	...	...	...	...
1ES1928+738	19 28 56	+73 51 28	$0.34^{+0.13}_{-0.11}$	11/7	2.39E−07	28.3	7	2A	...	...	x1H1922+746	0.5	VV	AGN:0.302	4C 73.18	0.5
1ES1932+695	19 32 28	+69 33 36	$0.11^{+0.04}_{-0.04}$	13/6	4.62E−05	88.8	5	3A	4267	0.4	...	...	WLY	S:K0V	WLY 764	1.0
1ES1934−063	19 34 53	−06 19 38	$1.48^{+0.46}_{-0.39}$	13/3	1.00E−10	8.6	7	3A	...	...	1H1934−063.A	0.3	A3	AGN:0.011	SS 442	0.3
1ES1935+501	19 35 09	+50 07 07	$0.12^{+0.04}_{-0.03}$	24/7	3.86E−08	144.1	3	3A	4269	0.5	...	...	SAO	S:F4V	SAO 031815	0.7
1ES1948+087	19 48 23	+08 44 20	$0.07^{+0.02}_{-0.02}$	25/5	1.86E−05	228.1	5	3A	4294	0.4	x	...	SAO	S:A7V	SAO 125122	0.3

TABLE 6—*Continued*

Slew Desig.	RA 1950	DEC 1950	IPC Rate (cts s^{-1})	NP/NS	P_{rand}	Exp. (s)	PI	QI	EOS # EMSS	Δ2E (′)	A3 EXO	Δ1H (′)	Cat.	Class.: Type/z	Name	ΔC (′)
1ES1948+085	19 48 47	+08 34 35	$0.08^{+0.03}_{-0.03}$	25/6	2.14E−05	189.7	4	3A	4295	0.6	x	...	2E	S	AG+08 2640	0.3
1ES1957+405	19 57 47	+40 35 54	$0.40^{+0.11}_{-0.10}$	23/1	8.66E−10	46.3	8	3E	4309	0.3	1H1958+406	0.5	A3	AGN:0.056	CYG A*	0.6
1ES1959+650	19 59 35	+65 00 14	$1.59^{+0.28}_{-0.26}$	38/10	1.00E−10	23.1	6	3A	...	...	...	...	...	...	...	...
1ES2001+068	20 01 41	+06 51 03	$1.19^{+0.58}_{-0.46}$	7/1	2.02E−05	5.2	4	2A	...	...	...	...	SBD	S:K2	HD 190342	2.4
1ES2005+175	20 05 20	+17 33 30	$0.20^{+0.04}_{-0.04}$	32/3	1.00E−10	132.0	5	3A	4322	0.2	x	...	SHA	CV	WZ SGE	0.1
1ES2005−489	20 05 47	−48 58 45	$1.44^{+0.70}_{-0.55}$	6/4	1.50E−07	4.0	6	3A	...	...	x	...	VV	BL:0.071	PKS	0.1
1ES2008−570	20 08 23	−57 01 20	$0.45^{+0.21}_{-0.17}$	9/6	9.99E−05	15.9	6	2A	4331	2.6	...	...	SBD	GAL:0.055	ESO 186- 11	2.8
1ES2010+463	20 10 33	+46 20 06	$0.38^{+0.07}_{-0.06}$	43/12	1.00E−10	99.0	7	3A	4336	0.3	...	...	2E	S	31 CYG	0.4
1ES2013+448	20 13 12	+44 52 37	$0.17^{+0.07}_{-0.06}$	11/7	7.43E−06	52.9	6	3A	...	...	...	...	SAO	S:K0	SAO 049357	0.4
1ES2018+436	20 18 49	+43 41 30	$0.36^{+0.12}_{-0.10}$	14/7	1.37E−08	33.9	6	3A	...	...	x1H2018+439	0.4	SAO	S:WC7P+O5	SAO 049491	0.4
1ES2025+573	20 25 19	+57 22 34	$0.24^{+0.12}_{-0.09}$	7/5	1.95E−05	26.1	8	3A	...	...	...	...	...	...	...	...
1ES2028+513	20 28 10	+51 19 47	$0.24^{+0.13}_{-0.10}$	5/5	5.10E−08	20.3	4	3A	...	...	...	...	...	...	...	...
1ES2030+407	20 30 39	+40 47 13	$14.21^{+0.10}_{-0.10}$	19909/26	1.00E−10	1384.8	8	3A	4376	0.4	x1H2030+407	0.2	A3	XRB	CYG X-3	0.3
1ES2031+411	20 31 28	+41 08 43	$0.11^{+0.01}_{-0.01}$	250/18	1.00E−10	1059.0	7	3A	4382	0.2	...	...	SAO	S:O6Ib	SAO 049781*	0.2
1ES2033+110	20 33 05	+11 00 18	$0.13^{+0.06}_{-0.05}$	12/2	6.88E−05	69.8	8	3A	...	...	...	...	...	...	...	...
1ES2037−010	20 37 35	−01 03 02	$0.16^{+0.07}_{-0.06}$	12/2	4.12E−05	56.8	4	3A	4404	0.3	x	...	SHA	CV	AE AQR	0.2
1ES2037+521	20 37 57	+52 09 42	$0.10^{+0.04}_{-0.03}$	16/7	6.99E−05	111.1	6	3A	4405	0.6	...	...	2E	...	...	...
1ES2038−007	20 38 18	−00 46 43	$0.10^{+0.04}_{-0.03}$	18/4	7.81E−06	123.6	6	3A	m4408	0.6	...	...	SAO	S:F8	SAO 144692	1.2
1ES2039+758	20 39 42	+75 51 07	$0.24^{+0.12}_{-0.09}$	7/5	1.44E−05	25.9	9	2A	...	...	...	...	...	...	...	...
1ES2042+335	20 42 49	+33 31 51	$0.10^{+0.04}_{-0.03}$	19/11	3.12E−05	127.8	6	3A	...	...	...	...	SAO	S:G5	SAO 070451	2.2
1ES2048+314	20 48 50	+31 25 17	$0.26^{+0.08}_{-0.08}$	185/11	1.00E−10	181.6	4	3A	...	...	...	...	SAO	S:K0	SAO 070569	0.9
1ES2052+441	20 52 08	+44 11 40	$1.00^{+0.21}_{-0.19}$	29/10	1.00E−10	27.3	5	3A	...	...	...	...	SAO	S:G2V	SAO 050198	0.5
1ES2055+298	20 55 55	+29 51 05	$0.25^{+0.12}_{-0.10}$	9/4	8.50E−05	29.2	7	3A	...	...	...	...	...	...	...	...
1ES2055+443	20 55 57	+44 20 43	$0.28^{+0.14}_{-0.11}$	8/4	9.27E−05	23.4	6	2A	...	...	...	...	...	...	...	...
1ES2056+504	20 56 53	+50 29 55	$0.20^{+0.08}_{-0.07}$	11/3	3.05E−06	45.6	7	2A	...	...	...	...	...	...	...	...
1ES2058+398	20 58 08	+39 52 07	$0.41^{+0.13}_{-0.11}$	14/7	1.00E−10	30.7	4	3A	...	...	...	...	WLY	AC:M3EV+M3EV	WLY 815AB	0.6
1ES2100+276	21 00 18	+27 36 26	$0.57^{+0.08}_{-0.07}$	69/8	1.00E−10	111.8	5	3A	4438	0.1	x	...	SAO	S:G0V+G5V	ER VUL	0.4
1ES2127+119	21 27 34	+11 56 56	$4.28^{+0.66}_{-0.61}$	47/5	1.00E−10	10.8	7	3A	...	...	x1H2128+120	0.3	A3	XRB	M15	0.3
1ES2128+231	21 28 47	+23 06 50	$0.46^{+0.18}_{-0.15}$	9/3	3.11E−10	18.8	5	3A	...	...	...	...	SBD	S:K8	BD+22 4409	0.7
1ES2129−026	21 29 31	−02 37 12	$0.22^{+0.10}_{-0.08}$	10/1	8.17E−05	35.4	5	3A	...	...	...	...	SBD	S	PHL 26	1.3
1ES2129+470	21 29 36	+47 04 11	$1.25^{+0.16}_{-0.15}$	70/2	1.00E−10	52.8	8	3A	4485	0.2	1H2131+473	0.1	A3	XRB	X2129+470	0.1
1ES2131+812	21 31 24	+81 17 38	$0.40^{+0.17}_{-0.14}$	8/5	7.63E−08	18.8	6	3A	...	...	...	...	...	...	...	...
1ES2135−147	21 35 01	−14 46 16	$0.14^{+0.04}_{-0.04}$	24/4	4.51E−08	132.1	7	3A	4497	0.1	x	...	VV	AGN:0.200	PHL 1657	0.2

TABLE 6—*Continued*

Slew Desig.	RA 1950	DEC 1950	IPC Rate (cts s^{-1})	NP/NS	P_{read}	Exp. (s)	PI	QI	EOS # EMSS	Δ2E (′)	A3 EXO	Δ1H (′)	Cat.	Class.: Type/z	Name	ΔC (′)
1ES2135+011	21 35 02	+01 10 38	$0.20^{+0.09}_{-0.07}$	11/8	7.33E−05	43.0	8	2A	...	...	...	...	SBD	S:K0	AG+01 2623	2.4
1ES2137+204	21 37 00	+20 26 22	$0.21^{+0.10}_{-0.08}$	8/7	8.51E−05	32.2	7	2A	...	...	...	...	...	...	...	...
1ES2137+241	21 37 26	+24 10 25	$0.75^{+0.37}_{-0.29}$	6/3	4.71E−07	7.6	5	3A	...	...	...	...	...	...	...	...
1ES2143+751	21 43 03	+75 10 25	$0.29^{+0.11}_{-0.09}$	11/5	1.37E−08	34.0	5	3A	...	...	...	...	...	...	...	...
1ES2149+054	21 49 40	+05 24 21	$0.19^{+0.06}_{-0.05}$	19/2	1.89E−08	82.2	5	3A	4536	0.5	...	...	2E	...	...	...
1ES2152−548	21 52 53	−54 52 47	$0.68^{+0.24}_{-0.20}$	12/3	8.52E−10	16.1	4	3A	...	...	...	...	...	...	...	...
1ES2153+441	21 53 14	+44 10 17	$0.59^{+0.13}_{-0.12}$	25/8	1.00E−10	40.1	6	3A	...	...	...	...	SAO	S:K0	SAO 051437	1.0
1ES2155−081	21 55 14	−08 08 32	$0.13^{+0.05}_{-0.04}$	14/3	9.44E−05	78.8	5	3A	...	...	...	...	SBD	S	BD-08 5773	0.7
1ES2155−304	21 55 58	−30 27 48	$5.08^{+0.16}_{-0.16}$	1043/5	1.00E−10	202.1	4	3A	4544	0.1	x1H2156−304	0.1	VV	BL:0.117	PKS	0.1
1ES2156+032	21 56 20	+03 15 35	$0.08^{+0.03}_{-0.03}$	19/1	8.10E−05	153.9	12	2A	...	...	...	...	...	...	...	...
1ES2159+436	21 59 29	+43 38 56	$0.12^{+0.02}_{-0.02}$	59/8	1.00E−10	360.0	6	3A	4550	0.1	...	...	SAO	S:G5	SAO 051563	0.5
1ES2200+826	22 00 09	+82 37 38	$0.59^{+0.27}_{-0.22}$	7/5	4.78E−07	11.0	7	3A	...	...	x	...	BSC	S:F6IV-V	HD 209942	0.2
1ES2200+420	22 00 40	+42 01 47	$0.27^{+0.07}_{-0.06}$	22/4	1.00E−10	72.2	7	3A	4558	0.5	x	...	VV	BL:0.070	BL LAC	0.4
1ES2201+315	22 01 02	+31 31 13	$0.22^{+0.10}_{-0.08}$	8/1	1.69E−05	31.2	6	3A	4561	0.3	...	...	HB	AGN:0.297	4C 31.63	0.2
1ES2202+469	22 02 56	+46 59 06	$0.30^{+0.11}_{-0.10}$	12/2	1.94E−07	33.9	4	3A	4567	0.4	1H2213+484	0.4	A3	AC	HK LAC	0.4
1ES2206+445	22 06 25	+44 30 34	$0.11^{+0.04}_{-0.04}$	17/2	6.45E−06	111.0	6	3A	...	...	...	...	...	...	...	...
1ES2206+455	22 06 40	+45 30 02	$1.86^{+0.08}_{-0.08}$	576/6	1.00E−10	302.0	5	3A	4573	0.2	x1H2207+455	0.3	A3	AC	AR LAC	0.3
1ES2207+643	22 07 06	+64 20 20	$0.14^{+0.06}_{-0.05}$	12/5	8.06E−05	62.8	7	3A	...	...	...	...	...	...	...	...
1ES2207−124	22 07 37	−12 25 27	$0.29^{+0.05}_{-0.04}$	55/5	1.00E−10	168.3	6	3A	4575	1.3	...	...	ABL	CG:0.084	A2420	1.3
1ES2216+845	22 16 16	+84 30 24	$0.28^{+0.13}_{-0.10}$	8/6	6.32E−06	25.0	5	3A	...	...	...	...	SAO	S:K2	SAO 003717	0.5
1ES2216+565	22 16 58	+56 35 39	$0.22^{+0.09}_{-0.08}$	11/6	4.15E−05	39.1	5	3A	...	...	...	...	...	...	...	...
1ES2221−018	22 21 22	−01 50 48	$0.18^{+0.06}_{-0.05}$	18/3	8.21E−08	81.1	8	3A	4597	1.6	1H2221−017.A	1.3	ABL	CG:0.090	A2440	1.0
1ES2223−051	22 23 09	−05 11 51	$0.17^{+0.03}_{-0.03}$	42/6	1.00E−10	200.4	7	3A	4603	0.5	x	...	VV	AGN:1.404	3C 446	0.7
1ES2236−208	22 36 04	−20 52 31	$0.66^{+0.09}_{-0.08}$	70/4	1.00E−10	99.4	4	3A	4632	0.4	x	...	SAO	AC:M2V+M4V	WLY 867AB	0.4
1ES2240+294	22 40 18	+29 28 17	$1.88^{+0.35}_{-0.32}$	33/7	1.00E−10	17.2	5	3A	...	...	1H2239+294	0.5	VV	AGN:0.025	AKN 564	0.5
1ES2244−019	22 44 48	−01 54 11	$0.15^{+0.05}_{-0.05}$	16/4	1.09E−06	82.4	13	2A	...	...	...	...	...	...	...	...
1ES2246−646	22 46 36	−64 41 41	$0.44^{+0.18}_{-0.15}$	9/6	7.94E−07	18.1	6	2E	...	...	1H2245−646	2.8	ABL	CG	A3921	2.8
1ES2247+106	22 47 53	+10 37 37	$0.76^{+0.33}_{-0.27}$	8/2	3.90E−07	9.7	6	3A	...	...	...	...	ABL	CG:0.077	A2495*	0.5
1ES2251+376	22 51 23	+37 40 29	$0.16^{+0.05}_{-0.04}$	20/2	9.67E−08	93.7	4	3A	4644	0.0	...	...	SAO	S:K0V	SW LAC	0.6
1ES2251−178	22 51 26	−17 50 20	$0.45^{+0.10}_{-0.09}$	31/2	1.00E−10	61.4	8	3A	4645	0.6	x1H2251−179	0.6	HB	AGN:0.068	MR 2251-178	0.6
1ES2254−371	22 54 52	−37 11 34	$0.28^{+0.07}_{-0.06}$	25/4	1.00E−10	76.2	4	3A	m4664	0.7	...	...	MS	AGN:0.039	MS	0.6
1ES2257−340	22 57 38	−34 01 28	$0.45^{+0.21}_{-0.17}$	7/4	1.53E−06	14.3	4	3A	...	...	...	...	SAO	S:G5VP	SAO 214237	1.7
1ES2257+620	22 57 39	+62 04 26	$0.15^{+0.06}_{-0.05}$	13/8	1.31E−05	68.5	7	3A	...	...	...	...	...	...	...	...

TABLE 6—*Continued*

Slew Desig.	RA 1950	DEC 1950	IPC Rate (cts s^{-1})	NP/NS	P_{rand}	Exp. (s)	PI	QI	EOS # EMSS	Δ2E (′)	A3 EXO	Δ1H (′)	Cat.	Class.: Type/z	Name	ΔC (′)
1ES2259+586	22 59 06	+58 36 31	$0.93^{+0.10}_{-0.10}$	128/10	1.00E−10	116.9	7	3A	4673	0.3	x1H2258+585	0.4	A3	SNR	G109.1-1.0	0.4
1ES2304+042	23 04 29	+04 16 40	$1.11^{+0.43}_{-0.36}$	9/2	2.43E−09	7.7	7	3A	...	...	x1H2303+039	0.3	VV	AGN:0.042	PG	0.3
1ES2304+252	23 04 38	+25 12 19	$0.11^{+0.04}_{-0.04}$	13/4	1.28E−05	92.0	7	3A	4682	0.9	1H2315+257	0.7	A3	AC	56 PEG B	0.7
1ES2307+476	23 07 33	+47 41 36	$0.54^{+0.15}_{-0.13}$	19/7	1.00E−10	32.0	4	3A	4687	1.2	...	...	SAO	AC:G5	KZ AND	1.6
1ES2310−219	23 10 20	−21 54 55	$0.20^{+0.04}_{-0.04}$	41/4	1.00E−10	160.5	7	3A	4695	0.7	1H2307−222.A	0.9	ABL	CG:0.086	A2556	1.3
1ES2311−430	23 11 13	−43 00 13	$1.03^{+0.13}_{-0.12}$	78/7	1.00E−10	71.6	6	3A	m4699	0.4	x	...	2E	CG:0.056	S1101*	0.8
1ES2316−423	23 16 22	−42 22 24	$0.12^{+0.03}_{-0.03}$	42/10	1.00E−10	240.1	6	3A	m4709	0.6	...	...	MS	CG:0.045	S1111	0.4
1ES2319−421	23 19 00	−42 10 15	$0.15^{+0.04}_{-0.04}$	26/9	3.04E−08	122.7	7	3A	m4721	2.0	...	...	ABL	CG	A3998	1.1
1ES2321+585	23 21 06	+58 33 08	$28.63^{+1.17}_{-1.17}$	612/12	1.00E−10	21.2	7	3A	4724	0.6	x1H2321+585	0.8	A3	SNR	CAS A	0.8
1ES2321+419	23 21 23	+41 54 59	$0.12^{+0.05}_{-0.04}$	12/4	3.04E−05	78.3	8	1A	4725	1.2	1H2318+417	1.1	A3	BL	H2321+419	1.0
1ES2321+143	23 21 47	+14 22 26	$0.14^{+0.04}_{-0.04}$	23/3	1.29E−07	123.0	8	2E	...	...	1H2320+146	2.6	A3	CG:0.041	A2593	2.7
1ES2322−409	23 22 02	−40 56 46	$0.70^{+0.29}_{-0.23}$	8/4	1.23E−09	11.0	6	3A	...	...	...	...	...	...	...	...
1ES2322−124	23 22 46	−12 24 27	$0.55^{+0.16}_{-0.14}$	17/2	1.00E−10	28.0	8	3A	4728	0.8	...	...	ABL	CG:0.085	A2597	1.7
1ES2326+411	23 26 59	+41 11 16	$0.38^{+0.16}_{-0.13}$	8/4	5.83E−07	19.4	2	3A	...	...	...	...	SBD	S:M2	G 190 -28	0.4
1ES2329+196	23 29 20	+19 39 44	$0.54^{+0.07}_{-0.06}$	88/6	1.00E−10	151.1	4	3A	4733	0.2	x	...	WLY	S:M4E+M6E	WLY 896AB	0.0
1ES2334+063	23 34 07	+06 18 05	$0.32^{+0.14}_{-0.11}$	9/3	7.38E−06	24.5	8	3A	...	...	...	...	SAO	S:G0	SAO 128282	0.8
1ES2335+461	23 35 06	+46 11 20	$2.85^{+0.18}_{-0.18}$	251/8	1.00E−10	86.6	5	3A	4740	0.2	x1H2336+462	0.2	A3	AC	λ AND	0.1
1ES2340−152	23 40 53	−15 12 37	$0.17^{+0.07}_{-0.06}$	11/1	3.46E−05	50.8	3	3A	m4755	0.6	x	...	ZCT	GAL:0.137	MS	0.8
1ES2342+089	23 42 25	+08 55 11	$0.38^{+0.06}_{-0.05}$	65/8	1.00E−10	150.4	6	3A	4758	0.5	1H2343+090	2.9	A3	CG:0.040	A2657	2.9
1ES2343−151	23 43 02	−15 06 15	$0.23^{+0.10}_{-0.08}$	9/2	1.15E−05	34.1	5	3A	4760	0.4	...	...	SBD	...	068.16-70.38	0.6
1ES2344+514	23 44 37	+51 25 50	$0.43^{+0.16}_{-0.14}$	10/7	1.22E−08	21.6	7	3A	...	...	...	...	...	...	...	...
1ES2347+485	23 47 58	+48 31 57	$0.40^{+0.19}_{-0.15}$	7/3	9.62E−06	15.9	4	3A	...	...	...	...	...	...	...	...
1ES2349−561	23 49 31	−56 11 39	$0.88^{+0.42}_{-0.33}$	6/4	7.55E−08	6.6	6	3A	...	...	...	...	ABL	CG	S1158	1.4
1ES2352−208	23 52 03	−20 51 58	$1.07^{+0.64}_{-0.48}$	4/1	3.69E−07	3.7	3	3A	...	...	...	...	...	...	...	...
1ES2352+283	23 52 32	+28 21 49	$2.98^{+0.57}_{-0.52}$	31/6	1.00E−10	10.2	4	3A	4789	0.5	x1H2354+285	0.9	HD	S:K0V	HD 224085	0.8
1ES2352+600	23 52 54	+60 03 32	$0.32^{+0.15}_{-0.12}$	6/4	3.66E−07	18.0	7	3A	...	...	...	...	...	...	...	...
1ES2352+512	23 52 59	+51 15 33	$0.76^{+0.41}_{-0.31}$	5/3	4.34E−07	6.4	4	3A	...	...	...	...	...	...	...	...

Column (8).—Mean pulse height bin. The average of the "pulse-invariant" (PI; Harnden et al. 1984) channel numbers (1–15) for each photon, which coarsely indicates the source spectrum.

Column (9).—Quality control index (Q) and *image code* (I). The Q (1, 2, or 3; 3 being highest quality) value is a visual estimate of the reliability of the source. The *image code* highlights cases where Prob1/Prob2 (defined in § 4.3) is large ($>10^3$), and which a visual inspection shows to be extended, or to have multiple sources within 15′ (see § 4.5). The *image code* has the following values:

A, generally acceptable Prob1/Prob2;
E, extended source (>15′);
M, multiple sources within 15′;
P, part of source (extended source existing in more than one field).

Columns (10) and (11).—EOSCAT number, Einstein Medium Survey membership (noted by *m*), and *offset from EOSCAT position* (Δ2E). For sources with counterparts in the 2E Catalog (Harris et al. 1991), we provide the EOSCAT number and the difference between the Slew Survey and catalog positions, in arc minutes. In addition, Medium Survey (Gioia et al. 1990; Stocke et al. 1991) sources are noted with a letter *m* preceding the EOSCAT number.

Columns (12) and (13).—HEAO 1 A-3 *counterpart, EXOSAT detections* (noted by *x*), and *offset from HEAO* A-3 *position* (Δ1H). For sources with counterparts in the *HEAO* 1 A-3 catalog (Remillard et al. 1991), we provide the "1H" name and the difference between the Slew Survey and catalog positions, in arcminutes. In addition, *EXOSAT* sources are noted with a letter *x* preceding the 1H name.

Columns (14)–(17).—Optical catalog (Cat.), *object classification* (Class.), *counterpart name* (Name), and *offset from catalog position* (ΔC). For sources with counterparts in (mainly) optical catalogs searched to date (see below for catalog list and references), we provide the name of the catalog, the classification (e.g., AGN), the counterpart name, and the difference between the Slew Survey and catalog positions, in arcminutes. If the redshift or stellar spectral type is known, it is listed after the object classification in column (15).

Composite spectral types in Table 6 indicate a binary (or other multiple star system). In general, we have tried to use the most common names of objects. For cases in which two objects (most commonly an SAO star and an extragalactic object) were found in the same error box, we compared their f_x/f_o ratios with those for the Medium Survey sources (Maccacaro et al. 1988). In most cases, only one of the objects was a plausible counterpart given these ratios. Cases in which more than one object is a likely counterpart are indicated with asterisks and noted below (§ 7.3).

If the counterpart name is the same as the Slew name in column (1) and the catalog is well known, only the catalog designator is listed in column (16) (e.g., PG, EXO, 2E). Woolley names with letters A, B, ··· indicate multistar systems (e.g., WLY 127AB). For each of the newly discovered X-ray sources, we list all the names known to us in Table 7.

Abbreviations for names of catalogs are as follows:

2E, Second *Einstein* IPC Catalog ('EOSCAT'; Harris et al. 1991);
A3, *HEAO* A-3 Catalog (Remillard et al. 1991);
ABL, Abell Catalog (1958; Struble & Rood 1987) and Southern Abell Catalog (Abell, Corwin, & Olowin 1989);
BMC, Bradt & McClintock (1983);
BSC, Bright Star Catalog (Hoffleit & Jaschek 1982);
EHG, *EXOSAT* High Galactic Latitude Survey (Giommi et al. 1991);
EXC, *EXOSAT* data base of optical and other astronomical catalogs;
GCV, General Catalog of Variable Stars (Kholopov et al. 1985–1988);
HB, Hewitt & Burbidge (1987);
HD, Henry Draper Catalog (Cannon & Pickering 1918–1924);
MCS, McCook & Sion (1987);
MS, *Einstein* Extended Medium-Sensitivity Survey (Gioia et al. 1990);
RNG, Revised NGC Catalog (Sulentic & Tifft 1973);
SAO, SAO Catalog (SAO Staff 1966);
SBD, SIMBAD data base;
SHA, Shara (1990);
UGC, Uppsala General Catalogue of Galaxies (Nilsson 1973);
VV, Véron-Cetty & Véron (1987);
WFC, ROSAT Wide-Field Camera (Cooke et al. 1991);
WLY, Woolley Catalog (Woolley et al. 1970);[2] and
ZCT, CfA Redshift Catalog; Huchra (1990).

Abbreviations for object classification are as follows:

AC, active star;
AGN, active galactic nucleus;
BL, BL Lacertae object;
CG, cluster of galaxies;
CV, cataclysmic variable;
GAL, normal galaxy;
P, pulsar;
S, normal star;
SNR, supernova remnant;
WD, white dwarf;
XRB, X-ray binary; and
(XRB-Be), X-ray binary (with Be star secondary).

6.2. *Notes on Individual Objects*

1ES 0013+195.—The error box also contains G32–7 (S:M4.5), but at $V = 14$ (cf. 13 for G32–6), it is an unlikely counterpart based on f_x/f_o (Maccacaro et al. 1988).

1ES 0100+405.—The stars G132–51B and G132–51C are in the error box and have acceptable f_x/f_o ratios, although both (at $V = 13.01$) are 2.2 mag fainter than G132–51A.

1ES 0120+004.—Besides the star, the error box contains MCG +00-04-103, a 16th mag galaxy which may be an AGN.

1ES 0122+084A and B.—Besides the cluster, the error box also includes the galaxy UGC 977, which may be a previously unknown AGN.

1ES 0237–531.—The error box also contains SAO 232842 (S:K5), which at $V = 8.3$ is 0.9 mag fainter than HD 16699.

1ES 0255+128.—Besides the cluster, the error box also contains the galaxy UGC 2438, another possible AGN.

1ES 0305–284.—The error box also contains LTT 1477 (S:M3), but this source has $V = 14.0$, and can be ruled out by f_x/f_o arguments.

[2] This is an extended version of the Gleise catalog, using the same numbering scheme as Gleise.

1ES 0316+413.—Besides the cluster, the error box also contains the AGN NGC 1275, a known X-ray source (Branduardi-Raymont et al. 1981).

1ES 0429+130.—The error box also contains HD 286839 (S:K0).

1ES 0538−019.—The Slew Survey error box contains part of the Orion star-forming region, based on an HRI detection.

1ES 0702+646.—Other than the AGN, the error box contains SAO 14073 (S: G0).

1ES 0716−248.—The error box contains a substantial portion of the globular cluster N2362, of which HD 57061 is the brightest star (at $V = 4.32$). There are more than 30 other possible counterparts, ranging from $V = 8.12$ to $V = 13$, with known spectral types B2–A0.

1ES 0953+693.—The error box also contains 0953+6917, a $B = 13.7$ galaxy which may have an active nucleus.

1ES 1035−268.—Error box contains the compact group HCG 048, which includes the galaxy counterpart.

1ES 1101+384.—The error box contains two identifications based on the 2E catalog: Mrk 421 (BL), and 51 UMA (S: A3), but the latter is 2.'1 from the 1ES position. Mrk 421 is a well-known source at high energies (Wood et al. 1984) and is clearly the preferred identification based on an HRI position (from *einline*).

1ES 1215+039.—The counterpart is a double galaxy.

1ES 1218−637.—The optical counterpart is a young SNR candidate, based on HRI data in *einline*.

1ES 1254−172.—The error box also contains 1254−1711 (GAL:0.049), a possible AGN.

1ES 1259+289.—The error box also contains 1259+2857 (GAL:0.030), a possible AGN.

1ES 1301−239.—Error box also contains A3541 (CG).

1ES 1351+695.—Error box also includes MCG +12-13-024 (AGN: 0.031). With $V = 17$ MCG +12-13-024 is a marginally acceptable candidate based on f_x/f_o (Maccacaro et al. 1984). Mrk 279 is the preferred identification based on an HRI position (in *einline*).

1ES 1503+017.—The counterpart, N5486, is part of a galaxy pair with the fainter N5486A (GAL: 0.007).

1ES 1549+203.—There are two acceptable identifications: LB 906 (AGN), and SAO 084044 (S: G0), but the latter is 1.'6 from the 1ES position.

1ES 1602+178.—The UGC counterpart is a galaxy pair. In addition, the error box contains an NGC pair at $z \sim 0.035$ and a Zwicky triple at $z = 0.038$.

1ES 1702+457.—The error box also contains two galaxies—1702+4544A (GAL:0.061) and 1701+4544B (GAL:0.007).

1ES 1704+545.—Triple system (with WLY 9584B, F6V; WLY 9584C).

1ES 1706+787.—The error box also contains a Zwicky triple (1706+7842), and another Zwicky galaxy.

1ES 1714+574.—Error box also includes NGC 6345 (GAL), 2.'7 from the 1ES position.

1ES 1731−325.—Error box also includes HD 159176 (S:O6 V+O6 V), possibly a member of the globular cluster.

1ES 1821+643.—Error box also includes K1-16 (WD: D0Z1), which had an *EXOSAT* detection, (1.'2 from the 1ES position). However, the PI bin value (=6) suggests that the AGN is the correct identification, since white dwarfs typically have a mean PI bin of 2 (Schachter et al. 1991).

1ES 1914+092.—Error box also includes SAO 124466 (S: F0).

1ES 1957+405.—Both the cluster and the radio galaxy are possible counterparts.

1ES 2031+411.—The Slew Survey field contains part of the OB association VI Cygni. The SAO star identification is based on IPC and HRI data in Harnden et al. (1979). There are two or more HRI sources present within a 0.'3 radius (also see Fig. 9).

1ES 2247+106.—Other than the cluster, the error box also contains MCG +02-58-021, a 16th mag galaxy which is possibly an AGN.

1ES 2311−430.—The error box also contains 2311−4300 (GAL:0.056), with the same redshift as the cluster, a possible AGN.

7. IDENTIFICATIONS

Identifications of Slew Survey sources with known X-ray sources have played an important role in producing this catalog (as detailed in § 3). Identifications with other, primarily optical, catalogs are also useful in providing a final check on the reality of the sources and the accuracy of the derived positions. All the identifications with counterparts presented here come from searching 3′ fields centered on the Slew Survey positions, slightly more conservative than the 95% confidence radius estimated in Figure 7*d*. A total of 313 (38%) of the Slew Survey sources are new as X-ray sources, and 637 (78%) have been identified with optical catalog sources, including 133 (16%) of the new X-ray sources. Few of these are likely to be chance coincidences since a 3′ radius search circle gives $\sim 5 \times 10^6$ independent bins on the sky. Thus, assuming that all the objects are randomly distributed, for the ~1000 Slew Survey sources, only about one in 5000 objects will accidentally associated with a catalog object. Most catalogs contain fewer sources than this, so one chance coincidence or less per catalog is expected. The SAO catalog (with ~100,000 entries) is an exception. A detailed examination of the identifications and their reliability will be presented in a forthcoming paper (Schachter et al. 1991).

In the case of extended objects, especially supernova remnants and clusters of galaxies, this technique may fail to identify some objects. A solution to this problem is to increase the search radius systematically while also checking for any duplicate counterpart identifications. A preliminary analysis suggests that increasing the radius to ~5′–15′ gives ~20%–30% more supernova remnant and cluster candidates.

We are presently extending the identification program to handle the extended sources in more detail and also to include the *IRAS* survey (including both the Point Source Catalog and the Faint Source Catalog), the HST Guide Star Selection System catalog, and the radio 87GB and UT 327 MHz surveys. Optical magnitudes for candidate identifications in all fields are being obtained from digitizations of the Palomar and UK Schmidt surveys. An on-line data base of identifications will be maintained at CfA, accessible remotely through the *einline* system. To allow for detailed follow-up, we will make available an on-line ascii version of the source identification list, which will be updated periodically. We welcome contributions to this identification list, which will be referenced in the data base.

TABLE 7

NEW IDENTIFIED X-RAY SOURCES

Name (1)	Type/z (2)	Counterpart Name (3)	Other Counterpart Names (4)
		AGNs	
1ES 0702+646	0.079	VII Zw 118*	...
1ES 0836+710	2.160	4C 71.07	S5 0836+710
1ES 0921+525	0.036	Mrk 110	PG
1ES 1149−110	0.049	PG	...
1ES 1309+355	0.184	TON 1565	PG
1ES 1320+084	0.050	Mrk 1347	...
1ES 1415+451	0.114	PG	...
1ES 1518+593	0.079	SBS 1518+593	...
1ES 1626+554	0.132	PG	...
		Galaxies[a]	
1ES 0257+442	...	U02468	...
1ES 0403−373	0.055	ESO 359−19	...
1ES 0412−382	0.050	ESO(B)303R	...
1ES 0543−555	0.015	NGC 2087	ESO 159−26
1ES 0559−399	...	GAL 0559−3959	...
1ES 1121−012	...	Z1121.0−0117	...
1ES 1141+799	...	UO6728	...
1ES 1215+039	0.075	4C+04.41*	PKS 1214+038
1ES 1234+459	...	Z1234.5+4556	...
1ES 1238−332	...	ESO 381−7	...
1ES 1254−172	0.046	GAL 1254−1710*	...
1ES 1318+274	...	G149−80	...
1ES 1323+717	0.072	GAL 1323+7145	...
1ES 1324−269	0.046	ESO 509−9	...
1ES 1324−268	...	ESO 509−14	...
1ES 1336+280	0.036	Z1336.4+2800	...
1ES 1714+574	0.028	NGC 6338*	U10784
		Clusters of Galaxies	
1ES 0122+084A	0.045	A193*	...
1ES 0122+084B	0.045	A193*	...
1ES 0644−541	...	A3404	...
1ES 0914+519	0.197	A773	...
1ES 1241+275	0.241	A1602	...
1ES 1256−039	0.083	A1651	...
1ES 1301−239	...	A1664*	...
1ES 1310−327	...	S724	...
1ES 2247+106	0.077	A2495*	...
1ES 2349−561	...	S1158	...
		White Dwarfs	
1ES 1631+781	DA	RE 1629+781	...
		Stars: Known to Be Active	
1ES 0957+247	K0VE+B	DH Leo	SAO 081134
1ES 2058+398	M3EV+M3EV	WLY 815AB	...
		Stars: Binaries	
1ES 0154−518	G5 IV+	WLY 81AB	SAO 23273, χ Eri, HD 11937
1ES 0309−291	F8 IV+	WLY 127AB	SAO 168373, α For, HD 20010
1ES 1314+172	K2 V+M2 V	WLY 505AB	SAO 100491
1ES 1833+169	G2 V+G2 V	HD 171746	SAO 103886
		Stars: Early-Type	
1ES 0157+706	A3 IV	SAO 4554	48 Cas, HD 12111
1ES 0324+095	B9 Vn	HD 21364	214 Tau, SAO 168373
1ES 0426−131	B1 Vne	DU Eri	HD 28497, SAO 149674
1ES 0510−119	B8 V	SAO 150223	309 Lep, HD 33802
1ES 0839−445	A0	HD 74209	...
1ES 1126−610	A	HD 306536	...

TABLE 7—*Continued*

Name (1)	Type/z (2)	Counterpart Name (3)	Other Counterpart Names (4)
1ES 1148−624	B8	HD 309207	...
1ES 1318−632	B	LS 3039	...
1ES 1348−588	B9 IV	SAO 241229	...
1ES 1414−197	A5 IV	SAO 158468	...
1ES 1650−417	B	SAO 227370	...
1ES 1920+223	A2	HD 344230	...
		Stars: Late-Type[b]	
1ES 0013+195	M4	G32−6*	...
1ES 0120+004	G0	HD 8358*	...
1ES 0143−253	F1 V	ϵ Scl	HD 10830, SAO 167275
1ES 0226−615	F8	SAO 248569	...
1ES 0238+057	M	BD +05 378	...
1ES 0305−284	K7 V	CD −28 1030*	...
1ES 0357−400	K0	HD 25300	...
1ES 0415+231	K0	HD 284303	...
1ES 0419+148	F8	HD 285758	...
1ES 0423+146	G7 III	SAO 093935	7316 Tau, HD 28100
1ES 0444−704	K7	HD 270712	...
1ES 0447+068	F6 V	SAO 112106	WLY 178, 116[3] Ori, HD 30652
1ES 0504−575	F8 V	WLY 189	Zeta Dor, HD 33262, SAO 233822
1ES 0603−484.....	G5	SAO 217708	HD 41824
1ES 0614+227	K2	HD 254475	...
1ES 0618−580	K2V	SAO 234448	...
1ES 0635−698	G3V	HD 47875	...
1ES 0637−614	G1-2 V	HD 48189	SAO 249604
1ES 0712−363	F6–7 V	SAO 197732	...
1ES 0717−572	G0 IV–V	SAO 235087	...
1ES 0738+612	K0	SAO 014296	...
1ES 0740+228	K0	SAO 079647	...
1ES 0919+404	K2 V	SAO 042826	...
1ES 0920−136	K0 IV	SAO 155136	...
1ES 0923−530	F7 V	SAO 236956	...
1ES 1002−559	K1-2 III	SAO 237656	...
1ES 1020+493	F5	HD 89944	...
1ES 1101−606	M0	SAO 251235	...
1ES 1105+833	K0	SAO 001824	...
1ES 1212−652	G0/G1 V	HD 106392	...
1ES 1212+078	K0	SAO 119284	...
1ES 1228−465	F5 V	SAO 223481	...
1ES 1239−011	F0 V	WLY 482A	SAO 138917, HD 110379, HD 110380
1ES 1252−060	K8 V	WLY 9424	...
1ES 1301−411	K0	CD −40 7655	...
1ES 1325−261	K5 III	HD 117033	...
1ES 1325−312	F5 V	SAO 204500	...
1ES 1326+789	G2.5 IIIb	HD 117566	SAO 007821
1ES 1327−313	K1 III	SAO 204527	...
1ES 1339−688	G2 IV–V	SAO 252423	...
1ES 1354−314	K0 V	SAO 205032	...
1ES 1414+203	F8 V	HD 125040	SAO 083259
1ES 1437−252	F0/F2 V	HD 129009	...
1ES 1456−400	F7/F8 V	HD 132349	...
1ES 1509+763	G5	SAO 008175	...
1ES 1606+218	K2	AG +21 1576	...
1ES 1614+446	G0	SAO 045997	...
1ES 1702+457	F8	SAO 046462*	...
1ES 1711−547	F0I V–V	SAO 244557	...
1ES 1716+551	K0	SAO 030326	...
1ES 1727+590	G0	SAO 030416	...
1ES 1737+612	M	HD 160934	...
1ES 1746+748	K0	SAO 008910	...
1ES 1824+151	K0	SAO 103722	...
1ES 1902−524	F7 V	ρ Tel	HD 177171
1ES 1914+092	K2 II	SAO 124465*	...
1ES 2001+068	K2	HD 190342	...
1ES 2013+448	K0	SAO 049357	...
1ES 2042+335	G5	SAO 070451	...
1ES 2048+314	K0	SAO 070569	...
1ES 2052+441	G2 V	SAO 050198	...

TABLE 7—*Continued*

Name (1)	Type/z (2)	Counterpart Name (3)	Other Counterpart Names (4)
1ES 2128+231	K8	BD +22 4409	...
1ES 2135+011	K0	AG+01 2623	...
1ES 2153+441	K0	SAO 051437	...
1ES 2216+845	K2	SAO 003717	...
1ES 2257−340	G5 VP	SAO 214237	...
1ES 2326+411	M2	G190−28	...
1ES 2334+063	G0	SAO 128282	...
		Stars: Type Unknown	
1ES 0437−046	...	BF Eri	...
1ES 0437+444	...	OU Per	...
1ES 0829+159	...	SAO 097895	...
1ES 1735−269	...	IRAS 17345−2656	...
1ES 1841−044	...	FT Sct	...
1ES 2129−026	...	PHL 26	...
1ES 2155−081	...	BD −08 5773	...

[a] These galaxies, although cataloged as normal, may possess active nuclei.
[b] Many of the late-type stars may be previously unknown active stars.

7.1. *New Identified X-Ray Sources*

Table 7 contains a list of the 133 new X-ray sources with optical identifications by object class. By a new X-ray source, we mean a Slew Survey source undetected in the *EXOSAT*, pointed IPC (Harris et al. 1991), or *HEAO* A-3 (Remillard et al. 1991) catalogs within 3′ of the Slew position. Some sources may not be in these catalogs, yet be detected in other X-ray missions (e.g., *HEAO* A-2, *Uhuru*, *Ariel V*). Therefore, we inspected other comprehensive X-ray source compilations (e.g., Bradt & McClintock 1983; Kowalski et al. 1984). Three (~3%) of the candidate new identified X-ray sources were eliminated in this manner: the X-ray binaries 4U 1755−338 and Aql X-1 (4U 1908+005), and the cluster A2315 (a *HEAO* A-2 source).

The entries in Table 7 are grouped by object type—AGN, galaxies, clusters, white dwarfs, and stars—while the stars are further subdivided as in Table 5 [active, binaries, early type (OBA), late type (≥F), unknown type]. The first column gives the 1ES (First *Einstein* Slew Survey) name of the object. If the redshift or stellar spectral type is known, it is indicated in column (2). We list in column (3) the common name of each object, including only a catalog designator such as PG for common catalogs, if the coordinate name is the same as in the 1ES name. An asterisk following the object name signifies an ambiguous identification (see § 6.2). Column (4) lists alternate names of the object, if any.

Based on their f_x/f_o ratios in comparison with the values given for Medium Survey sources by Maccacaro et al., we expect that the new "galaxies" are previously unknown active galaxies, primarily Seyfert galaxies.

8. PROPERTIES OF THE SLEW SURVEY

The Slew Survey contains 819 sources, which are concentrated toward the ecliptic poles (Fig. 17). Half of these sources are newly discovered as X-ray sources.

The range of source fluxes complements well that of the Medium Survey (Gioia et al. 1990, Fig. 1): there are similar numbers of sources in each survey; they each cover about a decade of flux with excellent statistics; and the Slew Survey sources are on average 10 times brighter. The uniform selection of the Slew Survey sources by soft X-ray emission will allow the formation of well-defined samples of most classes of X-ray emitter: stars, CVs, AGNs, clusters of galaxies, and BL Lacertae objects.

Some regions of the sky have especially favorable coverage. The Cygnus Loop has ~150 s exposure, which produces an image with over 100,000 photons (Fig. 18). Of more general interest is the north ecliptic pole region (Fig. 19) which has between 30 and 100 s exposure. In the region within 10° of the ecliptic pole, 21 sources can be seen, illustrating the ability of the Slew Survey to detect new "serendipitous" sources.

Two examples of the uses of the Slew Survey samples are given below, one for quasars and the other for BL Lacertae objects.

1. The steep luminosity function of AGN, means that low-luminosity AGNs (i.e., Seyfert galaxies) are likely to make up a major part of the AGN contribution to the diffuse X-ray background. Yet most optical studies cannot treat these AGNs because the host galaxy leads to fuzzy images and dilutes the AGN colors, both of which effects produce uncertain levels of incompleteness in the samples. Thus Schmidt & Green (1983), for example, could not extend their luminosity function fainter than $M_V = -23$. The Slew Survey will give a bright AGN survey, similar to the Palomar Bright Quasar Survey (BQS, 'PG', Schmidt & Green 1983), but with the advantage that it is free from the problem of galaxy starlight contamination. AGNs will be seen down to $M_V \sim -20$ with redshifts as high as $z \sim 0.1$, complementing the Medium Survey which reaches a similar absolute magnitude but has few AGNs at $z < 0.1$. The Slew Survey may also be a good means of finding high-luminosity quasars of moderate redshift since, being rare,

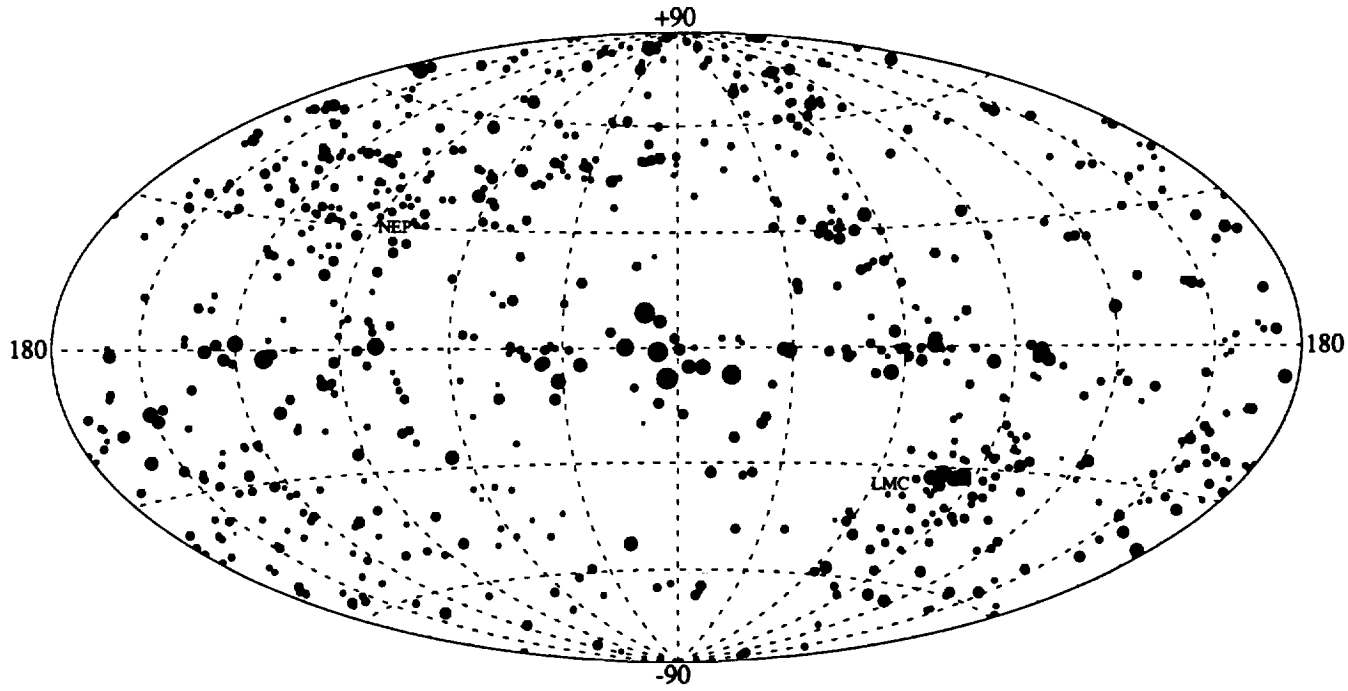

FIG. 17.—Distribution of Slew Survey sources in Galactic coordinates. The concentration of sources at the ecliptic poles ("NEP" and "LMC"), where the Slew Survey exposure time is greatest, is clear.

they require large sky coverage to be detected. Another problem, the dependence of AGN evolution on the unknown spectrum of the sources (Elvis et al. 1986; Tananbaum et al. 1986), can be removed empirically by using the Slew/A-2 flux ratios.

2. There is a peculiar break in the X-ray log N–log S for BL Lacertae objects, which may be related to relativistic beaming in these sources (Giommi et al. 1989) or to cosmological evolution (Wolter et al. 1991; Morris et al. 1991). The flux region of the break is not presently well sampled. This is the range covered by the Slew Survey. Recent X-ray surveys (Stocke et al. 1989) have clearly demonstrated that X-ray selection is currently the best method of discovering BL Lacertae objects. For the flux limit of the IPC Slew Survey, a uniform, X-ray–selected sample of ~80 objects will be detected (and identified through our ongoing program to identify all Slew Survey sources) in the high Galactic latitude sky. This compares with a *total* of 87 BL Lacertae objects, selected by all methods, in the Hewitt & Burbidge (1987) Catalog. There are about 40 known X-ray–selected BL Lacertae objects. All X-ray selected BL Lacertae objects are radio-loud (Stocke et al. 1989) and have well-defined and distinct X-ray/optical/radio flux ratios (Giommi et al. 1990). This tight α_{RO}/α_{OX} distribution implies that the BL Lacertae objects in the Slew Survey will have radio flux densities in the range 50–80 mJy. This, when combined with the correlation between radio and optical fluxes, gives an expected m_V in the range 18–19 for the faintest objects. The three fluxes alone are sufficient to select a large sample of BL Lacertae objects for further study.

Identification of the unidentified Slew Survey sources should be relatively easy since they are all bright. We can estimate their optical magnitudes using the nomogram constructed for Medium Survey sources (Maccacaro et al. 1988). The typical AGN will be at $V \sim 16$ mag and the faintest M dwarfs will be at ~14 mag. This is 2–3 mag brighter than the Medium Survey identifications and our error circles have only ~5 times their area, so the typical number of possible optical candidates, and possible spurious counterparts, will be few.

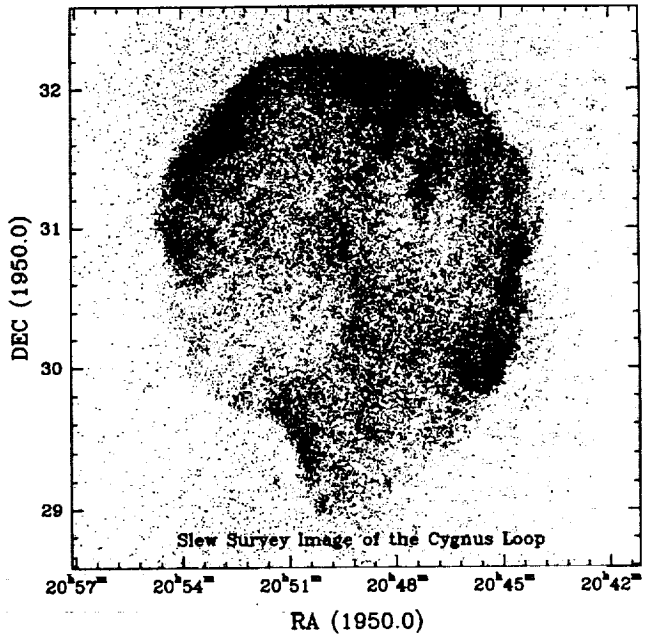

FIG. 18.—Slew Survey image of the Cygnus Loop. The mean exposure time in this image is ~150 s. A total of 108,000 photons are included in the image. The field shown is 4° × 4°.

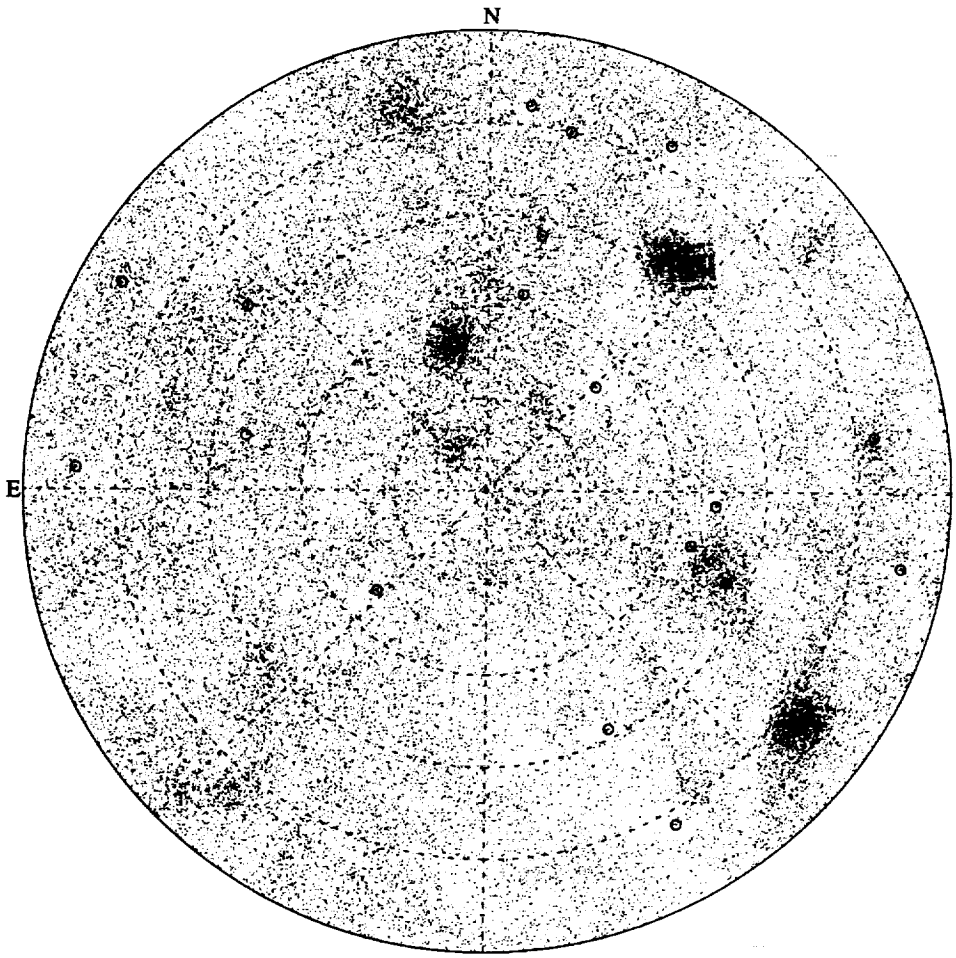

FIG. 19.—The region of the Slew Survey within 10° of the north ecliptic pole. The exposure time ranges from ~100 s (north) to ~30 s (south) which leads to the variations in photon density seen in the image. The image is not exposure corrected. The two darkest areas are short segments of data from the very beginning or end of slews when the spacecraft is virtually stationary. The 21 Slew Survey sources are circled. (One source is almost hidden in the heavily exposed region to the lower right.)

Many of the new sources will also show up in the IRAS Point Source Catalog, Version 2 1988 and the Green Bank (Gregory & Condon 1991) survey. We will use the Minnesota POSS (Humphreys 1991) and Edinburgh UK Schmidt digitizations to derive the bulk of our optical magnitudes. In this way relatively few new optical observations will be needed to make the remaining identifications.

We have not constructed a log N–log S for the Slew Survey in this paper. This obvious step is in practice quite difficult to do properly. The uncertainty on the count rates in the survey are mostly large, so that the "Eddington bias" is large. This is the effect by which sources below the formal flux threshold are detected while sources above the threshold are missed due to flux measurement errors. A simple flux threshold thus cannot be readily defined. Since the log N–log S is steep (Gioia et al. 1990), more sources will enter the survey than will drop out, systematically distorting and steepening the observed log N–log S at low fluxes. A proper treatment requires detailed simulations of the procedures used to produce the survey source list, and we defer this to a later paper.

9. CONCLUSIONS

We have presented a survey of the sky in soft (~0.1–3.5 keV) X-rays containing 819 sources. New, well-defined, samples of bright X-ray sources can be derived from this survey for many object types. The survey has a limiting flux a few times fainter than the largest previous all sky survey in X-rays (*HEAO* A-1, Wood et al. 1984) which took place in the ~2–10 keV band, and a factor ~10 brighter than the typical sensitivity of the *ROSAT* survey which covers the 0.1–2 keV band.

It is fair to ask what the value of the Slew Survey is in the context of the much larger and more sensitive *ROSAT* survey (Trümper 1991). This question has several answers: first, the Slew Survey makes available rapidly a large number of new bright X-ray sources suitable for follow-up study with *ROSAT* (and, in a few years, with *ASTRO-D*); second, virtually all of the existing faint source X-ray work has been carried out with IPC-selected sources as part of the *Einstein* Medium Survey (Maccacaro et al. 1988; Gioia et al. 1990) and the Deep Survey (Giacconi et al. 1979b; Primini et al. 1991), so that a compari-

son sample of bright identified sources selected with the same instrument can be put to use at once for source count and evolution work, without ambiguities due to different detector characteristics; third, a comparison of Slew Survey sources with *ROSAT* survey sources will allow the selection of unusual objects having extreme variability and/or extreme spectra; finally, the energy band of the *Einstein* IPC extends to significantly higher energies than that of the *ROSAT* survey, so that it will continue to be valuable (e.g., for the selection of hard X-ray sources) even when the *ROSAT* survey is published.

The large amplitude variations in exposure on a scale of a few arcminutes in the Slew Survey mean that it is not possible to derive upper limits for arbitrary positions on the sky from the present catalog. We are preparing two methods to allow this—an on-line service will be added to *einline* (the *Einstein* On-line Service; Harris et al. 1990); and the original, aspect-corrected, slew data is available on a CD-ROM as part of the SAO CD-ROM series of *Einstein* Data Products (Fabbiano 1990). This CD-ROM also allows timing, spectral, and structural information to be extracted from the Slew Survey via standard X-ray data reduction packages (e.g. IRAF/PROS, MIDAS).

The Slew Survey presently has only coarsely known completeness as a function of source flux. A program to derive accurate sky coverage and source detection efficiencies as a function of source flux and extent is being initiated. This will allow the derivation of statistical population properties such as luminosity functions from the Slew Survey.

We are pursuing a program of identifications for all Slew Survey sources. This is initially based on existing archival data and catalogs in an attempt to minimize the amount of optical observing needed. A first paper on these identifications is in preparation (Schachter et al. 1991). We shall maintain a data base of these identifications as part of the on-line *einline* system for general use. We welcome any contributions to these identifications. The on-line data base will include a reference for the source of each identification. We ask that any publication using this information reference its source as listed in the on-line system.

We have received many requests for information on sources in the Slew Survey. As a result, we are forming working groups for astronomers interested in pursuing the active galaxies and quasars, and the BL Lacertae objects in the survey. The aim of these groups is to exchange information and prevent unnecessary duplication of effort, not to direct anyone's research. Anyone interested in joining one of these groups or in forming another should send e-mail to the Slew Survey Project (slew@cfa.harvard.edu, cfa::slew). The *Einstein* Slew Survey data are part of the *Einstein* data bank. As such, they are part of the NASA Astrophysics Data Program and are available to all interested parties.

There exists some 50% more slew data in the *Einstein* data bank than was used for the present survey. These were originally rejected because of problems that would have complicated this first analysis, primarily long data dropouts that make the extrapolation of the gyro aspect solution less certain. Our experience now suggests that this problem can be overcome and we hope to include this data in constructing a second "definitive" Slew Survey, which should have roughly double the number of sources.

We thank John McSweeney and the *Einstein* data center team for assistance with data handling; Ron Remillard, Jonathan McDowell, Paolo Giommi, John Stocke, and Nick White for their assistance with the identifications; and John Stocke for a careful reading of the manuscript. This research has made use of the SIMBAD data base, operated at CDS, Strasbourg, France and also the NASA/IPAC Extragalactic Database (NED) which is operated by the Jet Propulsion Laboratory, California Institute of Technology, under contract with NASA. This work was supported by NASA contract NAS8-30751 (*HEAO 2*) and NASA grant NAG5-1201 (ADP).

REFERENCES

Abell, G. 1958, ApJS, 3, 211
Abell, G., Corwin, H., & Olowin, R. 1989, ApJS, 70, 1
Bradt, H. V. D., & McClintock, J. E. 1983, ARA&A, 21, 13
Branduardi-Raymont, G., Fabricant, D., Feigelson, E., Gorenstein, P., Grindlay, J., Soltan, A., & Zamorani, G. 1981, ApJ, 248, 55
Cannon, A. J., & Pickering, E. C. 1918–1924, The Henry Draper Catalogue, Ann. Astron. Obs. Harvard College, 91–99
Cooke, B. A., et al. 1991, Nature, submitted
Elvis, M., Green, R. F., Bechtold, J., Schmidt, M., Neugebauer, G., Soifer, B. T., Matthews, K., & Fabbiano, G. 1986, ApJ, 310, 291
Fabbiano, G. 1990, in Imaging X-Ray Astronomy, ed. M. Elvis (Cambridge: Cambridge Univ. Press), 155
Giacconi, R., et al. 1979a, ApJ, 230, 540
Giacconi, R., et al. 1979b, ApJ, 234, L1
Gioia, I. M., Maccacaro, T., Schild, R. E., Stocke, J. T., Liebert, J. W., Danziger, I. J., Kunth, D., and Lub, J. 1984, ApJ, 283, 495
Gioia, I. M., Maccacaro, T., Schild, R. E., Wolter, A., Stocke, J. T., Morris, S. L., and Henry, J. P. 1990, ApJS, 72, 567
Giommi, P., et al. 1989, in Proc. Workshop on BL Lac objects, ed. L. Maraschi, T. Maccacaro, & M.-H. Ulrich (Berlin: Springer), 231
Giommi, P., Barr, P., Garilli, B., Maccagni, D., & Pollock, A. M. T. 1990, ApJ, 356, 432
Giommi, P., et al., 1991, ApJ, 378, 77
Gorenstein, P., Harnden, R. F., & Fabricant, D. G. 1981, IEEE Trans. Nucl. Sci., NS-28, 869
Gregory, P. C., & Condon, J. J. 1991, ApJS, 75, 1011
Harnden, F. R., Branduardi, G., Elvis, M., Gorenstein, P., Grindlay, J., Pye, J. P., Rosner, R., Topka, R., & Vaiana, G. S. 1979, ApJ, 234, L51
Harnden, R. F., Jr., Fabricant, D. G., Harris, D. E., & Schwarz, J. 1984, Smithsonian Astrophys. Obs. Spec. Rep. 393
Harris, D. E. et al. 1991, *Einstein* IPC Source Catalog, NASA Publication, in press.
Harris, D. E., Stern, C. P., & Biretta, J. A. 1990, in Imaging X-ray Astronomy, ed. M. Elvis (Cambridge: Cambridge Univ. Press), 299
Hewitt, A., & Burbidge, G. 1987, ApJS, 63, 1
Hoffleit, D., & Jaschek, C. 1982, The Bright Star Catalogue (4th rev. ed.; New Haven: Yale Univ. Obs.)
Huchra, J. P. 1991, in preparation.
Huchra, J. P., & Geller, M. J. 1984, ApJ, 257, 423
Humphreys, R. 1991, private communication
IRAS Point Source Catalog, Version 2. 1988, Joint *IRAS* Science Working Group (Washington, DC: GPO)
Kholopov, P. N., et al. 1985–1988, General Catalogue of Variable Stars (4th ed.; Moscow: Nauka)
Koch, D., Hall, R., Tsao, H., Wollman, H., & Kilinski, R. 1978, IEEE Trans. Nucl. Sci., NS-25, 473
Kowalski, M. P., Ulmer, M. P., Cruddace, R. G., & Wood, K. S. 1984, ApJS, 56, 403
Kraft, R., Burrows, D., & Nousek, J. 1991, ApJ, 374, 344
Maccacaro, T., et al. 1988, ApJ, 326, 680

McCook, G., & Sion, E. 1987, ApJS, 65, 603
Morris, S., Stocke, J. T., Gioia, I. M., Schild, R. E., Wolter, A., Maccacaro, T., & Della Cecca, R. 1991, ApJ, 380, 49
Nilsson, P. 1973, Uppsala General Catalogue of Galaxies, Uppsala Astron. Obs. Ann. 6
Piccinotti, G., Mushotzky, R. F., Boldt, E. A., Holt, S. S., Marshall, F. E., Serlemitsos, P. J., & Shafer, R. A. 1982, ApJ, 253, 485
Plummer, D., Schachter, J., Garcia, M., & Elvis, M. 1991, CD-ROM issued by Smithsonian Astrophysical Observatory
Primini, F. A., Murray, S. S., Huchra, J., Schild, R., Burg, R., & Giacconi, R. 1991, ApJ, 374, 440
Remillard, R., et al. 1991, in preparation
SAO Staff. 1966, Star Catalog. Positions and Proper Motions of 258,997 Stars for the Epoch and Equinox of 1950.0 (Pub. 4652) (Washington: Smithsonian Institution)
Schachter, J., et al. 1991, in preparation
Schmidt, M. 1990, in Imaging X-Ray Astronomy, ed. M. Elvis (Cambridge: Cambridge Univ. Press), 201
Schmidt, M., & Green, R. F. 1983, ApJ, 269, 352
Shara, M. 1990, private communication
Stocke, J. T., Morris, S. L., Gioia, I. M., Maccacaro, T., Schild, R. E., and Wolter, A. 1989, in BL Lac Objects, ed. L. Maraschi, T. Maccacaro, & M.-H. Ulrich (Berlin: Springer), 242
Stocke, J. T., Morris, S. L., Gioia, I. M., Maccacaro, T., Schild, R., Wolter, A., Fleming, T. A., & Henry, J. P. 1991, ApJS, 76, 813
Struble, M. V., & Rood, H. J. 1987, ApJS, 63, 543
Sulentic, J. W., & Tifft, W. G. 1973, The Revised New General Catalogue of Nonstellar Astronomical Objects (Tucson: The University of Arizona Press)
Tananbaum, H., Avni, Y., Green, R. F., Schmidt, M., & Zamorani, G. 1986, ApJ, 305, 57
Trümper, J. et al. 1991, Nature, 349, 579
Véron-Cetty, M.-P., & Véron, P. 1987, A Catalogue of Quasars and Active Nuclei (3d ed.; Saint-Michel, France: Observatoire de Haute Provence), 102
Wolter, A., Gioia, I. M., Maccacaro, T., Morris, S. L., & Stocke, J. T. 1991, ApJ, 369, 314
Wood, K. S., et al. 1984, ApJS, 56, 507
Woolley, R., Epps, E. A., Penston, M. J., & Pocock, S. B. 1970, Catalogue of Stars within Twenty-Five parsecs of the Sun, R. Obs. Ann., 5

Appendix C
Other Slew Survey Publications

IDENTIFICATIONS OF *Einstein* SLEW SURVEY SOURCES

JONATHAN F. SCHACHTER, MARTIN ELVIS, DAVID PLUMMER, AND G. FABBIANO
Harvard–Smithsonian Center for Astrophysics
60 Garden St. Cambridge MA 02138 USA

ABSTRACT

We discuss the status of identifications of the *Einstein* Slew Survey, a bright soft X-ray catalog with 550 new X-ray sources. Possible counterparts have been found for > 95% of the Slew Survey based on positional coincidences and color-color diagnostics. The survey will be fully identified via upcoming radio and optical observations.

1. Introduction

The *Einstein* Slew Survey is an all-sky survey covering 50% of sky at an exposure of 6 s. It contains 1067 bright soft X-ray sources ($\gtrsim 5 \times 10^{-12}$ erg cm^{-2} s^{-1}, 0.1 – 3.0 keV) with a positional accuracy of 1.2′ (90% confidence radius), of which 550 were not previously known to emit X-rays. A paper which includes the details of source detection, derivation of positions and fluxes, and an extensive catalog of all 1067 sources has been submitted for publication (Elvis et al. 1991). All the photon data, useful lists, and software tools are available either on CD–ROM (from the *Einstein* Data Products Office at CfA; email: edpo@cfa.harvard.edu) or via *einline*.

2. Identified Sources

2.1 *Counterparts of Known Optical Type*

We have found possible counterparts for 96% (1021 sources) of the Slew Survey based on positional coincidences found in an extensive search of existing catalogs and databases. For 650 sources, the counterpart is a known optical type, including all known types of X-ray sources—AGN, BL Lacs, clusters, CVs, X-ray binaries, supernova remnants, pulsars, stellar coronal sources, and white dwarfs (Table 1).

2.2 *Counterparts of Unknown Optical Type*

Of the fraction lacking counterparts of known optical type, 363 have possible counterparts in the Hubble Guide Star Catalog (GSC). This reflects the GSC completeness ($B \sim 14.5$), and is consistent with the expected distribution of V magnitudes of unidentified sources, based on known X-ray–to–optical flux ratios (Stocke et al. 1991). There are 79 sources with only one GSC candidate in the Slew Survey error circle. We have tentatively identified new late-type stars ($V \sim 11 - 14$) and new AGN ($V \sim 14 - 16$) in this group. There are typically 3.7 GSC sources per Slew Survey

source, with a range of 1 – 3 magnitudes. An unambiguous identification requires information from catalogs at other wave bands.

Of 15 new counterparts in the *IRAS* Point Source Catalog, the low-Galactic latitude subset contains 2 probable new T Tauri stars (in Cassiopeia) and one molecular cloud core (near W44). Positions of molecular clouds are from Dame et al. 1987, and *IRAS* color-color diagnostics from Emerson 1986. In the high-latitude sources, we find 4 AGN candidates, and two starburst galaxies. Extragalactic *IRAS* color diagnostics are taken from Soifer, Houck, & Neugebauer 1987. We also find 6 new counterparts in the *IRAS* Faint Source Catalog.

There are 22 new 5 GHz CBS (Condon, Broderick, & Seielestad 1989) identifications lacking optical counterparts, with $f_{5GHz} = 27 - 4660$ mJy. Two of these sources are flat spectrum sources, and may be new BL Lac objects. The remaining sources are probably AGN, BL Lacs, and clusters, as these dominate the optically identified Slew Survey sources with CBS counterparts.

We find 45 sources lacking counterparts in any of the catalogs searched. These have the most extreme X-ray–to–optical fluxes of any Slew Survey sources, and are probably mainly BL Lacs and clusters. Radio spectral indices from the upcoming Becker et al. (1991) 1400 MHz and southern radio surveys will aid in identification. We are planning to obtain VLA and optical spectroscopy on these sources (starting in June, 1991) to progress the survey to 100% identification.

This work was supported by NASA grant NAG5-1201 (ADP).

References

Becker et al. 1991, ApJ, submitted.

Condon, J. J., Broderick, J. J., &, Seilestad, G. A. 1989, AJ, 97, 1064.

Dame T. M., Ungerechts, H., Cohen, R. S., de Geus, E. J Grenier, I. A., May, J., Murphy, D. C., Nyman, L.-A., & Thaddeus, P., 1987, ApJ, 322, 706.

Elvis, M., Plummer, D., Schachter, J., & Fabbiano, G. 1991, ApJS, submitted

Emerson, J. P. 1987, IAU Symp. 115, "Star Forming Regions," ed. M. Peimbert &J. Jugaku (Dordrecht: Reidel), p. 16.

Soifer, B. T., Houck, J. R., & Neugebauer, G. 1987, ARA&A, 25, 187.

Stocke, J. T., Morris, S. L., Fleming, T. A., & Henry, J. P. 1991, ApJS, in press.

Table 1: Identified Sources of Known Optical Type

Class	Num. New X-ray Src.	Total Num. IDs.
AGN	9	128
BL Lacs	0	32
Clusters	9	80
CVs	0	22
Stars	81	231
X-ray binaries and Pulsars	0	41
Other:	6	93
Norm. Galaxies	5	16
SN Remnant	0	27
White Dwarf	1	6
2E Sources	0	41
EXOSAT Sources	0	2

THE *Einstein* SLEW SURVEY CATALOG

JONATHAN F. SCHACHTER, MARTIN ELVIS, DAVID PLUMMER,
G. FABBIANO, and JOHN HUCHRA
Harvard-Smithsonian Center for Astrophysics
60 Garden St. Cambridge MA 02138 USA

Abstract

The Slew Survey catalog contains 1075 bright X-ray sources, including 557 objects with no previous X-ray detection. Two-thirds of the survey has been identified with counterparts of known optical type. Source samples to date provide insight on low-luminosity AGN and clusters. The remainder, which contains many uncatalogued BL Lacs and clusters, will be identified by using digitized photographic plates.

1 INTRODUCTION

All-sky surveys can help to address key problems in X-ray astronomy. Among these problems are (1) low-luminosity active galactic nuclei (LLAGN) and the soft X-ray background, and (2) the cluster X-ray luminosity function. We briefly summarize each of these problems below.

1.1 LLAGN and the Soft X-ray Background

The steep luminosity function of AGN (meaning emission-line objects only) means that low luminosity AGN (e.g. Seyfert nuclei) are likely to provide a major part of the AGN contribution to the diffuse X-ray background (Schmidt and Green 1986). Yet optical color-selected samples (e.g. the Palomar Bright Quasar Survey; Schmidt and Green 1983) are incomplete at low luminosities ($M_V \geq -23$) because of dilution by host galaxy starlight. New X-ray–selected samples can be far more complete down to significantly lower luminosities ($M_V \sim -18$).

1.2 The Cluster Luminosity Function

Edge *et al.* (1990) constructed a flux-limited sample [$f_x(2-10$ keV $) > 1.7 \times 10^{11}$ ergs cm^{-2} s^{-1}] of 55 clusters selected from the *HEAO-1* and *Ariel V* surveys. They found a statistically significant deficit of high-luminosity ($L_x \geq 5 \times 10^{44}$ ergs cm^{-2} s^{-1}) clusters at $z > 0.1$. If this effect is real, and not the result of a selection bias or their choice of a flux limit, then evolution must have occurred in $z > 0.1$ clusters. (But the Slew Survey clusters appear to be both high redshift and *over*luminous; see below).

1.3 The *ROSAT* All-sky Survey

Ultimately, the *ROSAT* all-sky survey will provide a wealth of information to bear on these important problems. But the *ROSAT* survey, which will contain up to 100,000 sources, cannot plausibly be ready before the end of 1991. Even then, the identification effort required for the *ROSAT* medium and deep surveys is immense. To identify ~ 800 sources with $18 < V < 22$ will take, optimistically, 50 clear dark-time nights on 4-meter class telescopes, i.e. almost 100% of a 4-meter's dark time for one year. The current MPE plan (Trümper 1991) is to identify ~2000 'medium survey' sources in a selected ~600 square degrees of the sky during the first three years (i.e. up to the end of 1993-94). This is only a factor ~2 more than the existing Extended *Einstein* Medium Survey (Gioia *et al.* 1990).

For a decade now X-ray *logN-logS* studies have been dominated by results from the *Einstein* IPC. The *Einstein* Deep and Medium surveys have effective *upper* limits to their flux range due to their limited sky coverage. As a result we have only limited knowledge of the bright X-ray sky at low (IPC) energies. The energy range of *ROSAT* is significantly lower than that of *Einstein* so that obscuration, both Galactic and intrinsic, is even more significant; thus, the population of sources *ROSAT* will detect will be biased toward softer spectra. These difficulties will enlarge the ambiguities in explaining the diffuse x-ray background since its spectrum is only well determined at energies significantly above the *ROSAT* energy range.

2 THE EINSTEIN SLEW SURVEY

We have constructed an all-sky soft X-ray survey from ~3000 individual slewing (i.e. traveling between pointings) observations of the IPC (Elvis *et al.* 1991). The Slew Survey covers 50% of sky at 6 s exposure,

and has a total effective exposure of $\sim 1/2 \times 10^6$ s (e.g., Fig. 1 of Plummer *et al.* 1991). Compared to the Medium Survey, the Slew Survey has a flux limit $\sim$ 10 times higher (3×10^{-12} erg s^{-1}cm^{-2}, 0.2–4.0 keV) and has 30 times the area.

All the photon data of the Slew Survey, useful lists, and software tools are available either on CD-ROM (from the *Einstein* Data Products Office at CfA; email: edpo@cfa.harvard.edu) or via *einline*. A paper with updated counterpart identifications, and containing multiwavelength data for the Slew Survey (radio, IR, optical, soft and hard X-ray) is in preparation (Schachter *et al.* 1991).

Sources were detected by a percolation algorithm, which is more efficient than a sliding box method for a spatially sparse data set. We accepted sources as real if the Poisson probability of the observed counts relative to the local background is greater than 3.95×10^{-4} and the total number of counts in the source is ≥ 3. This yields a catalog of 1075 objects, the largest bright X-ray catalog to date, including 557 new X-ray sources.

A positional accuracy of 1.2′ (90% confidence; 3′ at 95% confidence) was achieved. The principal limitation on source localization is the slew aspect solution (details in Elvis *et al.* 1991).

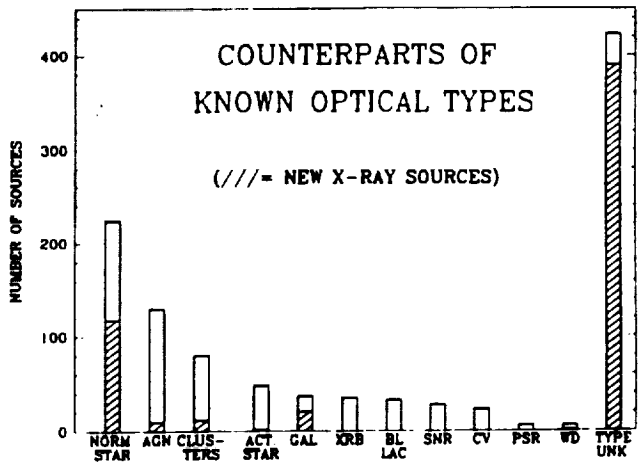

Figure 1: Bar chart showing breakdown of Slew Survey sources possessing counterparts of known optical types. For each type, the hatched region represents the proportion of new X-ray sources. Abbreviations used are *NORM.* and *ACT.* for normal and active.

3 COUNTERPARTS OF SLEW SURVEY SOURCES

3.1 Sources with Known Optical Types

We have performed an exhaustive search of standard catalogs of stars, galaxies, AGN and BL Lacs, clusters of galaxies, cataclysmic variables and X-ray binaries (see §6 of Elvis *et al.* 1991). In addition, we have searched the Simbad and NED databases. This program yields counterparts of known optical type (e.g., AGN, CV) for 2/3 of the survey. A bar graph (Figure 1) shows the relative numbers of sources with known optical types; also indicated are the fractions of each type that are new X-ray detections. Clearly, we have objects of every known type of X-ray source. Examples of new samples of sources are discussed below.

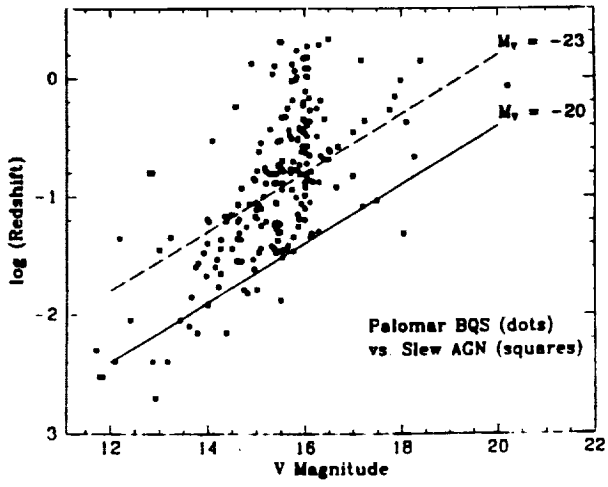

Figure 2: Redshift–V magnitude distribution for the Palomar Bright Quasar Survey (BQS; solid dots), and for identfied Slew Survey AGN to date (squares). The broader distribution in V magnitude for the Slew Survey AGN is a consequence of the X-ray selection. The Slew Survey AGN are seen to be intrinsically 3 magnitudes fainter in M_V.

Table 1: New Identified X-ray Clusters

Name	Slew Name	R	D	z	IPC Ct. Rate	log L_X
A193	1ES0122+084B	1	4	0.048	$0.21^{+0.07}_{-0.06}$	$45.81^{+0.13}_{-0.14}$
A773	1ES0914+519	0	6	~0.20	$0.22^{+0.10}_{-0.08}$	~47.06
A1602	1ES1241+275	0	6	~0.24	$0.32^{+0.15}_{-0.12}$	~45.39
A1651	1ES1256−039	1	4	0.083	$0.51^{+0.20}_{-0.17}$	$44.67^{+0.14}_{-0.17}$
A1664	1ES1301−239	2	6	...	$0.20^{+0.07}_{-0.06}$	...
A2495	1ES2247+106	0	5	...	$0.76^{+0.33}_{-0.26}$	...
A3404	1ES0644−541	1	5	...	$0.27^{+0.09}_{-0.08}$	...
A3866	1ES2217−354	0	5	...	$0.40^{+0.21}_{-0.16}$	...
S724	1ES1310−327	0	4	...	$1.78^{+0.42}_{-0.36}$	...
S1158	1ES2349−561	0	5	...	$0.88^{+0.43}_{-0.33}$	...
ZW 314	1ES0058+345	...	...	...	$1.14^{+0.71}_{-0.51}$	...

3.1.1 Identified Slew Survey AGN to date

There are 130 Slew Survey sources with counterparts in catalogs of AGN, of which 10 are new X-ray sources. One of the new X-ray sources is S5 0836+710, which has $z = 2.2$. To the list of identified AGN, we will probably add many of the new X-ray galaxies (21 to date) found in galaxy catalogs, but not currently known to possess active nuclei.

The identified Slew Survey AGN to date are compared with the Palomar Bright Quasar Survey sample in Figure 2. Clearly, the Slew Survey sample can detect sources at least 3 magnitudes fainter in M_V, showing the efficiency of detecting LLAGN. Plotting the Slew Survey and the Medium Survey AGN on a similar graph (not shown) shows that the two samples can be readily combined to sample a large range of luminosity-redshift space.

3.1.2 Identified Clusters

We find 80 cluster counterparts, of which 11 are new X-ray detections. The new X-ray clusters are listed in Table 1, with richness class (R), distance class (D), and redshift for each. IPC count rates have been converted to X-ray luminosities for the sources with known or estimated (Huchra *et al.* 1991) redshifts, using $H_0 = 50$ km s^{-1} Mpc^{-1}. Note that the clusters are all high z (or large D), i.e. $z \gtrsim 0.1$, and also high L_X. This would tend to go against the Edge *et al.* (1990) result (§1).

3.1.3 Identified Active Stars

Some 48 stars in the Slew Survey were previously known to be active (e.g., FK Com, RS CVn, AD Leo). Of the stars *not* known to be active, but identified in normal stellar catalogs, there are 151 late-type (> F) counterparts, including 91 new X-ray sources. The spectral types of these new X-ray sources often suggest coronal activity (e.g., FIII). Many cases (> 30) have been confirmed in ongoing observations by R. Remillard of MIT at the MDM 1.3 m, and S. Saar of CfA with the echelle spectrograph at the McMath 1.6 m.

3.2 Counterparts without Known Optical Types

3.2.1 Predicted Optical Properties

There are 502 Slew Survey sources without known optical magnitudes, of which 79 have known optical types (mainly supernova remnants and low Galactic-latitude X-ray binaries), and the remaining 423 lack counterparts of known type. For this last group, we can estimate the distribution of V-magnitudes. This distribution is a useful diagnostic of the amount of optical observing required for complete identification. We use values of the X-ray–to–optical flux ratio (f_X/f_o) from Stocke *et al.* (1991), and the relation 1.0 IPC cts s^{-1} = 3.26×10^{-11} erg cm^{-2} s^{-1} (0.2–4.0 keV), appropriate to a power-law energy index of 0.5 and $N_H = 2.0 \times 10^{20}$ cm^{-2} (Gioia *et al.* 1984).

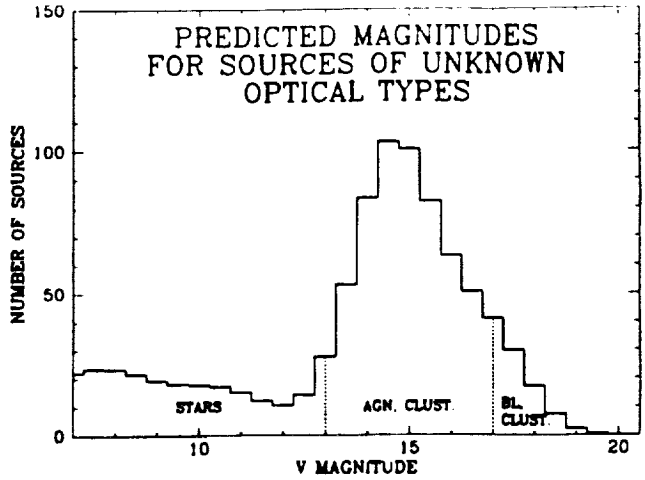

Figure 3: Histogram of predicted V magnitudes for the 423 sources in the Slew Survey currently lacking optical types. The distribution has been divided into three regions, containing bright, relatively bright, and faint objects. The main and secondary contributors to each of these three regions are listed.

The estimated V-magnitude histogram is given in Figure 3, where the typical uncertainty in determination of V is 1 mag. The bright end of the distribution ($V \leq 13$) is dominated by stars, where the lower limit depends on the completeness of stellar catalogs already searched. AGN account for the prominent $\sim$2 mag wide feature centered at $V = 15$, while clusters and BL Lacs dominate the faint end (to $V = 19-20$). There are some 24 objects expected to be fainter than $V = 18$.

We see that all the sources are expected to have readily detectable counterparts in either the Palomar Optical Sky Survey or the UK Schmidt plates. A sizable fraction (66%) are far enough from the Galactic plane ($|b| \geq 20°$) so that confusion is not a severe problem. The large number of unidentified sources and the large error radius suggest that we need other discriminants for a true counterpart determination.

3.2.2 Radio and IR Counterparts

We have searched the Becker, White & Edwards (1991) catalog compilation of the the Green Bank 5 GHz survey of the northern sky [$0° \leq |b| \leq 75°$; Condon, Broderick, & Seilestad 1989 (CBS)] to find counterparts to Slew Survey sources. Radio spectral indices (5 GHz - 0.365 Mhz) have also been tabulated by Becker *et al.* Figure 4 is an example of a diagnostic diagram to identify CBS counterparts. We show all the Slew Survey CBS counterparts known to be clusters, AGN, or BL Lacs; we also show the three CBS sources lacking optical counterparts (A, B, and C). On the basis of Figure 4, sources B and C are probably BL Lacs.

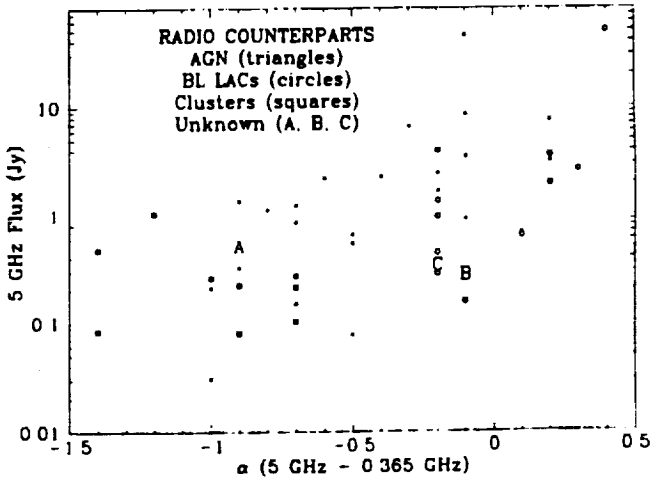

Figure 4: Technique for determining optical types for Slew Survey sources with radio counterparts. Known AGN, BL Lacs, and clusters of galaxies in the Slew Survey are indicated with triangles, circles, and squares. The letters A, B, and C indicate counterparts of unknown optical type.

We will obtain 1400 Mhz fluxes for all the northern objects using the sky maps of Condon and Broderick (1985, 1986). Existing southern sky surveys (PKSCAT90; Condon *et al.* 1991) are not nearly as deep as the CBS survey. Therefore, we plan to use the PMN survey, which is the southern complement of the CBS survey (at 5 GHz and 843 MHz; described elsewhere in these proceedings).

IRAS Point Source Catalog colors suggest two new candidate T Tauri stars, one new molecular cloud core, BL Lacs, AGN, and starburst galaxies (color-color diagnostics from Emerson 1986 and Soifer, Houck, & Neugebauer 1987).

3.2.3 Hubble Guide Star Catalog Counterparts

For the 502 Slew Survey sources lacking optical magnitudes, we find 364 possible identification in the Hubble Guide Star Catalog (GSC). This is consistent with the predicted magnitude distribution of the Slew Survey (Figure 3) and the GSC flux limit of $V \sim 16$. There are an average of 3.7 possible counterparts per Slew

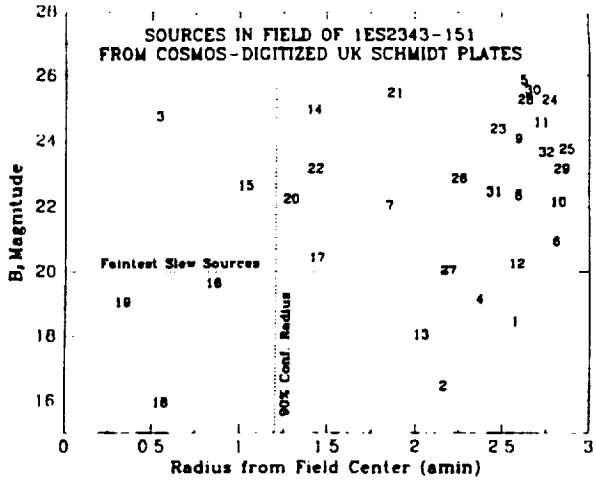

Figure 5: Magnitude distribution of sources in the field of the Slew Survey source 1ES2343−151 as a function of central radius. All sources detected in the digitized UK Schmidt plate are listed by number. The most likely Slew Survey counterparts lie in the box at the lower left.

Survey source, although one of these is probably just a chance superposition. The GSC has typically 100 sources per square degree (Lasker, these proceedings).

4 DIGITIZED RESOURCES

4.1 Overview

Using the results of the previous section, we find 45 sources (or only 4% of the survey) lacking any sort of counterpart. That is, these Slew Survey sources are (1) absent from standard catalogs, (2) absent from IRAS and radio surveys, and (3) absent from the GSC. These sources are expected to have the most extreme values of f_x/f_o and hence are mainly uncatalogued BL Lacs and clusters.

This again shows the advantage of X-ray selection. For example, the BL Lacs will be part of the ~100 total BL Lac objects in the Slew Survey. This can be compared with only 87 in the *entire* Hewitt & Burbidge (1986) catalog. The BL Lac sample of the Slew Survey will be uniform and X-ray selected, which is the most efficient way to detect these sources (Stocke *et al.* 1989).

4.2 Digitized Searches

We have used the COSMOS-digitized UK Schmidt plates, via the database at the Naval Research Laboratory (NRL). This work is in collaboration with H. Gursky and colleagues (principally B. Stuart, J. Wallin, and D. Yentis). Our initial interest was to obtain spectra of all objects in fields of sources favorable to the MMT ($\delta > -27°$). There are typically 25-50 objects within the conservative 3′ (95% confidence) radius down to the plate limit ($B_J \sim 23$). The brightest objects in our fields have $B_J \sim 16-17$, e.g. 1ES2343−151 (Fig. 5). We find typically 3 to 6 sources with $B_J \leq 19$. The faintest Slew Survey sources should lie near the upper limit.

In a recent run at the MMT Blue Channel (covering 3200-7000 Å) we observed three Slew Survey fields (1ES1355−086, 1ES2248−163, and 1ES2343−151). We suspect that object number 19 in the field of 1ES2343−151 is the optical counterpart, a faint galaxy with λ4686 absorption (Figure 6). This may be a member of a faint cluster.

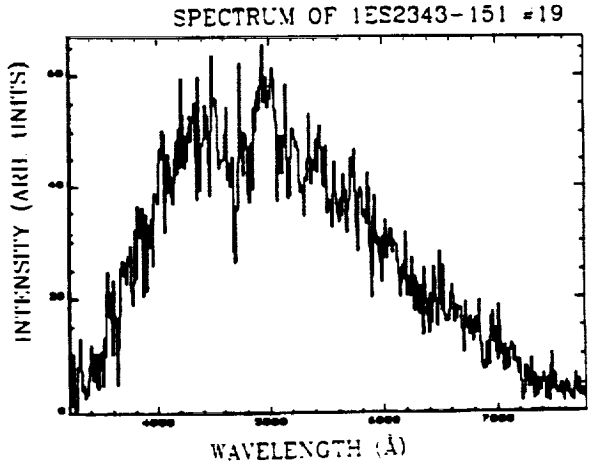

Figure 6: MMT Blue Channel spectrum of object no. 19 in the field of the Slew Survey source 1ES2343−151. He II λ4686 absorption is seen, suggesting that the counterpart is a member of a faint cluster.

In the near future, we will query the NRL database for all the southern sources. Our collaborators at the University of Minnesota are providing digitized magnitudes for the 4% of the Slew Survey with no counterparts from the the Palomar plates (Pennington, these proceedings). The usefulness of having two-color information for X-ray source identification is apparent.

We are committed to complete identification of the Slew Survey. We have ongoing observing programs to verify the new X-ray identifications, via optical spectroscopy at the Mt. Hopkins 60", the MMT, and southern telescopes, in addition to existing collaborations on the Kitt Peak telescopes described in an earlier section. Radio positions will be obtained with the aid of the VLA, which significantly reduces the number of possible counterparts in a given field. This can be used to pick out BL Lacs.

All of the Slew Survey sources are expected to be strongly detected (> 100 counts) in the *ROSAT* all-sky survey. In a collaboration with Dr. J. Trümper of MPE, we will search the *ROSAT* survey at the Slew Survey positions. Slew Survey sources constitute a *ROSAT* survey subsample of manageable size with some of its most interesting objects.

This research has made use of the Simbad database, operated at CDS, Strasbourg, France; and also the NASA/IPAC Extragalactic Database (NED) which is operated by the Jet Propulsion Laboratory, California Institute of Technology, under contract with NASA. Our work was supported by NASA grant NAG5-1201 (ADP).

5 REFERENCES

Becker, R. H., White, R. L., & Edwards, A. L., 1991, *Astrophys. J. Suppl.*, **75**, 1.
Condon *et al.* 1991, in preparation.
Condon, J. J., Broderick, J. J., & Seielstad, G. A., 1991, *Astr. J.*, **97**, 1064.
Condon, J. J., & Broderick, J. J., 1986, *Astr. J.*, **91**, 1051.
Condon, J. J., & Broderick, J. J., 1985, *Astr. J.*, **90**, 2540.
Edge, A. C., Stewart, G. C., Fabian, A. C., & Arnaud, K. A., 1990, *Mon. Not. R. astr. Soc.*, **245**, 559.
Elvis, M., Plummer, D., Schachter, J., & Fabbiano, G., *Astrophys. J. Suppl.*, 1991, accepted.
Emerson, J. P. 1987. In: *IAU Symp. 115, Star Forming Regions*, p. 16, eds M. Peimbert & J. Jugaku, Reidel, Dordrecht.
Gioia I.M., Maccacaro T., Schild R.E., Stocke J.T., Liebert J.W., Danziger I.J., Kunth D., and Lub J., 1984, *Astrophys. J.*, **283**, 495.
Gioia I.M., Maccacaro T., Schild R.E., Wolter A., Stocke J.T., Morris S.L., and Henry J.P., 1990, *Astrophys. J. Suppl.*, **72**, 567.
Hewitt A., & Burbidge G., 1986, *Astrophys. J. Suppl.*, **65**, 603.
Huchra et al. 1991, in preparation.
Plummer D., Schachter J., Garcia M., & Elvis M., 1991, CD-ROM issued by Smithsonian Astrophysical Observatory, Cambridge, MA.
Schachter, J., Elvis, M., Plummer, D., & Fabbiano, G., 1991, in preparation.
Schmidt M., & Green R.F., 1986, *Astrophys. J.*, **305**, 68.
Schmidt M., & Green R.F., 1983, *Astrophys. J.*, **269**, 352.
Soifer, B. T., Houck, J. R., & Neugebauer, G., 1987, *Ann. Rev. Astr. Astrophys.*, **25**, 187.
Stocke J.T., Morris S.L., Gioia I.M., Maccacaro T., Schild R.E., & Wolter A., 1989. In: *BL Lac Objects*, p. 242, eds L. Maraschi, T. Maccacaro & M.-H. Ulrich, Springer-Verlag, Berlin.
Stocke, J. T., Morris, S. L., Gioia, I. M., Maccacaro, T., Schild, R., Wolter, A., Fleming, T. A., & Henry, J. P. 1991, *Astrophys. J. Suppl.*, in press.
Trümper, J. 1991, private communication.

6 QUESTION AND ANSWER PORTION

L. Miller (ROE): Can you rule out the Edge *et al.* result? If so, do you have an explanation for what they see?

J. Schachter: Our new identified X-ray clusters are interesting, I think, because they are not what you would expect from the Edge *et al.* work. But we really need to have the all the Slew Survey clusters identified (all ~200 rather than just 80) before we can make a detailed quantitative comparison with other samples.

52-89
147932
p. 3

N93-20795

EINSTEIN SLEW SURVEY: DATA ANALYSIS INNOVATIONS

M. ELVIS, D. PLUMMER, J. SCHACHTER AND G.FABBIANO
Center for Astrophysics, 60 Garden St. Cambridge MA 02138 USA

ABSTRACT Several new methods were needed in order to make the *Einstein* Slew X-ray Sky Survey. These may be useful for other projects.

SCALE OF THE SLEW SURVEY PROJECT

The *Einstein* X-ray observatory was not intended to make a survey of the sky. However in moving between targets the instruments were left on, so that exposure was accumulated on most of the sky. Eventually this led to the *Einstein* Slew Survey containing 818 bright X-ray sources, 40% of which were unknown (Including almost doubling the number of known BL Lac objects).

The idea of a sky survey made from *Einstein* data was alluring. However the project faced a number of problems: the software was on obsolete 16-bit machines; the data had never been looked at, was poorly documented, and was dispersed on ~2500 magnetic tapes; the star tracker data was unusable so there was no known aspect system; the gyro aspect data needed extrapolation over ~ 120° slews; the data set was fairly large, ~ 400 Mbytes; we needed an arcminute, all-sky exposure map ; and the 'sliding box' detect has $\sim 4 \times 10^7$ cells over the sky. No manager could commit large resources to such an uncertain a project. Fortunately technology made the Slew Survey feasible. Below we summarize the innovations which enabled the Slew Survey to be done.

EXPERIMENTAL APPROACH TO LARGE PROJECTS

By greatly lowering the investment in time and manpower needed to process a satellite data set modern computer hardware allows an 'experimental' approach to large data analysis projects. Instead of deriving optimum analysis methods from first principles the data can be processed with 'quick and dirty' algorithms, and reprocessed many times until an successful result is obtained. This resembles *rapid prototyping.* A small team (one full time programmer and one part-time scientist) were able to carry out the whole Slew project in less than two years.

The two keys are: (1)**Large on-line storage** (a 1-Gbyte disk in our case; optical WORMs for larger archives) has removed the manual overhead and time involved in loading tapes. To process the original 2000 magnetic tapes of *Einstein* data even once was a major undertaking. Now the data are all on WORMs, on-line; (2)**Large amounts of CPU** available without being noticed by other users of the system mean that a complete reprocessing becomes a small decision. We had ~100 times the CPU power available to the original *Einstein* project.

The processing time was thus reduced from months to just days. The whole Slew Survey was re-processed at least a dozen times to reach an acceptable solution.

This approach is only possible for a data product, such as a survey. Projects with a software deliverable cannot operate this way. Our software is not intended for public distribution, is almost undocumented, and is certainly unsupported. The quality assurance lies in the scientific paper describing the survey results, which includes many checks on quality.

PARALLEL PROCESSING ON A LAN

A local area network of workstations was used in a quite simple and primitive way to run up to 10 parallel streams of processing. A complete re-analysis of the survey could in this way be accomplished in *3 days instead of 3 to 4 weeks.* This, as noted above, changes the whole approach to the project.

The main problem in implementing this parallel system was the control list since occasionally two machines would attempt access simultaneously. Unix does not handle file locks well, so we resorted to 10 separate lists. Several off the shelf packages now exist for SUNs that manage parallel processing more flexibly. These should enable the whole SAO High Energy LAN of ~60 4-Mflop SPARC 1 machines to be combined. Depending on the application such a 'network supercomputer' may reach of order 200Mflop (roughly 2/3 of a Cray Y/MP).

PERCOLATION SOURCE DETECTION

Standard source detection algorithms in X-ray astronomy have been of the sliding-box type. They are thus 'sky-centered' *i.e.* every part of the survey area is examined and there are 150×10^6 box positions on the sky. To keep compute time reasonable we were forced to a different approach. In the Slew Survey the sky is sparsely populated with photons. Since there are 3×10^6 photons in the Slew Survey a photon centered-approach is some 50 times more efficient than a sky-centered approach.

We developed a method to find photons which were too closely associated with their neighbors for mere chance. This approach turned out to be identical to that used to locate groups of galaxies in the CfA redshift survey (Huchra and Geller 1984), and is a simple version of the class of 'percolation algorithms'.

'MINIMUM ACTION' IDENTIFICATIONS

Archive material

Two thirds of the Survey sources have been identified using archival resources (NED, SIMBAD, z-cat). Of the remaining sources 75% have plausible counterparts in one or more of the existing digitally accessible sky surveys: the IRAS Point Source and Faint Source Catalogs; the 5GHz 300ft Green Bank (87GB) radio survey; the HST Guide Star Catalog (GSC); the ROE/NRL and Minnesota catalogs of the optical sky surveys.

These resources now make it possible to produce spectral energy distributions for many X-ray sources in the Slew Survey without any new observing.

We can isolate the most likely counterparts. Source classes can be assigned with reasonable probability based on these distributions. In this way ~96% of the sources have some likely counterpart. The follow-up observing time needed on optical telescopes is thus minimized. Only a couple of dozen high Galactic latitude fields have no counterparts and need be observed with large telescopes.

Statistical Sieveing

Many of our identifications will be with objects bright enough to be in the HST GSC, but within our 2 arcmin radius error circles there are typically several GSC objects. A maximum likelihood method (de Ruiter *et al.* 1977, Prestage and Peacock 1983) is powerful for picking out the correct identifications. This calculates the likelihood that an optical candidate in the error circle is correct given its position in the error circle and the local background optical object density at that magnitude. This yields 57 unambiguous identifications with GSC objects that had no previous counterpart (Schachter *et al.* 1992). This method readily allows the inclusion of other factors, such as X-ray to optical ratios, or a stellar/non-stellar flag to separate galaxies from stars.

RAPID DISSEMINATION OF THE WHOLE DATA BASE

Naturally astronomers working on on a large project tend to milk all the interesting information from it before making it public. Instead The Slew Survey source catalog and the complete photon and timing data used to construct it were released on CD-ROM (Plummer *et al.* 1991) as soon as the survey was complete (Jan '91) and well before the paper describing the survey was submitted to the Ap.J. (Sept '91) or published (April '92). As software is developed it is placed on-line to assist a user's own Survey analysis. This will encourage others to work on the data and the Slew Survey will become more widely known, used, and referenced. Self-interest and public interest can converge!

Our aim is to get the Slew Survey 100% identified as soon as possible, so we can begin population studies (*e.g.* AGN evolution). The best way to do this is to get others to help. An on-line, regularly updated, source identification list is maintained at CfA (on *einline*, Karakashian *et al.* these proceedings). We will put any proposed identifications sent to us into this data base with proper credit to the discoverers, providing them with an incentive to get there first.

REFERENCES

de Ruiter, H. R., Willis, A. G., & Arp, H. C. 1977, A&A Supp., 28, 211.

Elvis M., Plummer D., Schachter J. and Fabbiano G., 1992, *ApJS*, in press.

Huchra J.P. and Geller M., 1984, *ApJ*, **257**, 423.

Karakashian T. *et al.* 1991, these proceedings.

Plummer D. *et al.* 1991, CD-ROM issued by SAO.

Prestage, R. M., & Peacock, J. A. 1983, MNRAS, 204, 355.

Schachter J. *et al.*, 1992, in preparation.

THIRTEEN NEW BL LACERTAE OBJECTS DISCOVERED BY AN EFFICIENT X-RAY/RADIO/OPTICAL TECHNIQUE[1]

Jonathan F. Schachter[2], John T. Stocke[2,3], Eric Perlman[2,3], Martin Elvis[2], Jane Luu[4], John P. Huchra, Roberta Humphreys[5], Ron Remillard[6], and John Wallin[7]

Harvard-Smithsonian Center for Astrophysics, MS #4,
60 Garden St., Cambridge, MA, 02138.

Received: ——— ; *Accepted:* ———

ABSTRACT

We report the recent discovery of 13 serendipitous BL Lac objects in the *Einstein* IPC Slew Survey by means of X-ray/radio vs. X-ray/optical color-color diagrams and confirming optical spectroscopy. These 13 BL Lacs were discovered using a technique proposed by Stocke et al. (1989) which exploits the characteristic broad-band spectra of BL Lacs. New VLA detections provide accurate fluxes [$f(6\ cm) \sim 0.5$ mJy] and 2″ positions, facilitating the determination of an optical counterpart. All 13 new BL Lacs show essentially featureless optical spectra. Nine of these lie within the range of colors of known X-ray selected BL Lacs. Of the remaining four, one is apparently X-ray louder (by a factor of 1.5) or optically quieter (by 0.8 mags); and 3 are optically louder (by 1-1.3 mags) than X-ray selected BL Lacs. We expect ~50 new BL Lacs in total, from our VLA work and upcoming Australia Telescope observations, yielding a complete Slew Survey sample of ~90 BL Lacs.

Subject Headings: BL Lacertae objects: general — galaxies: nuclei — galaxies: X-rays — X-rays: sources — surveys

[1] Research reported here used the Multiple Mirror Telescope Observatory, which is a joint facility operated by the Smithsonian Institution and the University of Arizona.

[2] Visiting Astronomer at the National Radio Astronomy Observatory (NRAO), which is operated by Associated Universities, Inc., under contract with the National Science Foundation (NSF).

[3] Postal Address: University of Colorado, Dept. APAS, Campus Box 391, Boulder, CO 80309.

[4] Hubble Fellow.

[5] Postal Address: University of Minnesota, School of Physics & Astronomy, Minneapolis, MN 55455.

[6] Postal Address: Massachusetts Institute of Technology, Center for Space Research, Room 37-595, Cambridge, MA 02139.

[7] Postal Address: Naval Research Laboratory, Code 4129 6, 4555 Overlook Avenue SW, Washington, DC 20375.

I. INTRODUCTION

BL Lac objects have been hard to find: in the 20 years following the discovery of the first example (Schmidt 1968), their numbers grew by only a factor ~10 (Veron-Cetty and Veron 1991). By comparison, in the 20 years following the discovery of quasars (Schmidt 1963) their numbers grew 500-fold (Veron-Cetty and Veron 1991). Their elusiveness is due to the very lack of strong emission lines that make BL Lacs interesting. Even now less than 200 BL Lacs are known (Veron-Cetty and Veron 1991), ~2% of known active objects. BL Lac objects account for ~ 2% (162 out of 7765) of sources in the Veron–Cetty and Veron (1989) AGN catalog.

In the last few years, techniques using their distinguishing properties (Stocke et al. 1989) have made it possible to discover many new BL Lacs in the *Einstein* Extended Medium Survey (EMSS; Gioia et al. 1991; Stocke et al. 1991). This letter reports the extension of these efforts to the *Einstein* Slew Survey: we find 13 new BL Lac objects, which are the first results of a new, uniformly selected, sample of 85–90 bright BL Lacs.

II. AN X–RAY/RADIO/OPTICAL TECHNIQUE FOR IDENTIFYING BL LACS

The key to finding BL Lacs is to exploit their salient characteristics:

First, all BL Lacs are radio loud [$\alpha_{RO} > 0.3$, i.e. $f(6\ cm) > 1$ mJy for $V \leq 20$; Stocke et al. 1991]. For this reason, radio surveys with follow-up optical spectroscopy (e.g., Kühr et al. 1981), have been considerably more efficient than optical surveys (6–8%).

Second, 98% of BL Lacs have distinctive X–ray/radio/optical colors (Stocke et al. 1991). Thus, X–ray surveys, combined with radio and optical data, have been shown to be the best approach to date (~12% efficiency; Stocke et al. 1991). The X–ray/radio/optical approach was highly successful in identifying 36 BL Lacs in the EMSS.

Third, the surface density of X–ray—selected BL Lacs flattens at fluxes below 10^{-12} ergs s^{-1} cm^{-2} (Wolter et al. 1991). Therefore, wide–angle (all–sky) surveys are better for detecting BL Lacs than narrow–beam deep surveys. Because the EMSS covers only 2% of sky (up to $\sim 5 \times 10^{-12}$ ergs s^{-1} cm^{-2}), we need to use a shallow X–ray survey: the *Einstein* Slew Survey. The Slew Survey, constructed from 2799 individual slews of the IPC, covers 50% of sky at an exposure of 6 s (or, equivalently, to $\sim 1 \times 10^{-9}$ ergs s^{-1} cm^{-2}; Elvis et al. 1992). We estimate from the EMSS that a large number ($\sim$ 50) of new Slew BL Lacs will be identified, increasing the currently known number of BL Lacs by more than 30%.

Together these properties allow us to define a multi–step approach to identify BL Lacs, starting from the 193 unidentified Slew Survey sources:

1. Choose sources at high Galactic latitudes ($|b| > 15°$), with previous radio detections or a suggestive X–ray/radio flux upper limit;

2. Observe them with the VLA (hybrid CnB configuration, 2″ resolution, cf. 2′ X-ray position), giving an accurate flux (~ 0.5 mJy);

3. Select point sources from the VLA maps as likely BL Lacs;

4. Use arcsecond VLA positions to find optical counterparts and magnitudes from digitized sky survey plates;

5. Place objects in the X-ray/radio/optical color–color diagram;

6. Obtain optical spectra of candidates with correct colors.

III. CURRENT APPLICATION OF THE TECHNIQUE

The EMSS (Gioia et al. 1990) showed that the presence of a centimeter radio source of the proper flux within an X-ray error circle will yield a BL Lac object at $\geq 80\%$ efficiency (Stocke et al. 1991). In Figure 1 (after Stocke et al. 1991), identified BL Lacs occupy a unique area in the radio/optical/X-ray (or α_{OX}–α_{RO}) color–color diagram, compared to other extragalactic classes. The few ($\leq 20\%$) non-BL Lacs in the region of Figure 1 bounded by $\alpha_{RO} = (0.6, 0.3)$ and $\alpha_{OX} = (1.2, 0.55)$ are either highly variable AGN or dominant galaxies in cooling-flow clusters, which are easily distinguished from BL Lacs with optical spectra.

Sources likely to be BL Lacs were selected primarily from the 193 unidentified Slew Survey sources, i.e. sources currently lacking proposed optical counterparts. As most of the unidentified sources are accessible from the North (76% with $\delta > -40°$), we obtained VLA observing time, as described below. Only 10% (19) of the targets had previous radio survey detections [$f(6\ cm) > 25$ mJy in Condon & Broderick 1985, 1987; or $f(6\ cm) > 60$ mJy in Condon and Broderick 1992]. We therefore prioritized sources as follows:

1. All high-latitude ($|b| > 15°$) unidentified sources (both radio detections and nondetections; see Table 1).

2. Slew sources with proposed optical counterparts of questionable validity, due to the lack of previous X-ray detections or confirming spectroscopy. These were all (a) stellar identifications, which are possible superpositions of foreground objects, or; (b) "normal" galaxy identifications, which may have active nuclei, or; (c) cluster identifications.

3. Unidentified sources at low latitudes, where a radio detection may indicate the presence of a pulsar.

4. Slew sources rejected from the source list because of a 10%–15% false-source rate and the requirement of high source reliability > 98% (Elvis et al. 1992). In the 203 rejected unidentified sources, the false-source rate is slightly smaller (9%; from Figure 12 of Elvis et al.), but VLA detections would be highly significant.

In January, 1992, we observed a prioritized list of 152 Slew Survey sources at 6 cm with the VLA CnB hybrid configuration. The list contained 100 objects of Priority 1 (see above), 20 of Priority 2, 13 of Priority 3, and 19 of Priority 4. Using snapshot exposures of 3 minutes each, we achieved a 5σ flux sensitivity of 0.5 mJy, and a positional accuracy of 2–3 ″. The angular resolution clearly shows double–lobed, wide–angle–tail, or head–tail structure in many cases. Some 52 of the VLA detections identified with Slew sources (within the 80″ 91% confidence radius of the Slew Survey) have the point–source radio morphology typical of BL Lac objects. Five of these have a second VLA point source within the Slew error box, where the ambiguity will be resolved using our color–color criteria once we have magnitudes for all sources. The 47 remaining BL Lac candidates are divided into 21 strong sources [$f(6cm) > 10$ mJy], and 26 weaker sources [0.5 mJy $< f(6\ cm) \leq 10$ mJy].

To find optical magnitudes for the VLA sources, we are primarily using two $B \sim 22$ digitized catalogs: in the South, the NRL catalog of objects derived from ROE scanning of the UK Schmidt plates; in the North, the Minnesota catalog derived from scanning the POSS plates. At this writing, the UK Schmidt plates (in the B_J band) are easier to work with, as NRL has all of the scanned UK Schmidt plates on EXABYTE tape. The U. Minnesota analysis is more time consuming, but provides both O and E band plate data, which is important for identifying optical counterparts to Slew Survey sources. In the case of either the POSS or the UK Schmidt digitized data, magnitudes are typically accurate to better than 0.5 mag, and positions to 0.5″. These values are completely adequate for our analysis.

We obtained the magnitudes of optical counterparts in the VLA error circle. In no case has there been more than one possible counterpart, and we have found only one case without any possible counterparts, suggesting extreme optical variability (the Slew source 1ES1218+237). This is consistent with our expectation that the faintest expected Slew Survey objects will have $B \sim 19$ (Schachter et al. 1992). Using star counts from the Galactic models of Bahcall & Soneira 1980, it is easy to show that even at the POSS or UK Schmidt plate flux limit of $B \sim 22$, and $b = 20°$, the probability of a foreground source in the VLA error circle is small ($\leq 5\%$).

Using optical magnitudes derived from digitized plate data, we can place 13 of the VLA sources in Figure 1. We scale POSS O–magnitudes and UK Schmidt B_J–magnitudes by +0.5 to obtain approximate V magnitudes, using the median $(B - V)$ of 0.5 in Veron–Cetty & Veron 1989. Bearing in mind the uncertainties in the IPC flux and V magnitude (shown graphically in Figure 1), 9 sources have the correct colors to be BL Lacs. These only require confirming spectroscopy for an absolute identification (see below). The remaining four sources have systematically smaller values of either α_{OX} (1ES0347−121) or α_{RO} (1ES0303+067, 1ES1440+122, 1ES1544+820) relative to EMSS BL Lacs.

The simplest explanation of the 4 outlier points is X–ray or optical flaring, which is plausible given the non–simultaneity of the X–ray, optical photometric, and radio observations, and the variability of BL Lacs at all known wavelengths (e.g., Schwartz et al. 19??). The low–α_{RO} sources 1ES0303+067, 1ES1440+122, and 1ES1544+820 could have flared optically while observed by the POSS by 1.3, 1.1, and 1.0 magnitudes and could still lie in the proper region of the diagram. Similarly, the low–α_{OX} source 1ES0347−121 could have been caught in a flaring X–ray state by the Slew Survey. A reduction in the observed Slew flux by a factor of 1.5 would give this sources the correct BL Lac colors. This value, which

cannot be attributed to uncertainty in determination of the Slew Survey flux (18%), is within the range of known BL Lac variability. Equivalently, 1ES0347−121 could have been fainter optically when observed in the sky survey plates by 0.8 mags and still have the correct colors. Finally, the third and most speculative explanation is that 1ES0347−121 is a prototype of a new class of X–ray loud BL Lac objects. In the mean, these would be a factor of ∼4 more X–ray loud than EMSS BL Lacs.

Optical spectra, beginning in June, 1991, were obtained by us at the Michigan/Dartmouth/MIT 1.3 m (R. R.), and the MMT (Blue Channel: J. P. H; Red Channel: J. L., J. T. S). No attempt was made at this stage to identify a complete sample; we simply aimed to identify as many sources favorable in each observing season as possible. For the 13 objects with correct colors (or discrepancies explainable by flaring), we obtained spectra, all of which turned out to be featureless.

Figure 2 shows spectra of the 13 confirmed BL Lac objects. The positions of these objects are also marked in the X-ray/radio/optical color–color diagram (Figure 1). Differences in signal–to–noise ratios result from different detectors and telescopes used in the observations. Despite these differences, it is clear that the spectra are uniformly featureless. Table 2 provides VLA positions, 6 cm fluxes, optical magnitudes and colors (if available), for the 13 confirmed BL Lacs. In addition, there are 4 more featureless spectra (not shown), which are VLA nondetections, but which have the correct colors to be BL Lacs in Figure 1 (based on Condon nondetections; §3*b*).

IV. DISCUSSION

The combined X–ray/radio/optical technique for identifying BL Lacs is evidently very efficient. There have been no cases in which a VLA point source in the BL Lac part of the α_{RO}/α_{OX} diagram has not turned to be in fact a BL Lac object, as defined by the featurelessness of its optical spectrum. The payoff is large, considering the small amount of observing time required per source (5 min snapshot at the VLA, then 10–20 min at an optical telescope).

We can compare the new 13 Slew Survey BL Lacs identified to date with the complete BL Lac sample of the EMSS, and the optically selected BL Lacs in Veron–Cetty and Veron (hereafter, VV; VV 19??). The median V magnitudes are 17.0 for VV, 19.1 for the EMSS, and 18.2 for the Slew Survey. This illustrates that we are filling in an important gap in presently known optically and X–ray—selected BL Lac samples. In units of 10^{-12} ergs s^{-1} cm^{-2}, the mean Slew Survey BL Lac X–ray flux is 2.6, compared to 1.5 for the EMSS. The Slew Survey BL Lacs are apparently ∼2–2.5 times brighter than the EMSS BL Lacs, although (except for the two objects noted above) the X–ray—to–optical flux ratios between the two groups are consistent.

There are 38 more VLA point sources to be identified; using the EMSS as a guide, we eventually expect a yield of ∼ 40 BL Lacs from the 52 point sources detected at the VLA. Our observational program is accelerating. We have Australia Telescope time scheduled to pursue the deep southern ($\delta < -40°$) radio sources. Some 33 of these lie at high latitude.

Assuming a detection efficiency similar to our VLA work, we expect $\sim$ 15 AT detections, from which we will identify a dozen new BL Lacs. Hence, together with the 35 Slew Survey sources known from catalogs to be BL Lacs, and the complete VLA sample, we expect about 90 BL Lacs in the whole Slew Survey. Since they will be relatively bright and uniformly selected, they should prove valuable for both detailed follow–up observations of individual objects, and statistical population studies.

This work was supported by NASA grants NAG5–1746 (Slew Survey ADP), NAGW–2201 (Long Term Space Astrophysics), and NAS8–3751 (*Einstein* Data Center) to SAO; and by NASA grant NAGW–2645 and NSF grant AST–9020008 to the University of Colorado.

Table 1: VLA Observations of BL Lac Candidates

Source Group	Number Unidentified	Number Observed at VLA (Pct.)
Slew Survey[a]	193	113 (59%)
Northern ($\delta > -40°$)	147	113 (77%)
High Latitude ($\|b\| > 15°$)	111	100 (90%)
Low Latitude	36	13 (36%)
Southern	46	0[b]

a. From source list of 809 objects.

b. Southern sources will be observed at the Australia Telescope in July, 1992.

Table 2: New BL Lac Identifications

Index	Name	Posn. J2000	RA Off.(″)	DEC Off.(″)	f(6 cm) (mJy)	m_O (mags)	$m_O - m_E$ (mags)	Spec. Note[a]
1	1ES0229+200	02 32 48.6 +20 17 17	+25	−12	41.5	18.0	4.7	Luu/Rem.
2	1ES0303+067	03 06 09.7 +05 58 28	+71	−116	3.9	17.6:	...	Rem.
3	1ES0347−121	03 49 23.2 −11 59 27	+3	−1	7.6	19.1(J)	...	Rem.
4	1ES0502+675[b]	05 07 56.2 +67 37 24	−4	−1	31.3	16.5:	...	Sto./Rem.
5	1ES0525+713[c]	05 31 41.7 +71 22 17	+3	+68	8.6	19.9:	...	Rem.
6	1ES0647+250	06 50 46.5 +25 03 00	−11	+11	61.0	15.3:	...	Rem.
7	1ES0806+524[b]	08 09 49.2 +52 18 58	0	+3	169	15.3	1.8	Sto.
8	1ES1028+511	10 31 18.5 +50 53 36	−1	+1	42.5	17.0	0.7	Sto.
9	1ES1440+122	14 42 48.3 +12 00 40	−9	−1	40.2	15.3:	...	Sto.
10	1ES1544+820	15 40 15.7 +81 55 06	+2	+3	45.1	15.3:	...	Sto.
11	1ES1927+654	19 28 19.5 +65 33 55	+13	−3	16.0	18.7:	...	Rem.
12	1ES1959+650	19 59 59.9 +65 08 55	−5	+14	241.0	14.6:	...	Sto./Rem.
13	1ES2343−151	23 45 38.4 -14 49 29	+16	−11	7.7	19.2(J)	...	Huch.

a. Notes on spectra: *Huch.*—J. Huchra, MMT Blue Channel, *Luu*—J. Luu, MMT Red Channel, *Rem.*—R. Remillard, MDM 1.3 m, *Sto.*—J. Stocke, MMT Red Channel.

b. Priority 4 source; see §3.

c. Possible wide–angle–tail source.

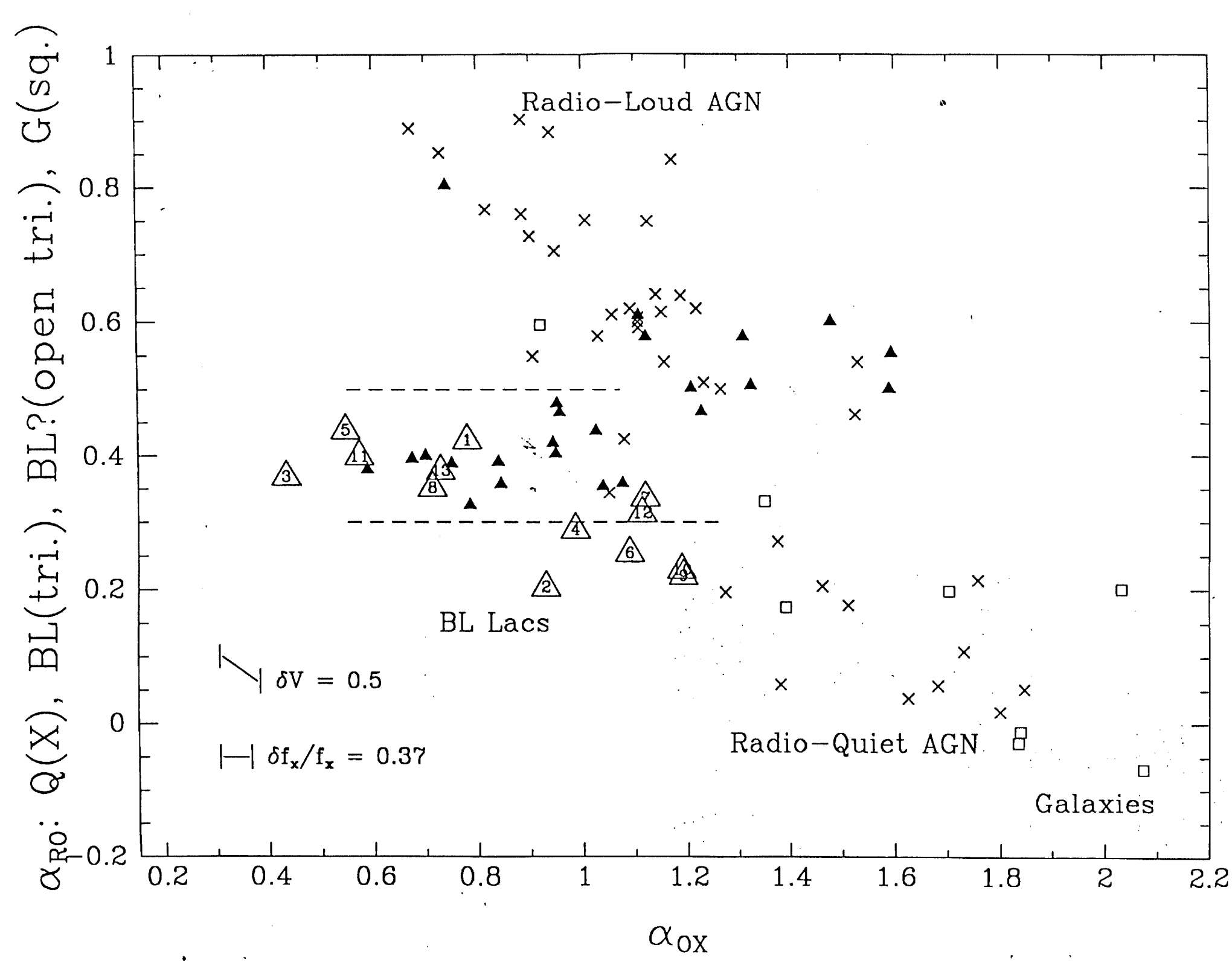
Radio−Loud AGN
BL Lacs
Radio−Quiet AGN
Galaxies
δV = 0.5
δf_x/f_x = 0.37
α_RO: Q(X), BL(tri.), BL?(open tri.), G(sq.)
α_OX
1
0.8
0.6
0.4
0.2
0
−0.2
0.2
0.4
0.6
0.8
1
1.2
1.4
1.6
1.8
2
2.2

FIGURE CAPTIONS

Figure 1: Color–Color diagram for the 13 new BL Lac objects reported in this paper (open triangles; numbered as in Table 2), compared with identified Slew Survey AGN (x's), BL Lacs (closed triangles), and normal galaxies (squares) known from positional coincidences in optical catalogs. Definitions of the quantities α_{OX} and α_{RO} are taken from Stocke et al. 1991. Changes in the spectral indices expected from typical uncertainties in V–magnitude and relative IPC flux are shown.

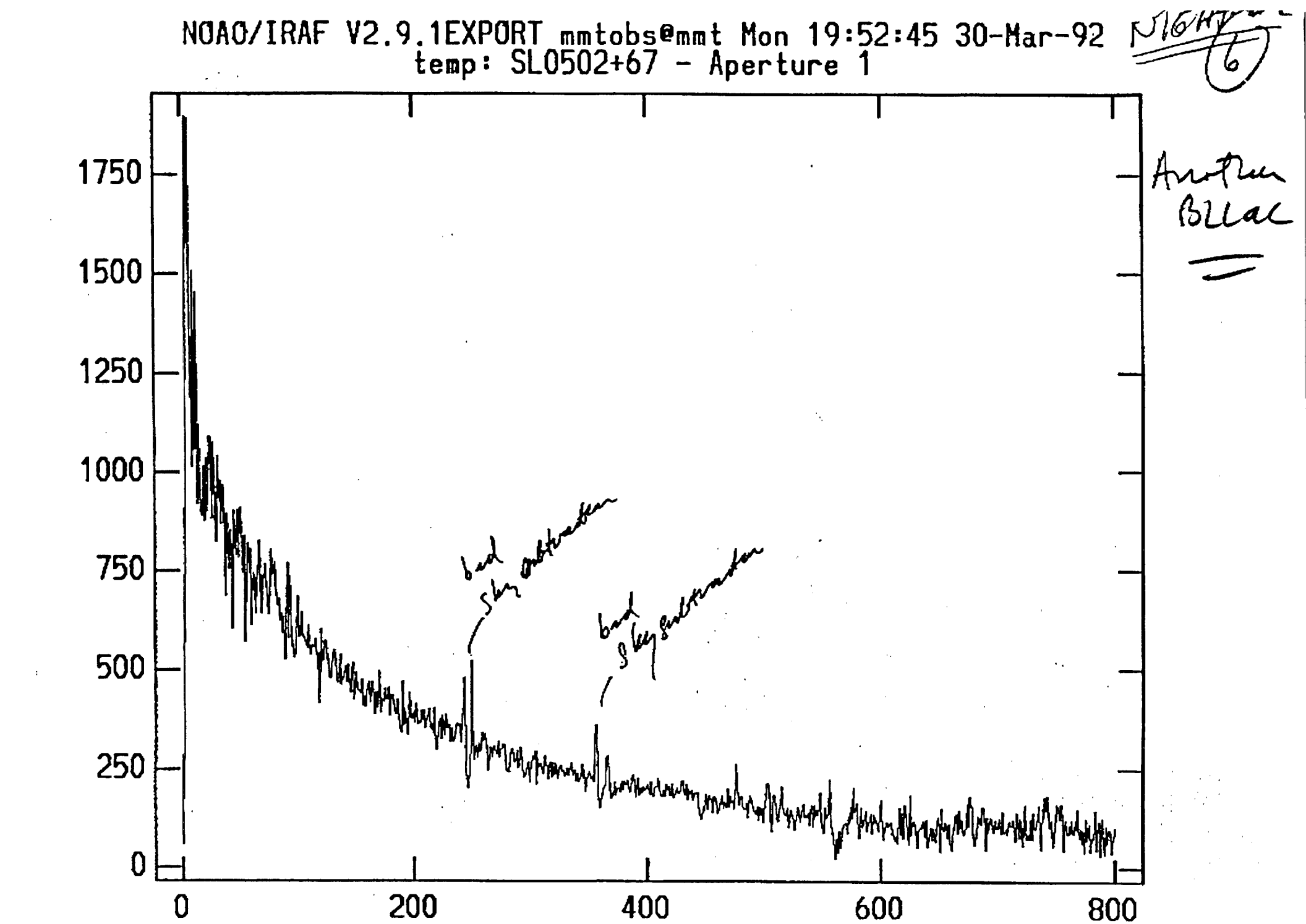
NOAO/IRAF V2.9.1EXPORT mmtobs@mmt Mon 19:52:45 30-Mar-92
temp: SL0502+67 - Aperture 1
1750
1500
1250
1000
750
500
250
0
0
200
400
600
800
bad sky subtraction
bad sky subtraction

REMILLARD — MDM
1.3 m

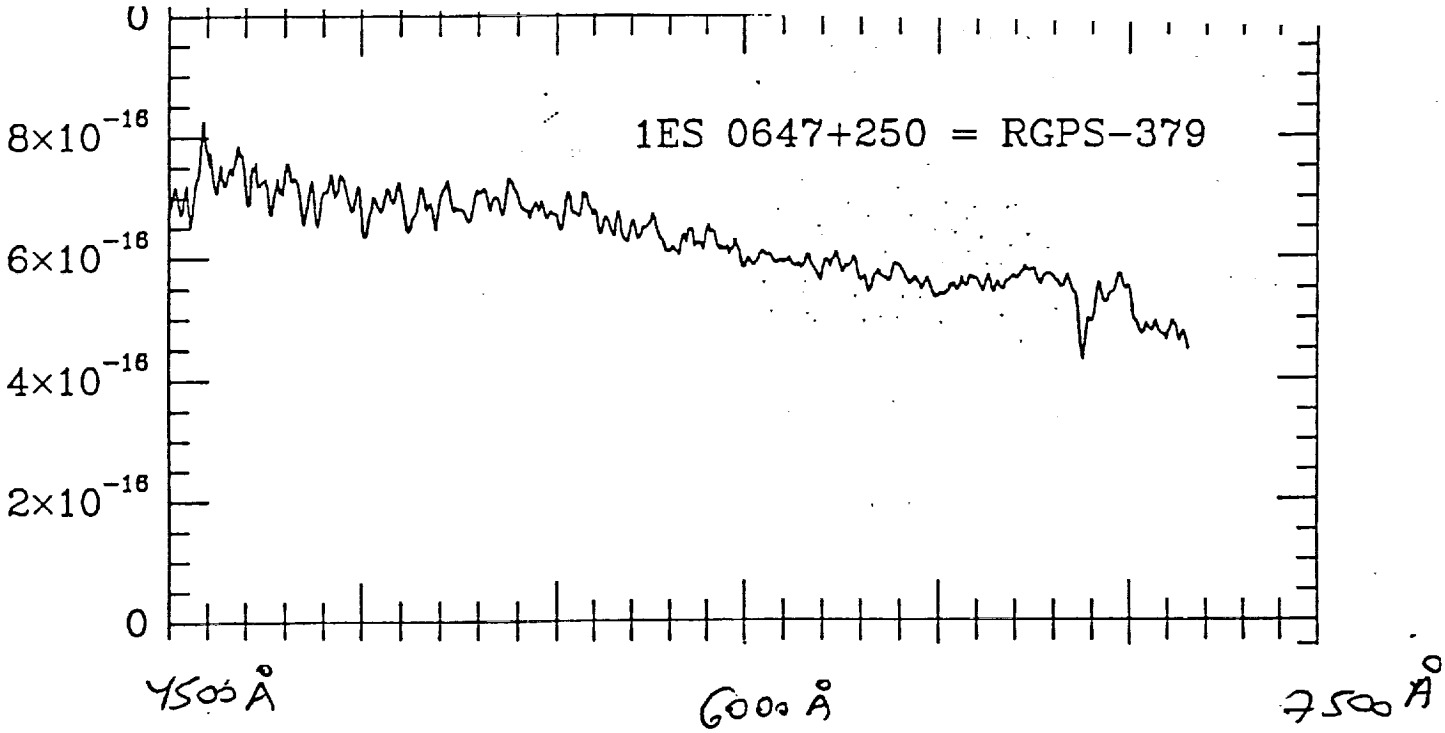

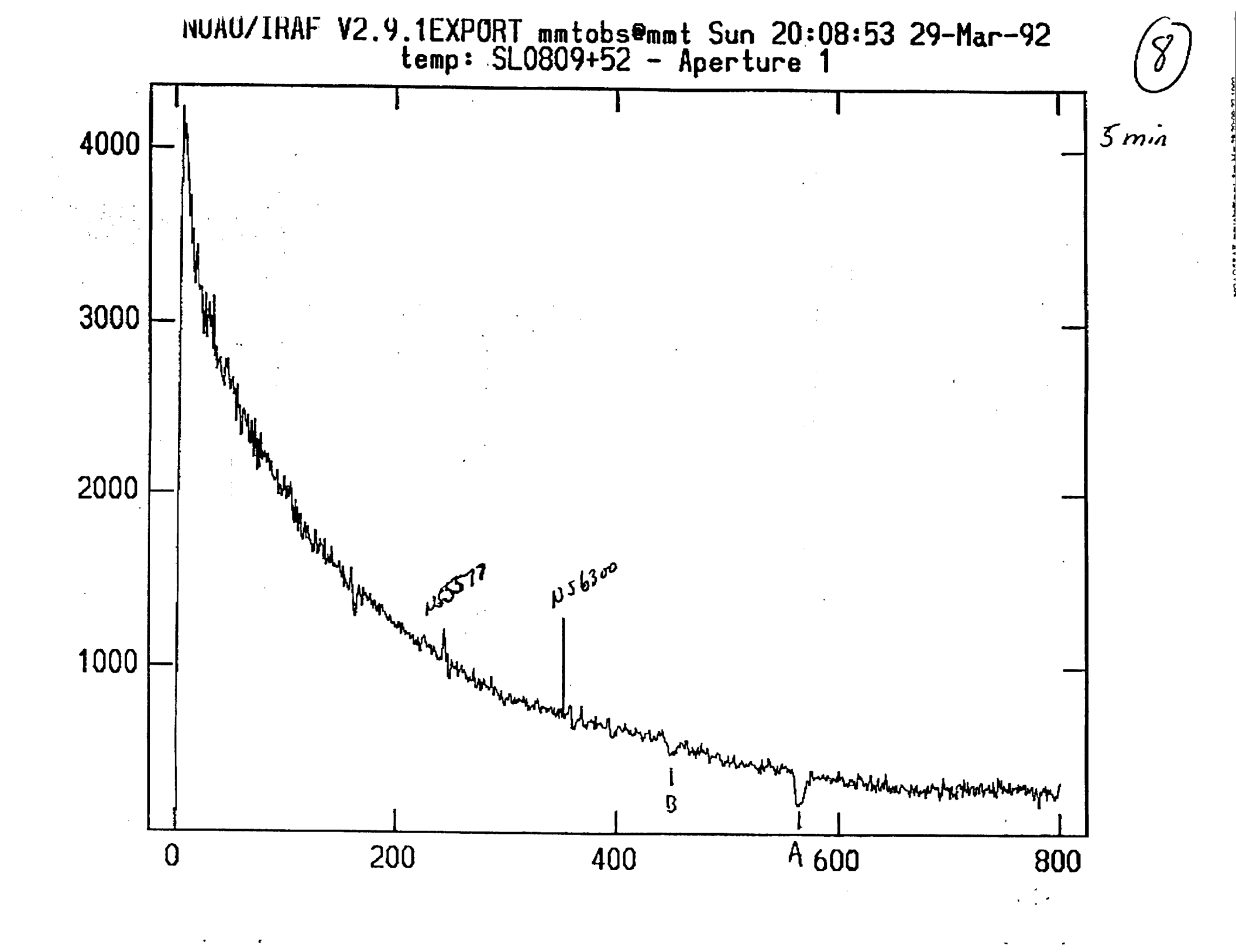
NOAO/IRAF V2.9.1EXPORT mmtobs@mmt Sun 20:08:53 29-Mar-92
temp: SL0809+52 - Aperture 1
8
5 min
4000
3000
2000
1000
0
200
400
600
800
λ5577
λ6300
I
B
I
A

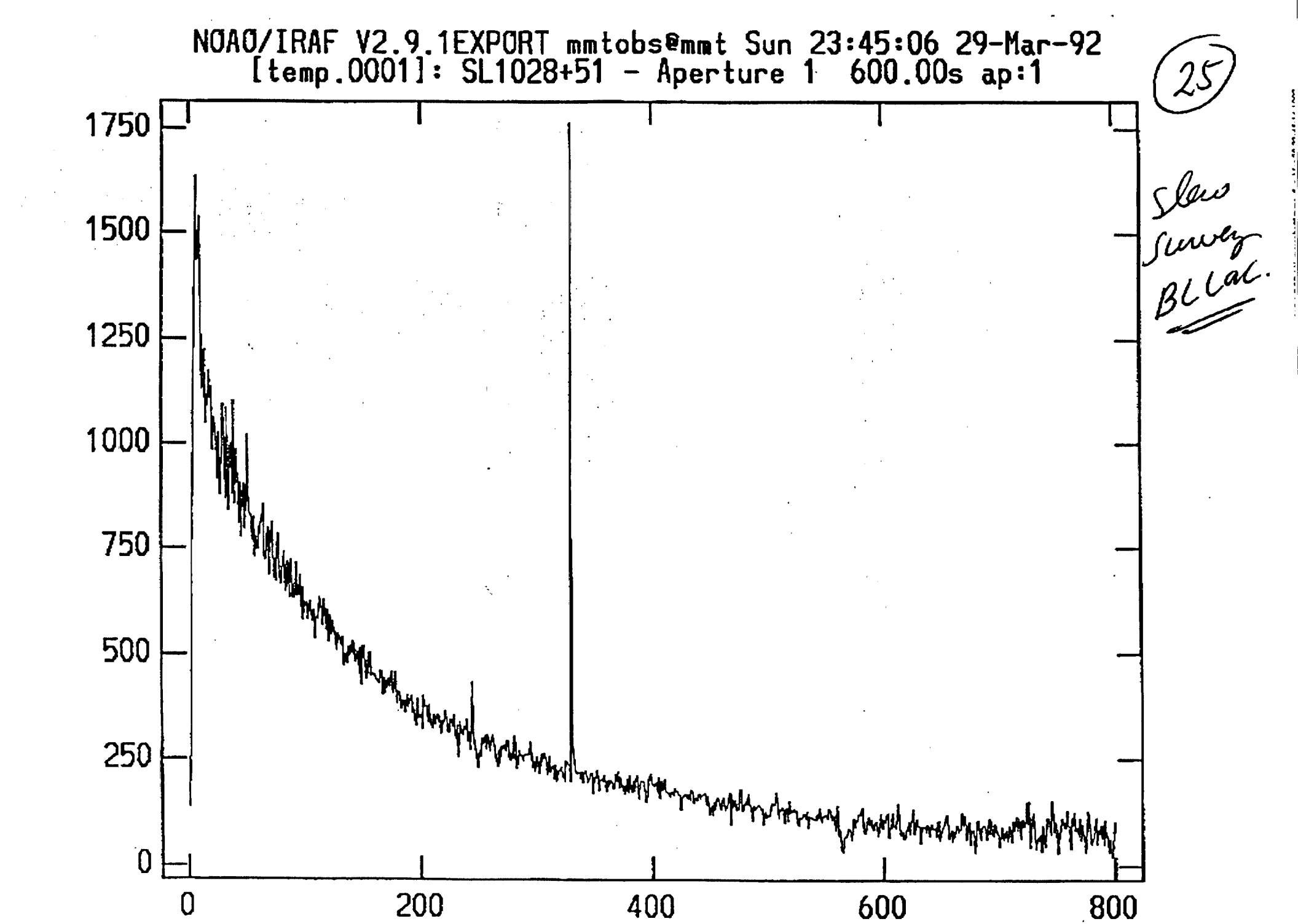

25

Slow Survey BL Lac.

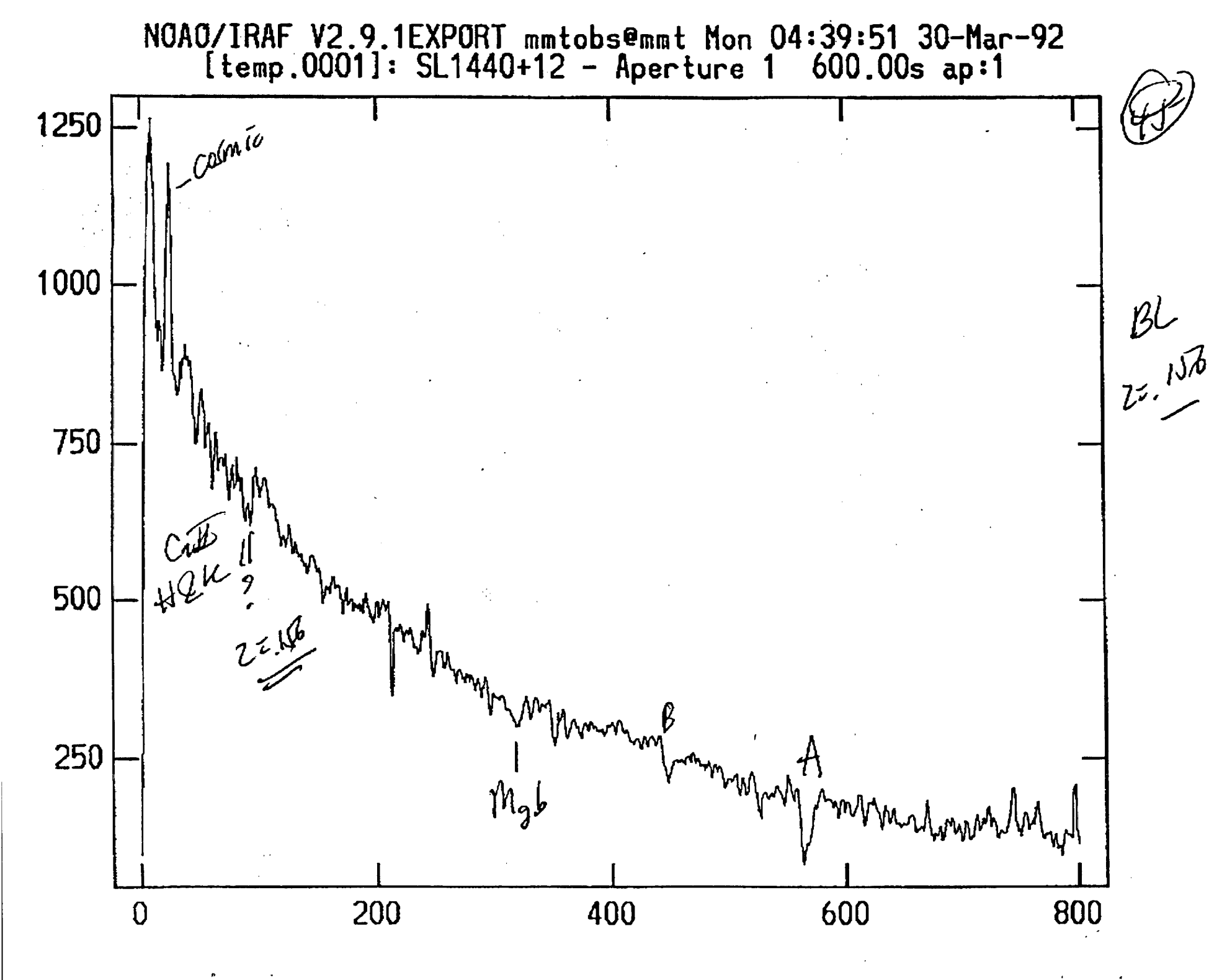
NOAO/IRAF V2.9.1EXPORT mmtobs@mmt Mon 04:39:51 30-Mar-92
[temp.0001]: SL1440+12 - Aperture 1 600.00s ap:1
1250
1000
750
500
250
0
200
400
600
800
cosmic
CaII H&K
?
z=.156
Mgb
B
A
BL
z=.157

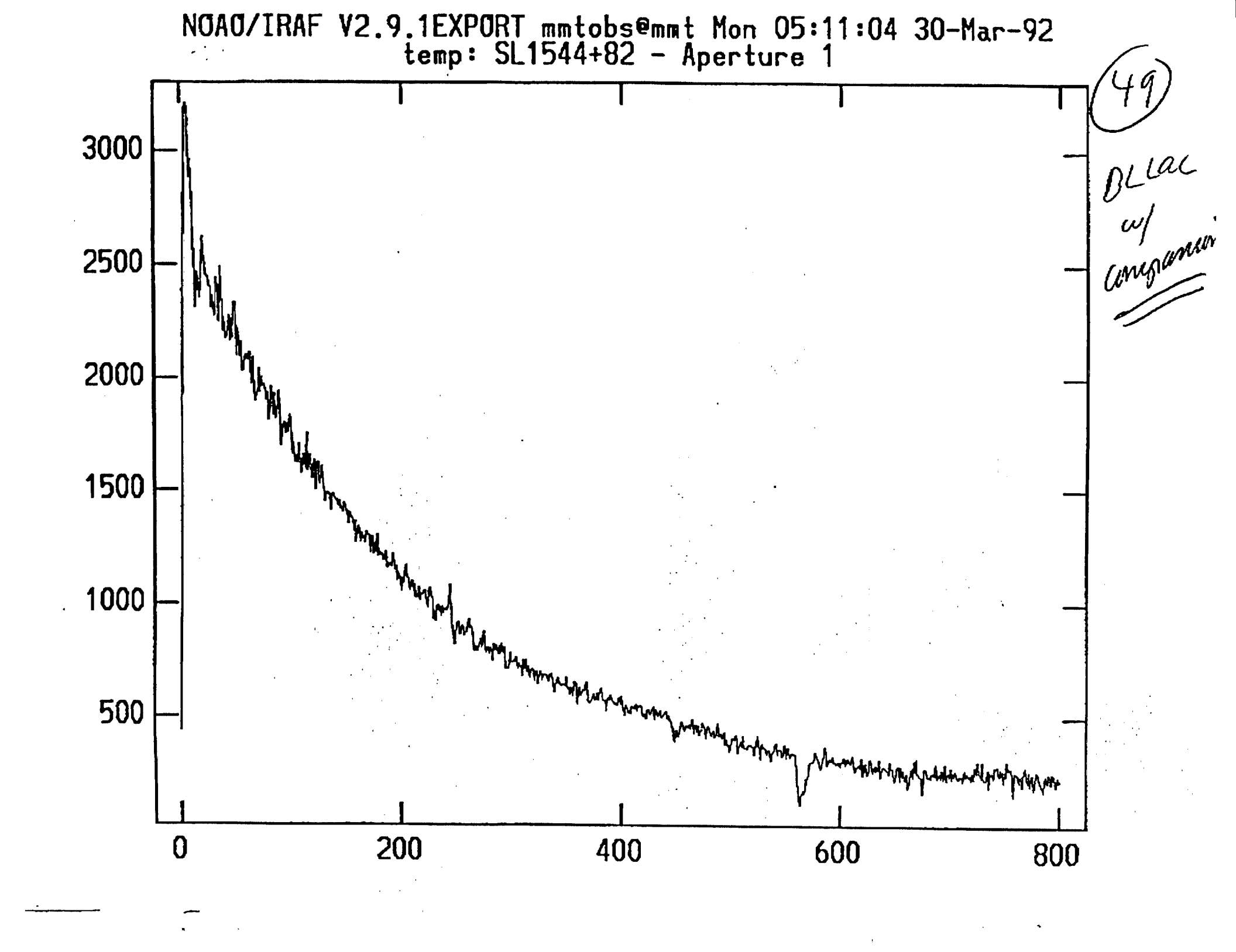
NOAO/IRAF V2.9.1EXPORT mmtobs@mmt Mon 05:11:04 30-Mar-92
temp: SL1544+82 - Aperture 1
3000
2500
2000
1500
1000
500
0
200
400
600
800
49
DLac
w/
companion

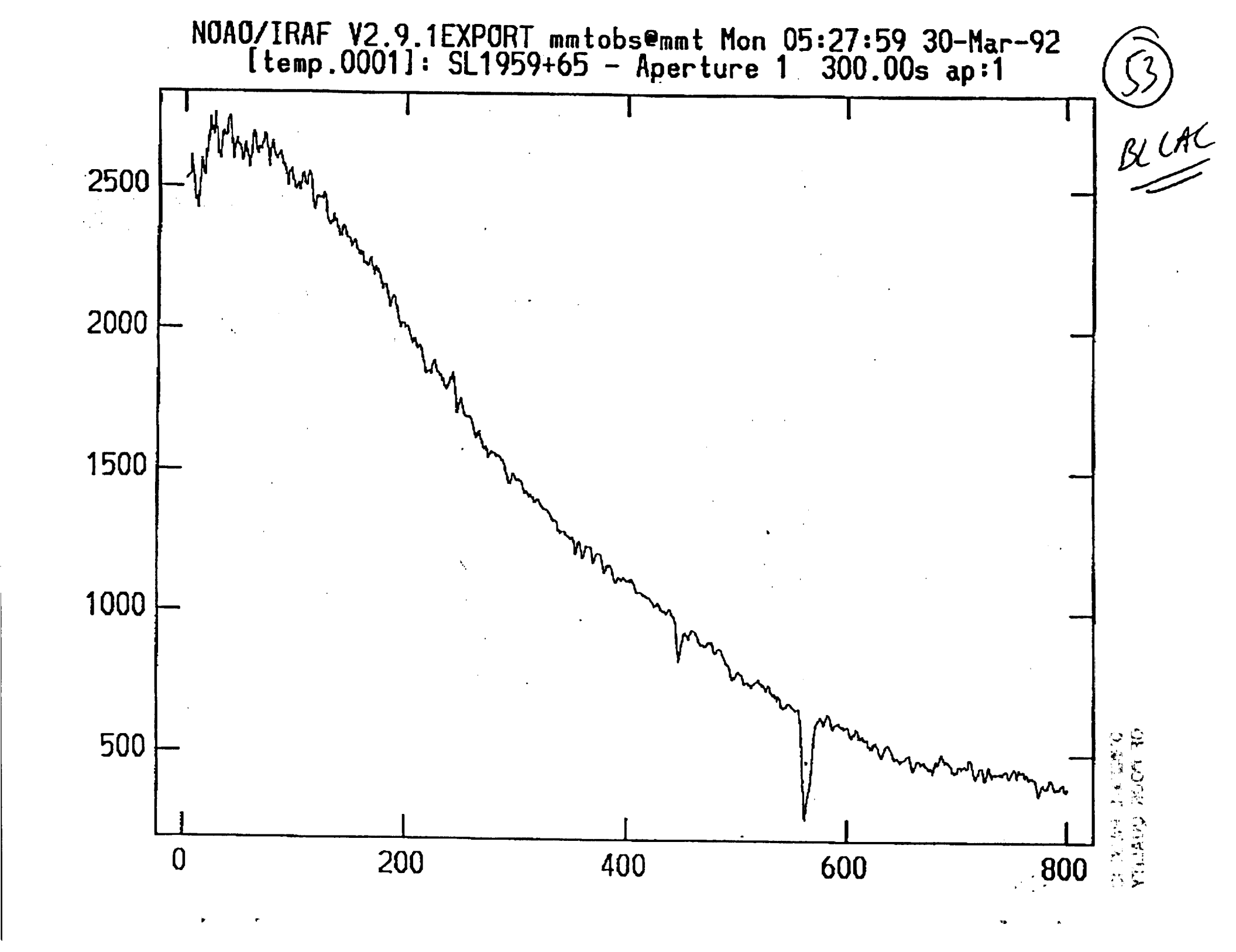
NOAO/IRAF V2.9.1EXPORT mmtobs@mmt Mon 05:27:59 30-Mar-92
[temp.0001]: SL1959+65 - Aperture 1 300.00s ap:1
2500
2000
1500
1000
500
0
200
400
600
800
53
BL CAL

HJCHRA – MMT Blue Channel

IES 2343-15 #19